Bi-directional flux of 2-chloroadenosine by equilibrative nucleoside transporter 4 (ENT4)

by

David Tandio

A thesis submitted in partial fulfilment of the requirements for the degree of

Master of Science

Department of Pharmacology

University of Alberta

Abstract

Introduction: Cardiac ischaemia-reperfusion injury (IRI) remains a life-threatening injury with no effective treatments. Though the mechanisms remain unknown, we know that ischaemic tissues are acidic. This is where equilibrative nucleoside transporter 4 (ENT4), which mediates an increased adenosine influx under acidic conditions (Barnes *et al.*, 2006), can potentially be a therapeutic target for cardiac IRI. It has been found to be expressed in cardiomyocytes, and vascular smooth muscle cells. Although ENT4 is part of the nucleoside transporter family, it was initially only found to transport monoamines, and therefore it is also identified as the plasma membrane monoamine transporter (Engel *et al.*, 2004). We hypothesise that ENT4 activity increases following ischaemia and that ENT4 may mediate the loss of intracellular adenosine during reperfusion which is detrimental for the recovery of contractile function in cardiomyocytes.

Methods: To better understand ENT4 as a nucleoside transporter and to study ENT4 in isolation, the pig kidney epithelial nucleoside transporter deficient cells (PK15-NTD) was stably transfected with ENT4 to create the PK15-hENT4 cells. To investigate if ENT4 plays a significant role in ischaemia-reperfusion injury, HL-1 cardiomyocytes were used to explore how ENT4 activity changes during ischaemia-reperfusion injury. In collaborative studies, hearts and mesenteric vascular beds isolated from ENT4-knockout (KO) and control mice were subjected to global no-flow ischaemia (20 min) and reperfusion (30 min), and assessed for their functional recovery. Therefore, we investigated any compensatory messenger ribonucleic acid (mRNA) changes in the ENT4 KO animals using quantitative reverse transcription polymerase chain reaction (RT-qPCR).

Results: Our data shows that ENT4 is capable of mediating not just adenosine uptake, but also a more stable adenosine analogue, 2-chloroadenosine (2CADO). 2CADO was then used as a substitute for the more labile adenosine to show that ENT4 mediates nucleoside efflux in an acidic pH-sensitive manner and that a proton gradient is not needed for its pH sensitivity. This suggests that ENT4 is capable of mediating bi-directional adenosine flux in ischaemic tissues, and during early reperfusion, before the recovery from acidic pH. In HL-1 cells, an acidic pH-sensitive purine influx was observed. This acidic pH-sensitive influx was reduced during ischaemia, but recovered following reperfusion; this was supported by reduced ENT4 transcript levels in ischaemic conditions. In ENT4 KO animals, compensatory changes in adenosine related genes (and not those related to monoamines) was mostly observed.

Conclusion: Our data showed that ENT4 can mediate adenosine efflux under acidic conditions and, therefore, blocking ENT4 during early reperfusion may prevent the rapid loss of intracellular adenosine pools that limits the recovery of contractile function. The suppression of ENT4 activity and expression following simulated ischaemia suggests that this might be a protective mechanism that the heart adopts to prevent further loss of intracellular adenosine pools. As an acidic pH-sensitive adenosine uptake was still observed following simulated ischaemia, this also suggests that inhibition of ENT4 will still be more selective for ischaemic tissues (compared to ENT1, for e.g.). This was further supported by data from ENT4 KO animals which suggests that the adenosine transport function of ENT4 might play an important role *in vivo*. The findings in this thesis add to our current understanding of ENT4, with data from a cellular to an organ level to determine if ENT4 can be used as a novel therapeutic target for a clinically unmet condition.

Preface

The work in this thesis was started by Gonzalo Vilas, a research associate in the Hammond laboratory. A version of chapter 4.1. will be published as David Tandio, Gonzalo Vilas, James R Hammond. Human equilibrative nucleoside transporter 4 (hENT4)-mediated influx and efflux of 2-chloroadenosine. I was responsible for data collection, data analysis, and manuscript composition. G. Vilas was responsible for data collection as shown in a figure legend and with creation of the PK15-hENT4 cell line. J.R. Hammond provided manuscript edits and was the corresponding author and was involved with concept formation, manuscript composition and submission.

There are ongoing collaborations on this project with Drs Frances Plane, Gary Lopaschuk, and Stephane Bourque. Molecular analysis of data produced in chapter 4.3 will be used to complement data produced in those respective laboratories. Supplementary figures shown in appendices were produced in the Bourque (Supplementary Figure 1), Plane (Supplementary Figure 2 – 5) and Lopaschuk labs (Supplementary Figure 6).

Acknowledgements

First and foremost, I would like to express my gratitude and thank my supervisor, James Hammond, for having me as a graduate student. I am thankful for his scientific mentorship and guidance during my graduate programme. Though this was not the journey I imagined when I started, the skills I have obtained here would be crucial to my lifelong journey of learning. I would also like to express my appreciation to my committee members, Frances Plane and Gary Lopaschuk. They have both provided thoughtful comments and suggestions to help provide a more enriching learning environment. I am also grateful for their contributions as collaborators in this project. I am thankful to Richard Schulz for initially being a course organiser and eventually agreeing to be a mentor, providing invaluable career advice and assistance for scholarships and PhD applications. I would also like to acknowledge Xiuju Li and Larry Fligel for technical assistance and expertise in helping me better complete my thesis work, and Danny Galleguillos for the occasional technical assistance and scientific discussion.

I am grateful to the Heart & Stroke Foundation of Canada for funding my project and the Alberta Innovates for partially providing stipend support.

Thank you to members of the Hammond laboratory, Monika Dabrowska, Nicholas Ruel, Nayiar Shahid, Chan Kim, and Michelle Ntiamoah, for making this such a unique learning environment and experience. These are the memories that will be cherished and remembered. I will also cherish the experiences I've had with my PGSA team – Nicholas Ruel, Filip Reformat and Daniel Fajonyomi. All the events we agreed to organise was unexpectedly a fulfilling and fun experience to say the least, especially the fundraisers. Thank you also to Rafid Feisal and the lab class for being part of my journey here. Special thanks to Department of Pharmacology members, especially Jennifer Beattie, Dancy Bogdanovic, and Linda Burke for providing logistical support and sorting out stipend and signatures. Finally, I am forever indebted for the support I have received from my family and friends who are thousands of miles away but made all this possible. This thesis is dedicated to the loving memory of my Dad.

Table of Contents

List of Tables

List of Figures

Abbreviations used

2CADO – 2-chloroadenosine
2-PCPA – (±)-trans-2-Phenylcyclopropylamine hydrochloride
5-HT – 5-hydroxytryptamine
5-HT_{1B}R – 5-HT 1B receptor
5-HT_{1D}R – 5-HT 1D receptor
5-HT_{1F}R – 5-HT 1F receptor
5-HT_{2A}R – 5-HT 2A receptor
5-HT_{2B}R – 5-HT 2B receptor
5-HT_3R – 5-HT 3 receptor
5-HT_4R – 5-HT 4 receptor
5-HT_7R – 5-HT 7 receptor
5-HTP – 5-hydroxytryptophan
5-HTR – 5-HT receptors
5-HIAA – 5-hydroxyindole acetic acid
6-MP – 6-mercaptopurine
A_1AR – adenosine A1 receptor
A_{2a}AR – adenosine A2a receptor
A_{2b}AR – adenosine A2b receptor
A_3AR – adenosine A3 receptor
ABT-702 – 5-(3-Bromophenyl)-7-[6-(4-morpholinyl)-3-pyrido[2,3-d]byrimidin-4-amine dihydrochloride
ADA – adenosine deaminase
ADK – adenosine kinase
ANOVA – analysis of variance
ATP – adenosine triphosphate
BECEF-AM – 2',7'-Bis-(2-Carboxyethyl)-5-(and-6)-Carboxyfluorescein, Acetoxymethyl Ester
BP – blood pressure
B_{max} – total specific binding
cAMP – cyclic adenosine monophosphate
CD39 – ecto-apyrase
CD73 – ecto-5'-nucleotidase
cDNA – complementary deoxyribonucleic acid
CNT – concentrative nucleoside transporter
Corticosterone – (11β)-11,21-Dihydroxypregn-4-ene-3,20-dione
COX – cyclooxygenase
D22 – decynium-22
Desipramine – 10-11-Dihydro-N-methyl-5H-dibenz(Z)[b,f]azepine-5-propanamine
$DiBAC_4(3)$ – Bis-(1,3-Dibutylbarbituric Acid)Trimethine Oxonol
Dilazep – (N,N'-bis[3-(3,4,5-trimeth-oxybenzo-yloxy)propyl]-homo-piperazine)
Dipyridamole – [2,6,-bis (diethanolamino)-4,8-dipiperidinopyrimido-[5,4-d]pyrimidine]
DMSO – dimethyl sulfoxide
DNA – deoxyribonucleic acid

Draflazine – [2-(aminocarbonyl)-4-amino-2,6-dichlorophenyl]-4-[5,5-bis(4- fluorophenyl) pentyl]- 1-piperazine acetamide 2HCl]
ENT – equilibrative nucleoside transporter
Fluoxetine – N-Methyl-3-[(4-trifluoromethyl)phenoxy]-3-phenylpropylamine
GAPDH – glyceraldehyde-3-phosphate dehydrogenase
GBR12935 – 1-(2-Diphenylmethoxyethyl)-4-(3-phenylpropyl)piperazine
GPCR – G-protein coupled receptor
HEK-293 – human embryonic kidney 293 cells
HIF – hypoxia inducible factor
HMEC – human microvascular endothelial cells
HR – heart rate
HUVEC – human umbilical vein endothelium cells
IPC – ischaemic pre-conditioning
iNOS – inducible nitric oxide synthase
IRI – ischaemia-reperfusion injury
K_D – binding affinity
K_m – substrate affinity for transporter
LDH – Lactate Dehydrogenase
KO – knock-out
MAO – monoamine oxidase
MDCK – Madin-Darby canine kidney cells
MEM – Modified Eagle Medium
Metformin – N,N-Dimethylimidodicarbonimidic diamide hydrochloride
MPP^+ – 1-methyl-4-phenylpyridinium
mRNA – messenger ribonucleic acid
MTT – 3-(4,5-Dimethylthiazol-2-yl)-2,5-Diphenyltetrazolium Bromide
MYC – protein tag, EQKLISEEDL amino acids
NBMPR – nitrobenzylmercaptopurine riboside
Nigericin – (2R)-2-[(2R,3S,6R)-6-[[(2S,4R,5R,7R,9R,10R)- 2-[(2R,5S)-5-[(2R,3S,5R)-5-[(2S,3S,5R,6R)-6-Hydroxy- 6-(hydroxymethyl)-3,5-dimethyl-2-tetrahydropyranyl]-3-methyl- 2-tetrahydrofuranyl]-5-methyl-2-tetrahydrofuranyl]-9-methoxy- 2,4,10-trimethyl-1,6-dioxaspiro[4.5]decan-7-yl]methyl]-3-methyl- 2-tetrahydropyranyl]propanoic acid
NMG – N-methylglucamine gluconate
NO – nitric oxide
NOS – nitric oxide synthase
NT – nucleoside transporter
OCT – organic cation transporter
PBS – phosphate buffered saline
PCR – polymerase chain reaction
PGEsyn – prostaglandin E synthase
PGIsyn – prostaglandin I2 (prostacyclin) synthase
PK15-hENT4 – ENT4-transfected pig kidney epithelial cells derived from the PK15 cell line
PK15-NTD – nucleoside transport deficient pig kidney epithelial cells derived from the PK15 cell line

PKC – protein kinase C
PMAT – plasma membrane monoamine transporter
Quinidine – (S)-(6-Methoxyquinolin-4-yl)((2R,4S,8R)- 8-vinylquinuclidin-2-yl)methanol
RIPA – radioimmunoprecipitation assay
RNA – ribonucleic acid
Quinine – (R)-(6-Methoxyquinolin-4-yl)((2S,4S,8R)- 8-vinylquinuclidin-2-yl)methanol
RT-qPCR – Real-time quantitative polymerase chain reaction
SDS-PAGE – sodium dodecyl sulfate polyacrylamide gel electrophoresis
SEM – standard error of the mean
SERT – sodium dependent serotonin transporter
sI – simulated ischaemia
sIR – simulated ischaemia reperfusion
SLC – solute carrier family
Soluflazine – 1-Piperazineacetamide,3-(aminocarbonyl)-N-(2,6-dichlorophenyl)-4-[4-(4-fluorophenyl)-4-(3-pyridinyl)butyl]-,hydrochloride (1:2)
TC-T6000 – 2,2'-[[4,8-Bis[bis(2-methylpropyl)amino]pyrimido[5,4-d]pyrimidine-2,6-diyl]diimino]bis-ethanol
TM – transmembrane
Tph – tryptophan hydroxylase
Verapamil – α-[3-[[2-(3,4-Dimethoxyphenyl)ethyl]methylamino]propyl]-3,4-dimethoxy-α-(1-methylethyl)benzeneacetonitrile hydrochloride
V_{max} – maximum transport rate
WT – wild-type

1. Introduction

1.1 Nucleoside Transporters

Nucleoside transporters (NT) are integral membrane proteins responsible for the transport, both influx and efflux, of nucleosides and nucleobases across the plasma membrane. These nucleosides would otherwise be unable to cross the plasma membrane due to their hydrophilic nature (Aymerich *et al.*, 2005). NTs are important for cell growth and proliferation as nucleosides uptake via these transporters is integral to the nucleoside salvage pathway, involved in the synthesis of deoxyribonucleic acid (DNA), ribonucleic acid (RNA), and adenosine triphosphate (ATP). Although many cells have the ability to synthesis these nucleosides *de novo*, it would cost the cell an abundance of energy to produce. The salvage pathway is therefore important as recycling is energetically more favourable than *de novo* biosynthesis (Aymerich *et al.*, 2005). NTs are formed by two different gene families: SLC28 and SLC29 which encode for the concentrative NT (CNT) and the equilibrative NT (ENT) respectively (Dos Santos-Rodrigues *et al.*, 2014).

CNT1-3, encoded by SLC28A1-3, make up the CNT family (see Fig 1.1). CNTs are predicted to have 13-transmembrane domains, with an intracellular N-terminus and an extracellular C-terminus (Dos Santos-Rodrigues *et al.*, 2014). CNTs are known to be Na^+-dependent symporters whereby nucleosides are co-transported with Na^+. This is a secondary active transport process as substrates are moved against its concentration gradient (Young *et al.*, 2013). CNT1 is primarily expressed in epithelial cells and is known to favour pyrimidine nucleosides but is also a high affinity, low capacity transporter for adenosine (Loffler *et al.*, 2007). CNT2 favours purine nucleosides while CNT3 transports both purine and pyrimidine nucleosides (Gray *et al.*, 2004).

The ENT family is formed of ENT 1-4, and are encoded by SLC29A1-4 (see Fig 1.1 and 1.2). They are predicted to have 11-transmembrane domains, and like CNTs, have an intracellular N-terminus and an extracellular C-terminus (Sundaram *et al.*, 2001). Unlike CNTs, however, nucleoside transport via ENTs are Na^+-independent and diffusion limited, whereby the transport of nucleosides is dependent on the concentration gradient of the substrate across the plasma

membrane. All ENTs are capable of transporting adenosine but differ in their ability to transport other nucleosides and nucleobases.

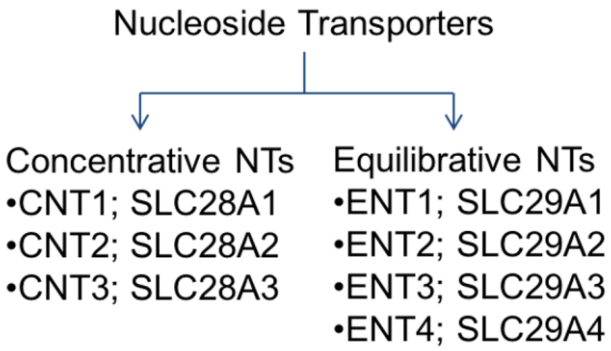

Figure 1.1. Nucleoside Transporters; CNTs and ENTs

The 2 main families of transporters involved in the transport of nucleosides. Na^+-dependent concentrative nucleoside transporter (CNT) 1-3 and Na^+-independent equilibrative nucleoside transporter (ENT) 1-4.

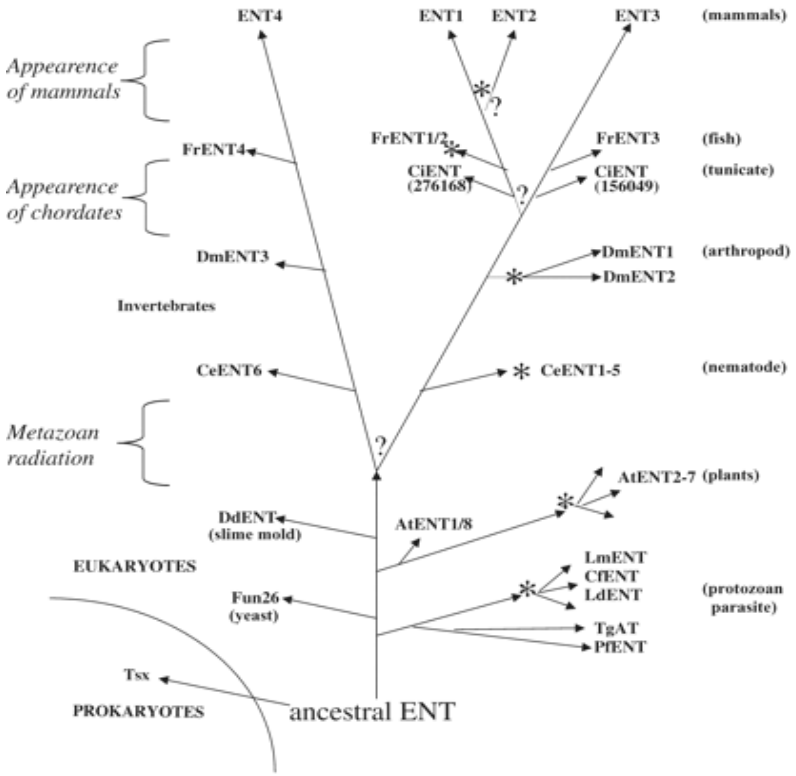

Figure 1.2. Evolutionary history of the ENTs

Asterisks indicate putative taxon-specific gene duplication events leading to ENT paralogs; question marks indicate putative gene or genome duplication events leading to new ENT lineage. Length of branches do not imply any time frame (Acimovic *et al.*, 2002). Re-print permission from Oxford University Press, License Number: 4553181191083.

Before the completion of the human genome project, ENT1 and 2 were the two transporters functionally identified as *es* (nitrobenzylthioinosine [NBMPR]-sensitive) and *ei* (NBMPR-insensitive), respectively. The former corresponds to ENT1 which is inhibited by NBMPR at nanomolar concentrations whilst the latter corresponds to ENT2 and is not inhibited by NBMPR at nanomolar concentrations (although it is at micromolar concentrations) (Ward *et al.*, 2000). Similarly, ENT1 was found to be more sensitive to inhibition by coronary vasodilators, including dipyridamole (DY) and dilazep (Ward *et al.*, 2000; Visser *et al.*, 2002). ENT1 and 2 are expressed in a wide range of tissues, including the vasculature and the heart (Crawford *et al.*, 1998; Archer *et al.*, 2004). ENT1 is known to transport a wide range of nucleosides, with the highest affinity for adenosine amongst the ENTs, at a K_m of 40 μM (Ward *et al.*, 2000). Although ENT2 has a lower affinity for both purine and pyrimidine nucleosides than ENT1 and is normally overshadowed by ENT1 activity, it has a higher affinity for inosine and hypoxanthine, suggesting that it has a function distinct from ENT1 (Ward *et al.*, 2000). ENT2 was also reported to be highly expressed in skeletal muscle and thus suggested to play an important role in muscle recovery after exercise (Crawford *et al.*, 1998). The N-terminus half of ENT1/2, transmembrane (TM) 1-6, was implicated in nucleoside, nucleobase, NBMPR, and coronary vasodilators binding (Yao *et al.*, 2001; SenGupta *et al.*, 2002; Visser *et al.*, 2002; Yao *et al.*, 2002; Endres *et al.*, 2005).

ENT1 and 2 are also used for the transport of anti-cancer and anti-viral nucleoside analogue drugs into the cells (Young *et al.*, 2013). Similar to endogenous nucleosides, these nucleoside analogue drugs are hydrophilic. Without ENT1 or 2, these drugs would be unable to cross the plasma membrane and reach their site of action to exert their therapeutic effects.

ENT3 was found to be unique whereby it is mainly expressed in intracellular vesicles (Baldwin *et al.*, 2005), and for that reason, has not been as extensively studied as ENT1 or 2. The long N-terminus hydrophilic motif that is responsible for its localisation to intracellular vesicles was mutated in a study to direct trafficking of ENT3 to the plasma membrane, allowing its physiological and pharmacological functions to be studied (Baldwin *et al.*, 2005). It was found to be weakly inhibited by NBMPR and coronary vasodilators such as DY and dilazep. Like ENT1 and

2, it has a broad selectivity for nucleosides, and is also able to transport adenine but not hypoxanthine (Baldwin *et al.*, 2005). Interestingly, ENT3 was reported to have a unique pH-dependent transport, with optimal activity at pH 5.5 (Baldwin *et al.*, 2005). Mutations in ENT3 are known to be associated with a range of human disease including the H syndrome and pigmented hypertrichotic dermatosis with insulin-dependent diabetes syndrome (Kang *et al.*, 2010) and pigmentary hypertrichosis; and non-autoimmune insulin dependent diabetes mellitus (Riachi *et al.*, 2019).

1.2 Fourth Member of the Equilibrative Nucleoside Transporter family – ENT4

ENT4, the last member of the family, was found initially to not transport nucleosides at physiological pH (Engel *et al.*, 2004), and for this reason, it was not identified as an ENT member until later. ENT4 is likely to have diverged much earlier on the evolutionary scale and became more distinct from ENT1 – 3 (Acimovic *et al.*, 2002) (see Fig 1.2.). It was shown to transport monoamines instead (mainly serotonin and dopamine), and thus was identified as the plasma membrane monoamine transporter (PMAT) (Engel *et al.*, 2004). Unlike the ubiquitous expression of ENT1, ENT4 was found to be mainly expressed in the brain, cardiomyocytes, vascular endothelial cells and skeletal muscle (Engel *et al.*, 2004; Barnes *et al.*, 2006). It was found to be most abundant in ventricular cardiomyocytes, compared to the atrium, and is almost absent in the sinoatrial node (Barnes *et al.*, 2006).

ENT4/PMAT is a low affinity and high capacity transporter, and was suggested to be the transporter responsible for uptake$_2$ of serotonin and dopamine uptake and clearance from extra-neuronal sites (Duan *et al.*, 2010). Like ENT3, ENT4 activity demonstrated a pH sensitivity and was shown to be able to transport nucleosides, specifically adenosine, at an acidic pH, with a K_m of 0.78 and 0.13 mM for the human and mouse ENT4, respectively, in *Xenopus oocytes* (Barnes *et al.*, 2006). Although this pH sensitivity was initially reported only for adenosine, transport of other monoamine substrates was also found to be pH sensitive (Zhou *et al.*, 2010). Conversely, increasing extracellular pH to 8.2 was shown to abolish ENT4 activity (Xia *et al.*, 2007). It was also

shown that decreasing pH affects the capacity of the transporter (increased V_{max} of a substrate) but does not affect affinity (K_m values) (Xia *et al.*, 2007; Itagaki *et al.*, 2012).

The K_m for each substrate of human ENT4 is shown in Table 1.1, with the highest affinity seen for 1-methyl-4-phenylpyridinium (MPP^+), a neurotoxin causing Parkinson's-like symptoms, and almost no affinity for adrenaline (Engel *et al.*, 2004). ENT4 is unique as a nucleoside transporter in that it transports adenosine exclusively and not any other endogenous nucleosides (Zhou *et al.*, 2010). As shown in Table 1.2, ENT4 is very weakly inhibited by ENT1 inhibitors such as NBMPR and DY. It is more potently inhibited by decynium-22 (D22), with an IC_{50} of 0.1 µM, although D22 also inhibits organic cation transporter 3 (OCT3) at that concentration (Wang, 2016). Two more selective inhibitors for ENT4 are lopinavir, an HIV protease inhibitor with an IC_{50} of 1.4 µM (Duan *et al.*, 2015) and a DY analogue, TC-T 6000, with an IC_{50} of 74.4 nM (Wang *et al.*, 2013).

ENT4 activity is also affected by membrane potential whereby hyperpolarisation increases, while depolarisation decreases its activity (Engel *et al.*, 2004). Engel *et al.* showed that ENT4-mediated MPP^+ uptake in Madin-Darby Canine Kidney (MDCK) cells was significantly inhibited when performed in the presence of 131 mM KCl. To eliminate the possibility that this effect was specific to potassium, 10 mM barium was used with a normal extracellular potassium concentration as a potassium channel blocker and can greatly reduce membrane potential in MDCK cells (Paulmichl *et al.*, 1985). As the same effect was observed with barium, collectively, these data suggest that the effect of high extracellular potassium concentration on ENT4-mediated MPP^+ uptake was related to changes in membrane potential.

To better understand the function of ENT4 under physiological conditions, a mouse model lacking exons 3-7 of ENT4 has been developed (Duan *et al.*, 2013). This results in the generation of a short peptide with no ENT4 transporter activity in these mice. ENT4 KO mice were viable with no overt physiological abnormalities and no compensatory increase of other monoamine transporters in the brain (Duan *et al.*, 2013). The uptake of MPP^+, 5-HT, and dopamine, however, was significantly reduced in the brain in these ENT4 KO mice (Duan *et al.*, 2013).

Substrate	*K_m (μM)*	*V_{max} (nmol/min/mg protein; pH 7.4)*	*V_{max} (nmol/min/mg protein; pH 6.0/6.6)*	*Reference*
MPP^+	33	2.8	~4 fold higher (6.6)	(Engel *et al.*, 2004; Xia *et al.*, 2007)
Serotonin	114	6.5	~3 fold higher (6.6)	(Engel *et al.*, 2004; Zhou *et al.*, 2010)
Dopamine	329	18.2		(Engel *et al.*, 2004)
Noradrenaline	2,606	20.6		(Engel *et al.*, 2004)
Adrenaline	15,323	38.4		(Engel *et al.*, 2004)
Histamine	10,471	99.6	~3-4 fold higher (6.0)	(Engel *et al.*, 2005; Itagaki *et al.*, 2012)
Tetraethyl-ammonium	6593	5.8		(Engel *et al.*, 2005)
Tyramine	283	5.1		(Engel *et al.*, 2005)
Metformin	1320	16.86	~4 fold higher (6.6)	(Zhou *et al.*, 2007)
Adenosine	413	2	~2.5 fold higher (6.6)	(Zhou *et al.*, 2010)

Table 1.1. ENT4 substrates

Table listing kinetics data (K_m and V_{max}) of known hENT4 substrates. Where available, potentiation of ENT4 activity, shown by increased V_{max}, is shown. Parenthesis on the 4th column represents the pH it was tested on, pH 6.0 or pH 6.6.

Inhibitor	*IC_{50} (μM)*	*Reference*
NBMPR	11.074	(Zhou *et al.*, 2010)
Dipyridamole	5.901	(Zhou *et al.*, 2010)
Dilazep	10.236	(Zhou *et al.*, 2010)
Lopinavir	1.4	(Duan *et al.*, 2015)
TC-T 6000	0.074	(Wang *et al.*, 2013)
Decynium -22	0.1	(Engel *et al.*, 2004)
Corticosterone	450	(Engel *et al.*, 2004)
Verapamil (Ca^{2+} blocker)	18.6	(Engel *et al.*, 2005)
Quinidine (Na blocker)	25.3	(Engel *et al.*, 2005)
Quinine	26.9	(Engel *et al.*, 2005)
Rhodamine123	1.02	(Engel *et al.*, 2005)
Tryptamine (Tryptophan analogue)	62.9	(Engel *et al.*, 2005)
Pargyline (MAOB inhibitor)	77.0	(Engel *et al.*, 2005)
GBR12935 (Dopamine uptake inhibitor)	7.9	(Engel *et al.*, 2004)
Fluoxetine (SSRI inhibitor)	22.7	(Engel *et al.*, 2004)
Desipramine (NA reuptake inhibitor)	32.6	(Engel *et al.*, 2004)

Table 1.2. ENT4 inhibitors

Table listing IC_{50} of known ENT4 inhibitors. K_i values calculated using K_m values from Table 1.1. showed an almost identical value compared to the IC_{50} value.

1.3 Serotonin (5-hydroxytryptamine; 5-HT) and its role in the cardiovascular system

Modulation of ENT4 is likely to result in a therapeutic and physiological effect that is dependent on the physiological actions of its substrates. A predominant endogenous substrate transported by ENT4 is serotonin (5-hydroxytryptamine; 5-HT), which is largely known for its function in the brain as a major neurotransmitter and plays a role in sleep, satiety, and mood, but also has

cardiovascular effects (Watts, 2005). Biosynthesis of 5-HT depends on the availability of a precursor amino acid, tryptophan, and the presence of the rate-limiting enzyme, tryptophan hydroxylase (Tph) (Watts, 2005). Tph transfers a hydroxyl group to the benzyl ring of tryptophan to form 5-hydroxytryptophan (5-HTP) which in turn undergoes decarboxylation to form 5-HT (Watts, 2005). Two forms of Tph exist: Tph1 and Tph2 mainly expressed in the periphery and the central nervous system (CNS) respectively (Walther *et al.*, 2003). 5-HT is inactivated by being metabolised to 5-hydroxyindole acetic acid (5-HIAA), catalysed by monoamine oxidase (MAO) (Watts, 2005). MAO is an intracellular enzyme, and therefore, 5-HT has to be taken up into the cell by its transporters (including ENT4) for it to be metabolised and inactivated. Two MAO isoforms, MAOA and MAOB, have been identified and can be classified according to their substrate specificities. MAOA is known to have a higher affinity and activity for 5-HT (Youdim *et al.*, 2006). In the periphery, it is mainly stored in platelets which constitutively take up 5-HT via the high-affinity sodium-dependent serotonin transporter (SERT) (Watts, 2005).

Seven subtypes of 5-HT receptors have been discovered: 5-HT_1–5-HT_7, with several isoforms within each subtype (see Table 1.3). All known 5-HT receptors (5-HTR) couple to a G-protein (GPCR), with the exception of 5-HT_3R which was found to be a non-selective cation channel (Watts, 2016). Of relevance, only 5-HT_{1B}R, 5-HT_{1D}R, 5-HT_{1F}R, 5-HT_{2A}R, 5-HT_{2B}R, 5-HT_3R, 5-HT_4R, and 5-HT_7R have been shown to be able to influence the cardiovascular system (Table 1.3).

Receptor	*Function*	*Second Messenger*	*Affinity (K_D;nM)*
5-HT_{1B}R	Vasoconstriction	G_i - GPCR	16.01
5-HT_{1D}R	Vasoconstriction	G_i - GPCR	10.05
5-HT_{1F}R	Vasoconstriction	G_i - GPCR	67.5
5-HT_{2A}R	Vasoconstriction Platelet aggregation	$G_{q/11}$ - GPCR	970.8
5-HT_{2B}R	Vasodilatation and Vasoconstriction Important in cardiac development, structure, and function	$G_{q/11}$ - GPCR	11.35
5-HT_3R	Bradycardia (Vagus Nerve)	Cation permeable ligand-gated ion channel	190.33
5-HT_4R	Positive inotropic, chronotropic and lusitropic effect	G_s - GPCR	117
5-HT_7R	Vasodilatation	G_s - GPCR	3.55

Table 1.3. Characteristics of 5-HT receptors

Table listing 5-HT receptors with known cardiovascular phenotype and their respective second messenger system and affinity for 5-HT. Table was adapted from Watts, 2016.

Though 5-HT clearly has effects on the cardiovascular system, the mechanism and receptors involved remain unclear. Different effects of 5-HT on the cardiovascular system have been reported in the literature. For instance, centrally administered 5-HT was reported to increase blood pressure (BP) in most studies (Sukamoto *et al.*, 1984; Dalton, 1986; Pergola *et al.*, 1991; Tsukamoto *et al.*, 2000), although another study showed a reduced BP instead (Okada *et al.*, 1994). This discrepancy might be explained by the lower dose used in the former study, consistent with the idea that since 5-HT_7R has the highest affinity for 5-HT, 5-HT will act on 5-HT_7R before acting on other receptors at higher concentrations. The negative chronotropic effect of centrally administered 5-HT, however, seems to be quite consistent (Sukamoto *et al.*, 1984; Pergola *et al.*, 1991; Okada *et al.*, 1994).

In *in-vitro* isolated vessel experiments, most papers reported a vasoconstriction phenotype in response to 5-HT administration, although a vasodilatation phenotype has also been reported by some (Watts, 2005). Therefore, one would expect a hypertensive (vasoconstrictive) phenotype when 5-HT is given *in-vivo*. This was studied by Watts and co-workers in a rat model of hypertension (Diaz *et al.*, 2008). The authors expected an exacerbated hypertension in the hypertensive rats administered 5-HT peripherally (using an osmotic mini-pump). Surprisingly, they observed a reduced BP in normotensive rats and a normalisation of the raised BP in the hypertensive rat (Diaz *et al.*, 2008), suggesting that there is an indirect action of 5-HT (rather than a direct action of 5-HT on the vasculature) that results in an overall reduction of BP.

The inconsistent reports on the actions of 5-HT are likely due to differential expression and activation of 5-HT receptors, which have different effector functions and affinities for 5-HT. It is important to note that modulation of ENT4 would be expected to affect the overall concentration of 5-HT rather than affecting specific 5-HT receptors.

1.4 Adenosine and its role in the cardiovascular system

Adenosine, also a substrate for ENT4, has a myriad of actions on the cardiovascular system (Loffler *et al.*, 2007). Therefore, an additional mechanism by which ENT4 modulators may exert therapeutic effects is via modulation of adenosine bioactivity. Adenosine can also potentially act in a paracrine and/or autocrine manner to regulate ENT4 expression and activity. For ENT1, for instance, activation of adenosine A1 receptors was shown to result in the phosphorylation of ENT1 at S281 in a protein kinase C-dependent manner, increasing ENT1-mediated adenosine uptake (Coe *et al.*, 2002; Hughes *et al.*, 2015).

Extracellular adenosine is formed from the breakdown of ATP to AMP, catalysed by ecto-apyrase (CD39), which is subsequently converted to adenosine, catalysed by the ecto-5'-nucleotidase (CD73) (Loffler *et al.*, 2007). As soon as adenosine is taken up into the cell, it is metabolised to inosine and AMP by intracellular enzymes adenosine deaminase (ADA) and adenosine kinase (ADK) respectively (Eltzschig *et al.*, 2006; Morote-Garcia *et al.*, 2008). ADA is a low affinity and

high capacity enzyme while ADK is a high affinity and low capacity enzyme. Due to the rapid metabolism of adenosine by these enzymes, it has an exceptionally short half-life ($t_{1/2}$ < 10 seconds) (Conti, 1991).

Adenosine is known as a retaliatory metabolite (Newby, 1984) as its extracellular concentration increases in response to an ischaemic insult as an attempt by the heart to limit the damage. The increase in extracellular adenosine concentration during hypoxia was attributed to an increase in CD39 and CD73, increasing the breakdown of extracellular ATP to form adenosine (Eltzschig *et al.*, 2003). The half-life of adenosine is increased up to 3-fold during hypoxia (Eltzschig *et al.*, 2005). The importance of extracellular adenosine generation was demonstrated whereby the cardioprotection conferred by adenosine was lost in CD39 or CD73 KO mice (Eckle *et al.*, 2007; Kohler *et al.*, 2007). Induction of CD39 and CD73 during hypoxia was shown to be dependent on the presence of a transcription factor, Sp1 (Eltzschig *et al.*, 2009), and hypoxia inducible factor (HIF)-1α respectively (Synnestvedt *et al.*, 2002).

Adenosine is able to act on 4 subtypes of adenosine receptors: A_1AR, A_{2A}AR, A_{2B}AR, and A_3AR. A_1AR and A_3AR couples to G_i, while A_{2A}AR and A_{2B}AR couples to G_s; each receptor is able to exert a different effect on different cells (Loffler *et al.*, 2007). By acting on these receptors, adenosine acts to re-balance the oxygen demand and supply; these actions include vasodilatation to increase supply and a negative chronotropic action to decrease demand (Young *et al.*, 2013).

Using A_1AR KO mice, A_1AR activation have been shown to be important in mediating ischaemic pre-conditioning (IPC) and protection from myocardial IRI (Lankford *et al.*, 2006). The anti-arrhythmic effect of adenosine (Blomstrom-Lundqvist *et al.*, 2003) is also a result of A_1AR-mediated bradycardia (Prystowsky *et al.*, 2003). By inhibiting cyclic adenosine monophosphate (cAMP) production, A_1AR activation results in an attenuation of the β-adrenoceptor-mediated increase in cAMP and thereby reduces cardiac oxygen demand. Catecholamines are known to have a positive chronotropic effect on the heart resulting from the activation of G_s-coupled β_1-adrenoceptors, which in turn activates the pacemaker current, voltage gated calcium channels,

and the repolarising potassium currents in the sinoatrial node (Gordan *et al.*, 2015). The same β_1-adrenoceptors-cAMP-protein kinase A (PKA) signalling pathway also accounts for the positive lusitropy and inotropy effect of catecholamines. The former depends on the phosphorylation of troponin I and sarcoendoplasmic reticulum (SR) calcium transport ATPase interacting protein, phospholamban (Cairns *et al.*, 2015). This leads to an increased dissociation rate of the calcium-troponin C complex and in the enhanced uptake of calcium into the SR respectively (Cairns *et al.*, 2015). Increased SR calcium stores also contribute to the positive inotropic effect as this creates a larger gradient and influx of calcium into the cytoplasm during systole. The phosphorylation of the L-type voltage gated calcium channels and ryanodine receptors also contributes to the increased calcium influx from extracellular sites (Bers, 2002). An increased $[Ca^{2+}]_i$ in turn leads to a positive inotropic effect.

By virtue of adenosine-A_1AR cAMP-independent activation of the inwardly rectifying K+ current (IK_{Ado}), adenosine can lead to pro-arrhythmic effects as it hastens the repolarisation phase and thus reduces action potential duration (Belardinelli *et al.*, 1995; Mahmood *et al.*, 2011). This is pro-arrhythmic as it promotes and maintains re-entry circuits that occur when some of the myocardial tissue remains excitable after the initial wave of depolarisation and is usually due to a slow conduction in that region (e.g. myocardial infarction) (Gaztanaga *et al.*, 2012). This is explained by the fact that the minimum distance a wave-front has to travel to achieve a re-entry circuit observed in arrhythmia is defined as the product of the refractory period and conduction velocity (of I_{Na}) (Wiener *et al.*, 1946). This effect is observed in supraventricular tissues as the expression of IK_{Ado} is significantly less in ventricular tissues than in atrial tissues (Belardinelli *et al.*, 1995).

Adenosine was also shown to inhibit glycolysis and improve recovery of cardiac function following ischaemia in an A_1AR-dependent manner (Finegan *et al.*, 1996). This cardioprotection was associated with the improved coupling of glycolysis to glucose oxidation, and thereby decreasing proton production in ischaemic conditions.

A_{2A}AR activation has been shown to mediate the anti-inflammatory properties of adenosine. Adenosine was shown to inhibit platelet aggregation in human and mouse blood in an A_{2A}AR-dependent manner (Hart *et al.*, 2008). Global A_{2A}AR KO mice have increased platelet aggregation and have exacerbated outcomes in models of sepsis, liver, and lung inflammation (Ledent *et al.*, 1997; Ohta *et al.*, 2001; Thiel *et al.*, 2005). Adenosine produced during a hypoxic stress was also shown to be involved in preventing the unwanted accumulation of neutrophils by acting on A_{2A}AR and A_{2B}AR (Eltzschig *et al.*, 2004). A_{2A}AR activation has also been implicated in mediating protection against myocardial infarction, indirectly, by its anti-inflammatory effects. Activation of A_{2A}AR has been suggested to inhibit T-lymphocytes, which in turn can inhibit neutrophil or monocyte recruitment in the heart (Yang *et al.*, 2005).

A_{2A}AR KO mice also have an increased BP and heart rate (HR), suggesting that A_{2A}AR has a basal role in regulating cardiovascular physiology (Ledent *et al.*, 1997). Agonism of A_{2A}AR was shown to cause vasodilatation and tachycardia (Bonizzoni *et al.*, 1995; Ledent *et al.*, 1997). While the role of A_{2A}AR in vasodilatation explains the increased BP in A_{2A}AR KO mice, one would have expected a bradycardia phenotype if A_{2A}AR is deleted. The tachycardia phenotype, however, might be due to a complex interaction of cardiovascular haemodynamics, i.e. a phenotype secondary to the increased BP, or simply a compensatory increase in expression of other AR.

Adenosine also mediates a vasodilatory effect through A_{2A}AR. This action was shown to be dependent, in part, on the presence of the endothelium and nitric oxide (NO) both in an isolated vessel study and in humans (Abebe *et al.*, 1995; Smits *et al.*, 1995). By acting on the G_s-coupled A_{2A}AR in vascular smooth muscle cells (VSMC), cAMP and PKA production is increased. PKA, in turn, can phosphorylate myosin light chain kinase (Hathaway *et al.*, 1985). This leads to decreased myosin phosphorylation and contraction of VSMC, and therefore reduced contraction.

Clinically, intravenous adenosine is used to produce maximal coronary hyperaemia (Pijls *et al.*, 2011). It has been shown that adenosine affects small vessels (≤150 μm in diameter) more significantly than larger vessels (>150 μm in diameter) in the coronary vasculature (Kanatsuka *et*

al., 1989). Since micro-vessels account for majority of the total resistance in the vasculature (Chilian *et al.*, 1989), this suggests that adenosine can be very effective in increasing blood flow and reducing blood pressure when needed. A_{2A}AR activation has also been suggested to lead to inhibition of vascular smooth muscle cell proliferation, and thus limit the vascular remodelling seen in vascular diseases such as hypertension (Dubey *et al.*, 1996).

A_{2B}AR is a low affinity adenosine receptor with an EC_{50} of 24 μM, as opposed to an EC_{50} in the nM range like the other adenosine receptor subtypes (Fredholm *et al.*, 2001). This suggests that A_{2B}AR plays a more important role during pathophysiological conditions such as during hypoxia where the extracellular concentration of adenosine is markedly raised. Indeed, IPC-conferred cardioprotection was completely abolished in A_{2B}AR KO mice, while A_1AR KO, A_{2A}AR KO, and A_3AR KO only demonstrated an attenuation (Eckle *et al.*, 2007). This suggests that A_{2B}AR activation is likely to mediate IPC directly and that the cardio-protection afforded by the other receptor subtypes maybe due to an indirect mechanism. The protection against IRI in the intestine was also suggested to be mediated by A_{2B}AR (Hart *et al.*, 2009), suggesting that it is not cardiac-specific. Hypoxia was also shown to induce an increase in A_{2B}AR expression, specifically, in an HIF-1α dependent manner (Eltzschig *et al.*, 2003; Eckle *et al.*, 2008), further suggesting that A_{2B}AR mediates the cardioprotection afforded by adenosine during pathophysiological conditions.

A_{2B}AR activation was further suggested to be involved in enhancing barrier function and reducing endothelium permeability during hypoxia (Eltzschig *et al.*, 2003). The prominent anti-inflammatory role of A_{2B}AR was confirmed in A_{2B}AR KO mice which, basally, have elevated pro-inflammatory markers and significantly increased leukocyte adhesion in the vasculature (Yang *et al.*, 2006). It was further shown that A_{2B}AR KO mice are more susceptible to vascular injury and inflammation (Yang *et al.*, 2008). The important role of A_{2B}AR in controlling inflammation was confirmed by a separate group with a different A_{2B}AR KO mice which have increased mast cell degranulation compared to wild-type (WT) (Hua *et al.*, 2007).

A_3AR, the last member of the family, have been shown to be involved in adenosine-mediated IPC cardioprotection (Armstrong *et al.*, 1994; Chaudary *et al.*, 2004). A_3AR activation has also been implicated in mediating blood pressure by acting centrally (Stella *et al.*, 1998) and in mediating coronary vasodilatation (Hinschen *et al.*, 2003). In addition, activation of A_3AR has been shown to mediate mast cell degranulation (Jin *et al.*, 1997), suggesting that adenosine does have pro-inflammatory properties and not only anti-inflammatory and cardio-protective effects. Indeed, there are *in-vivo* studies showing that A_3AR KO are more resistant to IRI (Cerniway *et al.*, 2001; Guo *et al.*, 2001), suggesting that A_3AR can promote inflammation in the heart which, partially, mediates IRI.

Another way to limit IRI is known as post-conditioning, a term that has been coined more recently by Zhao *et al*., 2003. Rather than subjecting the organ to a repetitive cycle of ischaemia and reperfusion before the ischaemic insult as in IPC, post-conditioning involves performing this cycle of ischaemia and reperfusion after the ischaemic insult instead. Post-conditioning has been shown to be as effective as IPC in reducing infarct size but is more practical and clinically relevant than IPC (Zhao *et al.*, 2003). Similar to IPC, the beneficial effects of post-conditioning are known to be dependent on the actions of adenosine. The sub-type of receptors involved is not clear, but several different groups have implicated all of the 4 different ARs (Kin *et al.*, 2005; Philipp *et al.*, 2006; Morrison *et al.*, 2007; Xi *et al.*, 2008).

In summary, adenosine has well-established cardio-protective effects by acting on the 4 different receptors, by its direct actions on the heart and vasculature and its indirect action of limiting unwanted inflammation. It is, however, becoming clear that adenosine does have unwanted on-target cardiovascular side effects. This is either due to the direct activation of A_1AR or A_3AR which mediates the pro-arrhythmic, pro-inflammatory effect as described above, or a prolonged activation of A_{2A}AR that results in vasodilatation of micro-vessels, leading to unwanted reduced BP (hypotension).

1.5 Cardiac ischaemia-reperfusion injury: Potential implications of ENT4 and why it's a superior target compared to ENT1

Cardiac IRI remains a life-threatening injury with no effective treatments. By definition, ischaemia is a mismatch of oxygen demand of the heart and blood supply to the heart. Though the rapid restoration of blood flow will limit cardiac infarction, this reperfusion is paradoxically harmful, at least acutely (Zhao *et al.*, 2003). Amongst many other mediators, this reperfusion leads to the generation of oxygen free radicals, calcium overload, and platelet and neutrophil accumulation which are known to contribute to IRI (Verma *et al.*, 2002). Of note, it is known that ischaemia produces intracellular, and subsequently extracellular, acidification (Kawabata *et al.*, 2002). This acidification will, in part, impair recovery during reperfusion. Intracellular H^+ accumulates during ischaemia due to (1) anaerobic glycolysis which serves as the sole significant source of energy and (2) the breakdown of ATP to ADP and P_i where the attenuation of ATP breakdown was associated with a less severe intracellular acidification (Finegan *et al.*, 1996; Kawabata *et al.*, 2002; Frank *et al.*, 2012). Upon reperfusion, intracellular pH is rapidly restored to physiological levels. The sodium-hydrogen exchanger exchanges intracellular H^+ for extracellular Na^+ (Avkiran *et al.*, 2002; Frank *et al.*, 2012). The consequential increase in intracellular Na^+ activates the sodium-calcium exchanger, leading to the exchange of intracellular Na^+ for extracellular Ca^{2+}. This calcium overload is detrimental for the recovery of cardiomyocytes and can lead to the opening of mitochondrial permeability transition pore (Griffiths *et al.*, 1995).

Adenosine has been studied as a possible therapy for cardiac IRI. However, it is rapidly taken up into the cells and has a short half-life of <10 secs (Conti, 1991). Theoretically, ENT1 blockers are beneficial during an ischaemic attack by preventing the uptake of adenosine into cells, prolonging adenosine's half-life and consequently its cardioprotective actions. ENT1 blockers have been developed and extensively studied as an attempt to significantly reduce the uptake and subsequent catabolism of adenosine, increasing its half-life. The cardioprotection has been validated in a proof-of-concept study where ENT1 KO mice were resistant to cardiac IRI, with reduced infarct size (Rose *et al.*, 2010). In a small clinical study, this protection against IRI was further shown in humans treated with DY compared to controls (Riksen *et al.*, 2005).

ENT1 blockers, however, have not been successful as the same vasodilatation will be observed in both the healthy and ischaemic vessels. Instead of increasing blood flow to the ischaemic region, blood flow is further reduced as the healthy vessel 'steals' the blood. More vasodilatation in the healthy tissue will also occur, relative to the damaged tissue, as it is likely to receive more of the ENT1 blocker than the ischaemic tissue, further worsening the coronary steal effect. In addition, due to the ubiquitous expression of ENT1, cells that lack the ability to synthesise nucleosides *de novo*, such as red blood cells (Micheli *et al.*, 1983), will be adversely affected as they lack the ability to replenish intracellular nucleoside pools.

This is where ENT4 may be a superior target by utilising the known acidic environment in ischaemic tissues. ENT4 was reported to be specific for adenosine only under acidic pH (Barnes *et al.*, 2006), suggesting that it is not involved in the salvage pathway under normal physiological conditions and pH. This also means that it will be site-specific, acting mainly on the ischaemic tissues, and as opposed to healthy (non-acidic) tissues, and devoid of the coronary steal phenomena associated with ENT1 blockers.

As ENT4 affinity for adenosine is relatively low compared to ENT1, it is also less likely to be involved in the transport of nucleoside analogue drugs at therapeutic concentrations and consequently, the efficacy of anti-cancer and anti-viral chemotherapy drugs. Though it may not play a significant role in adenosine metabolism, even during an ischaemic insult for the above-mentioned reason, local adenosine concentrations in cardiomyocytes and the interstitial spaces of ischaemic tissues are significantly higher compared to basal levels. Extracellular adenosine concentration was estimated to be as high as 30 µM under ischaemic conditions (Pedata *et al.*, 2001) and ENT4 was demonstrated to be capable of mediating adenosine transport at 1 µM (Zhou *et al.*, 2010). ENT4 also plays an important role in the re-uptake of serotonin and other monoamines into the cells, and therefore, potential side effects due to disruption of monoaminergic systems must be carefully studied.

Though the extracellular actions of adenosine are clearly beneficial for cardiac IRI, it may be as important, if not more so, to preserve intracellular adenosine pools and have better recovery of contractile function by cardiomyocytes during reperfusion. The direction of ENT4-mediated adenosine flux under pathophysiological conditions and whether the inhibition of influx or efflux is more important remains unknown at this stage.

If ENT4 mediates efflux during reperfusion, this may have significant pathological consequences during IRI. One of the deleterious aspects of IRI is the depletion of intracellular ATP pools during ischaemia. ATP is eventually metabolised to adenosine, and upon reperfusion, this intracellular adenosine is released from the ischaemic tissues. This depletion of intracellular nucleosides worsens recovery from IRI as the ischaemic tissues are required to then synthesise intracellular nucleoside (and ATP) pools *de novo*. This is opposed to simply being able to phosphorylate adenosine and make ATP, which is energetically favourable. Indeed, prevention of this loss by blocking ENT1 transporters and inhibiting ADA has been shown to enhance cellular recovery after IRI in a dog model (Abd-Elfattah *et al.*, 1994; Abd-Elfattah *et al.*, 2013). Intracellular acidification due to anaerobic glycolysis followed by subsequent extracellular acidification is a hallmark of IRI (Finegan *et al.*, 1996; Kawabata *et al.*, 2002). Therefore, ENT4 may be specifically activated under these conditions and contribute to this loss (efflux) of intracellular adenosine.

2. Research Aims and Hypothesis

The overarching hypothesis of this research project is that the inhibition of ENT4 has therapeutic benefit against cardiac IRI. Since past studies have mostly looked at ENT4 as a monoamine transporter, we wanted to better characterise the nucleoside transporter function of ENT4. Although adenosine is the physiological substrate for ENT4, a confounding factor with adenosine is that it is rapidly metabolised by ADA and ADK, and therefore, rather than measuring transport kinetics function (of ENT4), both transport function and enzymatic function of ADK and ADA would be measured, as the tritium (^{3}H) signal will be trapped intracellularly as adenosine monophosphate (AMP) or inosine monophosphate (Figure 2.1). In addition, it is not feasible to study ENT4-mediated efflux using adenosine as most of the adenosine would be metabolised to impermeable adenine nucleotides. 2-Chloroadenosine (2CADO), an ADA-resistant adenosine analogue, has been commonly used as an alternative to study other NTs and overcome the limitation observed with adenosine (Hughes *et al.*, 2015). Though ENT4 has been demonstrated to take up adenosine, it has not been investigated whether ENT4 recognises adenosine analogues.

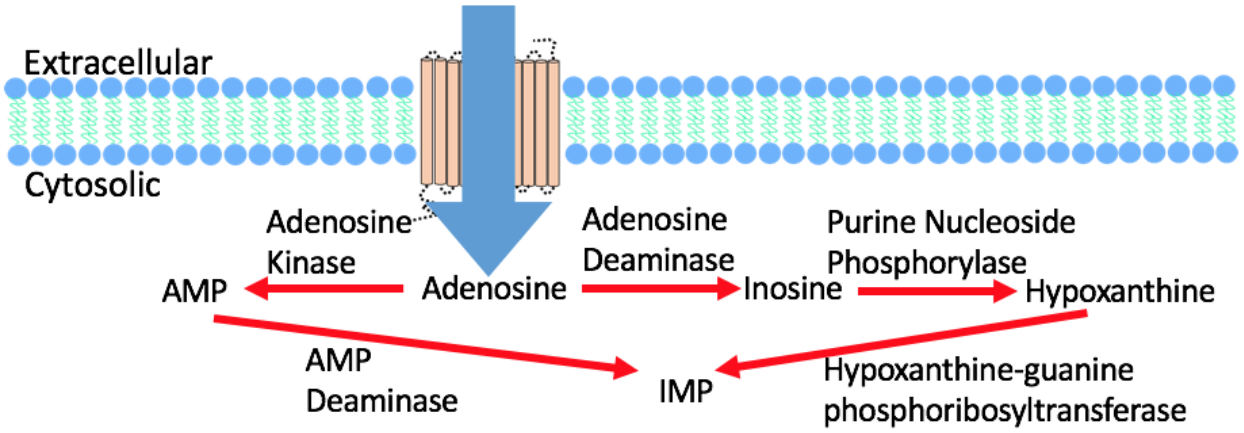

Figure 2.1. Intracellular metabolism of adenosine

Schematic diagram showing that adenosine is metabolised by their respective enzymes and eventually trapped as either adenosine monophosphate (AMP) or inosine monophosphate (IMP).

As with CNT3 where it can be coupled 1:1 proton:nucleoside, we hypothesised that ENT4 pH sensitivity depends on a proton gradient across the plasma membrane. In acute ischaemia, it is the cytosolic pH that decreases first due to the dependence on anaerobic glycolysis; and extracellular acidification of the tissue occurs with subsequent activity of the sodium-hydrogen

exchanger (NHE). Therefore, it might have important pathophysiological implications with regards to the directionality of ENT4 as a transporter if it is dependent on a proton gradient.

As adenosine has been described to be involved in IPC and mediating cardio-protection from IRI, we are going to explore how indirect regulation of adenosine via ENT4 under pathophysiological conditions might be beneficial. More specifically, we will explore its potential role in ischaemic heart disease which constitutes a significant proportion of cardiovascular diseases (Roth *et al.*, 2015). As ENT1 (Eltzschig *et al.*, 2005), ENT2 (Morote-Garcia *et al.*, 2009), and CNT2 and 3 (Medina-Pulido *et al.*, 2013) have been shown to be suppressed during hypoxia, we also hypothesise that ENT4 expression and activity changes with IRI. The role of ENT4 in cardiovascular diseases will, therefore, need to be investigated using an endogenous cardiovascular cell model *in vitro*. This will be complemented with *ex vivo* heart and mesenteric vascular bed experiments using ENT4 KO and control animals which are being performed in collaboration with Drs. Plane and Lopaschuk. They will be subjected to global no-flow ischaemia (20 min) and reperfusion (30 min), and have their functional recovery assessed.

To this end, we aimed to investigate whether:

1. 2CADO is a substrate for ENT4
2. ENT4 is capable of mediating nucleoside efflux, and how pH affects this efflux
3. ENT4 acidic pH sensitivity is dependent on a proton gradient across the plasma membrane
4. intracellular acidification affects ENT4 activity
5. ENT4 activity and/or expression changes with ischaemia-reperfusion injury
6. there are compensatory changes in ENT4 KO mice, with regards to expression of purinergic and serotonergic related genes in the heart and mesenteric vessels

3. Materials and Methods

3.1 Plasmid construction and transfection and cell culture

The DNA sequence corresponding to the coding region of SLC29A4 (NM_001040661.1) with an N-terminal myc-epitope tag was prepared by Integrated DNA Technologies (Coralville, Iowa, USA) in the pUCIDT-AMP vector (ATG**GAACAAAAACTCATCTCAGAAGAGGATCTG**GGTGGCGGAGGGGGT
GGCTCCGTGGGGAGCCAGCGCCTTGAGGAGCCCAGCGTGGCAGGCACACCAGACCCGGGCGTAGTGAT
GAGCTTCACCTTCGACAGTCACCAGCTGGAGGAGGCGGCGGAGGCGGCTCAGGGCCAGGGCCTTAGGG
CCAGGGGCGTCCCAGCTTTCACGGATACTACATTGGACGAGCCAGTGCCCGATGACCGTTATCACGCCAT
CTACTTTGCGATGCTGCTGGCTGGCGTGGGCTTCCTGCTGCCATACAACAGCTTCATCACGGACGTGGAC
TACCTGCATCACAAGTACCCAGGGACCTCCATCGTGTTTGACATGAGCCTCACCTACATCTTGGTGGCACT
GGCAGCTGTCCTCCTGAACAACGTCCTGGTGGAGAGACTGACCCTGCACACCAGGATCACCGCAGGCTA
CCTCTTAGCCTTGGGCCCTCTCCTTTTTATCAGCATCTGCGACGTGTGGCTGCAGCTCTTCTCTCGGGACC
AGGCCTACGCCATCAACCTGGCCGCTGTGGGCACCGTGGCCTTCGGCTGCACAGTGCAGCAATCCAGCT
TCTACGGGTACACGGGGATGCTGCCCAAGCGGTACACGCAGGGGGTGATGACCGGGGAGAGCACGGC
GGGCGTGATGATCTCTCTGAGCCGCATCCTCACGAAGCTGCTGCTGCCCGACGAGCGCGCCAGCACGCT
CATCTTCTTCCTGGTGTCGGTGGCGCTGGAGCTGCTGTGTTTCCTGCTGCACCTGTTAGTGCGGCGCAGC
CGCTTCGTGCTCTTCTATACCACACGGCCGCGTGACAGCCACCGGGGCAGGCCAGGCCTGGGCAGGGGC
TATGGCTACCGCGTGCACCACGACGTTGTCGCCGGGGACGTCCACTTCGAGCACCCAGCCCCGGCCCTG
GCCCCCAACGAGTCCCCAAAGGACAGCCCAGCCCACGAGGTGACCGGCAGCGGCGGGGCCTACATGCG
CTTTGATGTGCCGCGGCCAAGGGTCCAGCGCAGCTGGCCCACCTTCAGAGCCCTGTTACTGCACCGCTAC
GTGGTGGCGCGGGTGATCTGGGCCGACATGCTCTCCATCGCCGTGACCTACTTCATCACGCTGTGCCTGT
TCCCCGGCCTCGAGTCTGAGATCCGCCACTGCATCCTGGGCGAGTGGCTGCCCATCCTCATCATGGCTGT
GTTCAACCTGTCAGACTTCGTGGGCAAGATCCTGGCAGCCCTGCCCGTGGACTGGCGGGGCACCCACCT
GCTGGCCTGCTCCTGCCTGCGTGTGGTCTTCATCCCCCTCTTCATCCTGTGCGTCTACCCCAGCGGCATGC
CCGCCCTCCGTCACCCCGCCTGGCCCTGCATCTTCTCACTGCTCATGGGCATCAGCAACGGCTACTTCGGC
AGCGTGCCCATGATCCTGGCGGCAGGCAAAGTGAGCCCCAAGCAGCGGGAGCTGGCAGGGAACACCAT
GACCGTGTCCTACATGTCAGGGCTGACGCTGGGGTCCGCCGTGGCCTACTGCACCTACAGCCTCACCCGC
GACGCTCACGGCAGCTGCCTGCACGCCTCCACCGCCAATGGTTCCATCCTCGCAGGCCTCTGA; bold represents Myc-epitope tag and underline represents glycine linker). This construct was

transferred to pcDNA3.1 using the restriction enzymes XbaI (5') and HindIII (3'). The pcDNA3.1 construct was propagated in E. Coli DH5α, extracted using the QIAprep Spin Miniprep Kit (Qiagen, Canada) and sequenced in the Alberta Transplant Applied Genomics Centre, Canada, to confirm identity, using the primers 5'-CCC AAG CTT GGC TCC GTG GGG AGC C-3' (forward) and 5'-GCT CTA GAT CAG AGG CCT GCG AGG ATG-3' (reverse).

Approximately 1×10^6 pig kidney epithelial nucleoside transporter deficient cells (PK15-NTD) were grown in minimum essential media (MEM), containing no antibiotics, and were seeded into 16 well plates. The next day, 1.6 µg plasmid DNA and 4.8 µL LipofectAMINE 2000 (optimised ratio of 1:3) were each diluted into 100 µL Opti-MEM I Reduced Serum Medium and incubated at room temperature (~22°C) for 5 min. The mixtures were combined and incubated for an additional 20 min, then added to the PK15-NTD cells. After 24–48 hr incubation, the media was replaced with MEM supplemented with sodium pyruvate (1 mM), non-essential amino acids (0.1 mM), penicillin (100 U/mL), streptomycin (100 µg/mL), 10% fetal bovine serum (FBS), 50 µg/mL nystatin, and 0.5 mg/mL G418. Selection pressure was maintained for 3 weeks, after which surviving cells were moved to 6 well plates with MEM supplemented as above but containing 0.3 mg/mL G418 to maintain selection pressure. Individual colonies (derived from a single cell) were allowed to proliferate to ~300 cells before being isolated using cloning cylinders and transferred to new 6 well plates. Expression of the myc-SLC29A4 was confirmed by PCR analysis and hENT4 protein expression by immunoblotting. PK15-NTD cells were kept at 37^{o}C in a humidified incubator with 5% CO_2 and 95% room air, and grown in the supplemented MEM media, as above but without G418.

Human embryonic kidney 293 cells (HEK-293) and HEK293 cells with ENT2 deletion by CRISPR/Cas9 system (HEK-293 ENT2-KO) were cultured in Dulbecco's Modified Eagle Medium (DMEM) supplemented with sodium pyruvate (1 mM), penicillin (100 U/mL), streptomycin (100 µg/mL), 5% calf serum, 5% FBS, and amphotericin B (500 ng/mL).

Immortalised human dermal microvascular endothelial cells (HMEC-1) were grown in MCDB131 (Corning, Cellgro, Canada), supplemented with epidermal growth factor (EGF) (10 ng/mL), hydrocortisone (1 μg/mL), HEPES (2 mM), L-glutamine (20 mM), penicillin (100 U/mL), streptomycin (100 μg/mL), 10% FBS, and amphotericin B (500 ng/mL).

Immortalised murine HL-1 cardiomyocytes were cultured in Claycomb Media (Sigma, Canada) supplemented with penicillin (100 U/mL), streptomycin (100 μg/mL), 10% FBS, noradrenaline (0.1 mM) and L-Glutamine (2 mM) (Claycomb *et al.*, 1998).

3.2 Immunoblot analysis

Samples were prepared in radioimmunoprecipitation assay (RIPA) buffer (150 mM NaCl, 50 mM Tris, 1% NP-40, 0.5% sodium deoxycholate, and 1% SDS) containing a cocktail of protease inhibitors (MilliporeSigma, Canada, catalogue no: P8340). Samples were adjusted to 2% (v/v) β-mercaptoethanol, and then resolved by sodium dodecyl sulfate–polyacrylamide gel electrophoresis (SDS-PAGE) on 12.5% (w/v) acrylamide gels. Proteins were electro-transferred onto Immobilon-P polyvinylidene difluoride (PVDF) membranes (Millipore Corporation, USA) for 1.5 hr at a constant current of 280 mA. After transfer, membranes were rinsed in Tris-buffered saline (TBS; 0.15 M NaCl, 50 mM Tris, pH 7.5) and incubated with TBS containing 0.2% (v/v) Tween-20 and 5% (w/v) skim milk powder for 1 hr at room temperature (~22°C), with gentle rocking to block nonspecific binding. Membranes were then incubated for 16 hr at 4°C, with gentle rocking, in the presence of either mouse anti-Myc (Clone 4A6, 05-724, Lot #2585792; EMD Millipore, Canada) or mouse anti-glyceraldehyde-3-phosphate dehydrogenase (GAPDH) (v-18, sc-20357, Lot #B2113; Santa Cruz Biotechnology, Canada) at 1:1000 and 1:500 dilutions, respectively, in TBS containing 0.2% (v/v) Tween-20 and 1% (w/v) skim milk. After successive washes with TBS (+0.2% Tween-20/1% skim milk), the membranes were incubated with a 1:3000 dilution of the appropriate HRP-conjugated secondary antibody (Donkey anti-goat IgG-HRP, sc-2020, Lot #A1013, or m-IgGk BP-HRP, sc-516102, Lot #F1016, both from Santa Cruz Biotechnology, Canada) in TBS (+0.2% Tween-20/1% skim milk), for 1 hr at room temperature (~22°C) and further washed with TBS containing 0.2% (v/v) Tween-20. Proteins were detected using ECL western blot

substrate (EMD Millipore, Canada) and visualised using a ChemiDoc™ XRS + System (Bio-Rad Laboratories, Canada).

3.3 [^{3}H] substrate uptake

Cells were plated in a 6-well plate and allowed to grow for 2 days. Upon reaching 80-90% confluency, culture media was removed and cells washed with phosphate buffered saline (PBS; 137 mM NaCl, 2.7 mM KCl, 10 mM Na_2HPO_4, 1.8 mM KH_2PO_4, pH 7.4) twice and then incubated at room temperature (~22°C) in transport buffer (120 mM NaCl, 20 mM Tris, 3 mM K_2HPO_4, 10 mM glucose, 1 mM $CaCl_2$, 1 mM $MgCl_2$, pH 7.5) for 15 minutes. Uptake was initiated by exposing the cells to 10-100 µM [^{3}H] substrate in transport buffer, pH 6.0 or 7.5, for up to 15 minutes. Uptake was terminated by aspirating the uptake mixture and washing the cells 3 times with ice-cold PBS (~4°C). Cells were digested in 1N sodium hydroxide overnight at room temperature (~22°C), and radioactive content of each sample was measured using liquid scintillation techniques. Protein content of each sample was also measured and used for intra- and inter-assay normalisation. For the sodium-free experiments, they were performed in an NMG^+ buffer (140 mM NMG^+, 5 mM KCl, 4.2 mM $KHCO_3$, 0.36 mM K_2HPO_4, 0.44 mM KH_2PO_4, 10 mM HEPES, 0.5 mM $MgCl_2$, 1.3 mM $CaCl_2$, pH 7.5) instead of PBS and transport buffer. To estimate initial rate of uptake, accumulation of [^{3}H] 2-chloroadenosine at varying concentrations at 4 minutes was measured. hENT4-mediated uptake was defined as the difference between total uptake by the PK15-hENT4 cells (at pH 6.0 or 7.5) and that measured using the PK15-NTD cells (at the corresponding pH). Acidic pH-sensitive uptake was defined as the difference between total uptake by PK15-hENT4 cells at pH 6.0 and that measured at pH 7.5.

[^{3}H] Adenosine studies were performed in the presence of 100 nM EHNA [erythro-9-(2-hydroxy-3-nonyl)adenine] and 50 nM ABT-702 to minimise intracellular metabolism by adenosine deaminse and adenosine kinase respectively. 50 nM ABT-702 was also included in [^{3}H] 2CADO studies to minimise substrate metabolism by adenosine kinase.

[^{3}H] 5-HT studies were performed in the presence of 50 µM 2-PCPA (tranylcypromine hydrochloride) to minimise 5-HT intracellular metabolism by MAO and 20 µM corticosterone and 50 µM clomipramine to suppress endogenous 5-HT uptake by OCT3 and SERT, respectively.

For the inhibitor studies, cells were either pre-incubated with 2 µM D22 and 1 µM TC-T6000 for 15 minutes or given at the same time as [^{3}H]2CADO. MPP^+ and uridine were given competitively together with [^{3}H]2CADO.

To clamp intracellular pH to that of the extracellular surface, nigericin (10 µM), a proton and potassium ionophore, was used. Uptake was assessed as above, but in a high KCl transport buffer (120 mM NaCl was replaced with 120 mM KCl) at both pH 6.0 and 7.5. As nigericin is also a potassium ionophore, a high KCl transport buffer was used to match the physiological intracellular potassium concentration.

3.4 [^{3}H] 2-chloroadenosine efflux

Cells in 6-well plates were loaded with 30 µM [^{3}H]2CADO in transport buffer, at pH 6.0, for 12 min in the presence of 50 nM ABT-702 (concentrations and optimum loading times determined from the substrate uptake experiments) at room temperature (~22°C). After loading, cells were washed with ice-cold PBS 3 times (~4°C), and efflux initiated by adding room temperature (~22°C) substrate-free buffer (800 µL), pH 6.0, 7.5 or 8.2 (± D22 and TC-T6000) to the plates. After a defined incubation time, 500 µL of the extracellular media was removed and assessed for [^{3}H] content using liquid scintillation techniques. Background (t=0) [^{3}H] levels were estimated by adding room temperature (~22°C) substrate-free buffer to wells containing pre-loaded cells and then immediately (within 10 s) removing the extracellular media for analysis of [^{3}H] content. Cell protein content of each well was also measured and used for assay normalisation as described for the [^{3}H] substrate uptake assays.

3.5 Intracellular acidification by NH_4Cl

To study the effects of intracellular acidification on ENT4 activity, we employed the use of NH_4Cl (Amith *et al.*, 2016). Cells were pre-incubated with transport buffer and NH_4Cl or NMG^+ buffer (120 mM NaCl buffer replaced with 50 mM NH_4Cl or NMG^+ and 70 mM NaCl), pH 7.5, for a total of 15 minutes (11, 7, 3 minutes in transport buffer and 4, 8, 12 minutes in 50 mM NH_4Cl or NMG^+ buffer) at room temperature (~22°C). Uptake was subsequently performed as above in standard transport buffer, pH 6.0 or 7.5.

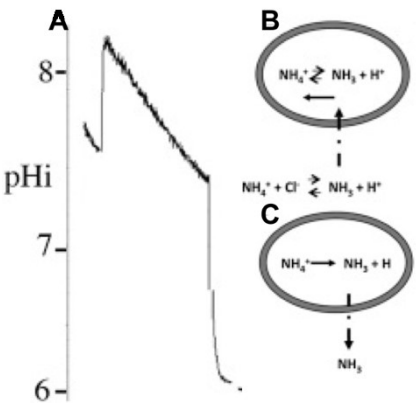

Figure 3.1. Changes in intracellular pH (pHi) in response to acid loading induced by ammonium chloride

A: A representative trace of how intracellular pH changes during an acid load is shown. B: During acid load with NH_4Cl, an initial alkalinisation was observed as uncharged NH_3, which is more permeable than the other cations, diffuses into the cell and associates with H^+. C: Following removal of extracellular NH_4Cl, NH_3 diffuses out, shifting the equilibrium to produce H^+ and therefore acidification. Image taken and modified from Amith *et al.*, 2016

3.6 Intracellular pH (pH_i) measurement

pHi was measured using a PTI Deltascan spectrofluorometer (Amith *et al.*, 2016). Cells were grown on glass coverslips (Thomas® RedLabel® Micro Cover Glasses) to ~90% confluency. Cells were loaded with BCECF-AM (20,70-bis(2-carboxyethyl)-5(6) carboxyfluorescein-acetoxymethyl ester) (Molecular Probes Inc., Eugene, OR, USA) at a final concentration of 2.5 µg/mL (1 µL of 1 mg/mL stock in DMSO in 400 µL serum-free culture media at 37°C for approximately 20 minutes). The AM group is de-esterified during this incubation, trapping BECEF within the cell. A dual excitation (440 and 502.5 nm), single emission (528.7 nm) ratio ensures that measurement is independent of cell number or amount of BECEF inside the cells. After loading, the coverslip was transferred to a cuvette holder in transport buffer, pH 7.5, with constant stirring by a magnetic stir bar at room temperature for 15 minutes. Following which, incubation times and conditions used for transport kinetic assays were applied to determine how pHi changes during uptake at the different extracellular pH conditions used (6.0, 7.5, 8.2). For each experiment, a three-point pH

calibration curve was made with a high KCl transporter Buffer (120 mM NaCl was replaced by 120 mM KCl) and 10 µM nigericin.

3.7 $DiBAC_4(3)$ membrane potential sensitive dye

Approximately $2x10^5$ PK15-hENT4 cells were seeded on a 24-well plate overnight and incubated with 2 µM $DiBAC_4(3)$ in transport buffer, pH 7.5, for 20 minutes in the dark, at 37°C. For experiments using NH_4Cl or NMG^+, they were incubated concurrently with 2 µM $DiBAC_4(3)$. Changes in membrane potential were assessed in the presence of 30 µM 2-chloroadenosine and 50 nM ABT-702 to simulate the conditions observed in uptake assays. Changes in $DiBAC_4(3)$ fluorescence were measured every 30 seconds for 20 minutes at excitation and emission wavelength of 493 and 515nm, respectively, at 25°C. The high K^+ positive control group was carried out in 120 mM KCl transport buffer, 120 mM NaCl replaced with 120 mM KCl, pH 7.5.

3.8 Polymerase chain reaction (PCR)

RNA was extracted from Trizol stabilized cells using chloroform phase separation. Briefly, 200 µL chloroform was added per mL of Trizol, the mixture vortexed, then centrifuged at 12,000 xg for 15 minutes at 4°C. The upper phase was then transferred to a clean tube and mixed with 700 µL of isopropanol per mL of sample and centrifuged at 10,000 xg for 10 minutes at 4°C. The supernatant was discarded and the pellet washed with 1 mL of 75% ethanol (with centrifugation at 7,500 xg for 5 minutes at 4°C). This supernatant was discarded and the pellet air-dried for 5 minutes and suspended in 100 µL RNase/DNase-free water. Total RNA content and purity was determined using a Nanodrop 2000 spectrophotometer (Life Technologies Inc., Canada). First-strand complementary DNA (cDNA) was synthesised from 1 µg of total RNA using M-MLV reverse transcriptase (Invitrogen, Canada).

Hearts and mesenteric vessels were dissected from ENT4 WT and KO animals and analysed with quantitative reverse transcription PCR (RT-qPCR). Both tissues were homogenised using the TissueLyser II (Qiagen, Canada) at max speed for 4 minutes. For the hearts, 200µL chloroform was

then added and processed as above. For mesenteric vessels, the upper phase was taken and RNA extracted using the Qiagen RNeasy microkit, as per manufacturers protocol.

PCR was performed using *Taq* DNA Polymerase (ThermoFisher, Canada) and on a T100™ Thermal Cycler (Bio-Rad Laboratories, Canada). Samples were heated to 95 °C for 3 minutes, 40 cycles of 30 seconds at 95 °C, 30 seconds at 58 °C, and 60 seconds at 72 °C, followed by 72 °C for 15 minutes. Primers used are listed in Table 3.1.

RT-qPCR was performed with the PowerUp™ SYBR™ Green Master Mix (Applied Biosystems, Canada) and on a Roche Light Cycler System (Cardiovascular Research Centre, University of Alberta, Canada). Samples were heated to 50 °C for 2 minutes, 95 °C for 2 minutes, followed by 45 cycles of 15 seconds at 95 °C, and 60 seconds at 60 °C, 95 °C for 15 minutes, and a temperature ramp from 60-95 °C, for a melting curve analysis to confirm product specificity. Reaction efficiency was also assessed, with results not being accepted if the efficiency was not >90%. For HL-1 cardiomyocytes, GAPDH, β-actin and α-tubulin were used as reference gene and their geometric mean was used to calculate a normalisation index. For ENT4 KO animals, gene expression were normalised to GAPDH and analysed relative to expression in WT mice. Expression of gene of interest was calculated using the $2^{-\Delta\Delta Ct}$ method.

Gene symbol	*Primer Sequence*	*Accession number*
Gapdh (Sus scrofa)	F: CCCTTCATTGACCTCCACTAC R: CCTGCTTCACCACCTTCTT	NM_001206359.1
SLC29A4 (Homo sapiens)	F: CTGGAGCTGCTGTGTTTCCT R: CAGTAACAGGGCTCTGAAGG	NM_001040661.1
Slc29a1	F: CCACCAACAGAAACCAGTCTAT R: ACCCAATGGTAACCGTGAAG	NM_001199113.1
Slc29a2	F: ATCCTCCTCTCCATCGTATGT R: CTTGGAGGAGCTCAGCTTTAG	NM_007854.3
Slc29a4	F: CAGGGACCTCCATCGTATTTG R: TTCAACCTCTCCACCACAAC	NM_146257.2
Slc22a1	F: CAACCTCTACCTGGACTTCTTT R: CCAGATTTGATGCCGCTATTG	NM_009202.5
Slc22a2	F: GTCCTTGTCTGCTCCTCTATG R: GGCCAACCACAGCAAATAC	NM_013667.3

Slc22a3	F: CACCCTCGGGATCATTATTCTT R: TCAGGGACCACCCAGTAATA	NM_011395.2
Slc28a2	F: GATTGCCTTTCTGGCTGTATTG R: GCAGATGACCTGGAAACTGA	NM_172980.3
Slc6a4	F: CCCTCTGTTTCTCCTGTTCATC R: GCAGTAGCCCAAGATGATACTC	NM_010484.2
Htr1a	F: CTGTTTATCGCCCTGGATGT R: CGTCCTCTTGTTCACGTAGTC	NM_008308.4
Htr1b	F: CCAAAGCAGAGGAGGAGATG R: GAGCAGGGTGGGTAAATAGAAA	NM_010482.2
Htr1d	F: CGTCCTTACCACCATTCTACTC R: CCAAGATAGAAACCAGGAGGTC	NM_001285482.1
Htr1f	F: CACCACCCAGCCAACTATTTA R: CTTGTCCCATAATCCAGCTCTC	NM_008310.3
Htr2a	F: CACCATTGCGGGAAACA R: AGGAAACCCAGCAGCATATC	NM_172812.3
Htr2b	F: CCTGATACTCGCGGTGATAATAC R: CTGCTATCGCCAAGGACATTA	NM_008311.3
Htr4	F: GCCTTCTACATCCCGTTTCTC R: GCCCGTTGTAACATCTGTATCT	NM_008313.4
Htr7	F: GCAGCCAAACACAAGTTCTC R: ACACTCTTCCACCTCCTTCT	NM_008315.3
Adora1	F: CCCTCATCCTCTTCCTCTTTG R: GATGAGGATGCTGGGTTTCT	NM_001039510.2
Adora2a	F: CTCACGCAGAGTTCCATCTT R: CCGTCACCAAGCCATTGTA	NM_009630.3
Adora2b	F: CTCACACAGAGCTCCATCTTTAG R: GTCCCAGTGACCAAACCTTTA	NM_007413.4
Adora3	F: GCCATTGCTGTAGACCGATAC R: CCAGCAAAGGCCCAAGAATA	NM_009631.4
Adk	F: GATGGCCGTCATGCCTTAT R: CCTGCGTCTTTCTGGCTATT	U26589.1
Ada	F: GAGGTGTTGGAGCTGTGTAAG R: GGCTACTTCCTTCAATGGTCTC	NM_001272052.1
Maoa	F: AAGAACCACAGGGCAGATAC R: GCTGAGGAATGGGACAAGATAA	NM_173740.3
Maob	F: GGGACTACATGACAATGAAAGA R: CTCCACACTGCTTCACATAC	NM_172778.2
Tph1	F: GACCATCTTCCGAGAGCTAAAC R: CTTCCCGATAGCCACAGTATTT	NM_009414.3
Entpd1	F: TCTCTCTCCTGCAAGGCTATAA R: TCAGCATGTAGCCCAAAGTC	NM_001304721.1
Nt5e	F: GGTGTGGAAGGACTGATTGAT R: CCGCCAACAGAGAGAACTTTA	NM_011851.4

Nos1	F: AAGAGGAGAGGAAGAGCTACAA R: CAAAGTTGTCTCTGAGGTCTGG	NM_008712.3
Nos2	F: CTTTGACGCTCGGAACTGTA R: GACCTGATGTTGCCATTGTTG	NM_010927.4
Nos3	F: GGATGAGTATGATGTGGTGTCC R: CTGCAAAGCTCTCTCCATTCT	NM_008713.4
Ptgs1	F: GGATACTGGCTCTGGGAATTTG R: GTAGTCATGCGCTGAGTTGTAG	NM_008969.4
Ptgs2	F: GTGCCTGGTCTGATGATGTATG R: TGAGTCTGCTGGTTTGGAATAG	NM_011198.4
Ptgis	F: GATGGGAAACGGCTGAAGAA R: GGTCGAAATGAGTCAGCAGTAG	NM_008968.4
Ptges	F: GCAACGACATGGAGACAATCTA R: TGTGAGGACAACGAGGAAATG	NM_022415.3
Ptges2	F: CATTAGTGCCCTCAAGACCTAC R: CCTTGCCCTGGTCATTCAT	NM_133783.2
Gapdh	F: GGGTGTGAACCACGAGAAATA R: GTCATGAGCCCTTCCACAAT	NM_001289726.1
Hif1a	F: CCCATTCCTCATCCGTCAAATA R: GGCTCATAACCCATCAACTCA	NM_001313919.1
Tnf	F: GCCTCCCTCTCATCAGTTCTAT R: CACTTGGTGGTTTGCTACGA	NM_013693.3
Il6	F: CCAGAGTCCTTCAGAGAGATACA R: CCTTCTGTGACTCCAGCTTATC	NM_031168.2
Icam1	F: CTGTTTGAGCTGAGCGAGAT R: AACGAATACACGGTGATGGTAG	NM_010493.3
Nfkbib	F: AGTACCTTGACCTGCAGAATG R: GGCTGCATACAACTTCTCTACT	NM_010908.5
Parp1	F: CAGGACGAAGAGGCAGTAAAG R: GTCAATCTCGTACTCCACCAAG	NM_007415.3
Ccl2	F: CCTGGATCGGAACCAAATGA R: CCGGTCAACTTCACATTCAAAG	NM_011333.3
Transferrin	F: AGCATCATCAGTGAGGGAAAG R: CATGTCCTCCATCCAAAGTCA	NM_133977.2
Gpx1	F: TGCGAAGTGAATGGTGAGAA R: CACCGGAGACCAAATGATGTA	NM_008160.6
Catalase	F: GATGGTAACTGGGATCTTGTGG R: GTGGGTTTCTCTTCTGGCTATG	NM_009804.2
Nox2	F: GCATGCCTTTGAGTGGTTTG R: CCCAGCCAGTAAGGTAGATATTG	NM_007807.5
Actb	F: CCTTCTTGGGTATGGAATCCTG R: AGCACTGTGTTGGCATAGAG	NM_007393.5
Tuba1a	F: CTCTCTGTGGATTACGGAAAGAAG R: GGTGGTGAGGATGGAATTGTAG	NM_011653.2

Table 3.1. Primer sequences used in PCR and qPCR studies

Sequence are all written from 5' to 3' and in *Mus musculus* unless stated otherwise. F: Forward, R: Reverse.

3.9 [^{3}H]NBMPR binding

Freshly isolated hearts were homogenised in PBS (as above but with 0.5 mM $MgCl_2$ and 0.9 mM $CaCl_2$, pH 7.4) in the presence of a cocktail of protease inhibitors (P8340, Lot #126M4016V, MilliporeSigma, Canada) and centrifuged for 10,000 xg for 60 minutes at 4°C. The supernatant was discarded and the pellet was re-suspended in ~4.2 mLs PBS (as above but with 0.5 mM $MgCl_2$ and 0.9 mM $CaCl_2$, pH 7.4). Crude membranes were incubated with various concentrations of [^{3}H]NBMPR, in the presence or absence of 10 µM DY, at room temperature (~22°C). Upon reaching steady state NBMPR binding (~45 min), membranes were filtered through Whatman GF/B filters with ~10 mLs of ice-cold (~4°C) 10 mM Tris buffer (pH 7.4) twice using a 24 port Brandel Cell Harvester. The radioactive content of each filter was determined using liquid scintillation techniques. Non-specific binding was defined as residual bound radioactivity in the presence of 10 µM DY. Specific binding was defined as the difference between total binding and non-specific binding. K_D and B_{max} values were determined by fitting a one-site specific binding curve of specific [^{3}H]NBMPR binding versus [^{3}H]NBMPR free concentration using GraphPad Prism 8.1.

3.10 Simulated ischaemia-reperfusion injury (sIR)

Cells were exposed to an ischaemia-mimetic buffer (125 mM NaCl, 8 mM KCl, 1.2 mM KH_2PO_4, 1.25 mM $MgSO_4$, 1.2 mM $CaCl_2$, 6.25 mM $NaHCO_3$, 5 mM sodium lactate, 20 mM HEPES, pH 6.6) and 95% N_2, 5% CO_2 at 37^{o}C for 2-5 hours to simulate ischaemia and then replaced with culture media for 1-2 hours in a 5% CO_2, 95% room air incubator to simulate reperfusion. In our qPCR study, 10 µM TC-T6000 or dimethyl sulfoxide (DMSO) was included during simulated ischaemia and reperfusion.

3.11 MTT (3-(4,5-Dimethylthiazol-2-yl)-2,5-Diphenyltetrazolium Bromide) assay

Following sham (control) or sIR conditions, cells were incubated at 37°C with 1 mg/mL MTT in PBS (as above but with 0.5 mM $MgCl_2$ and 0.9 mM $CaCl_2$, pH 7.4) for 90 minutes to allow the formation of water insoluble formazan. MTT was aspirated and the formazan was solubilised with DMSO and absorbance was assessed with a spectrophotometer at 570 nm.

3.12 Lactate Dehydrogenase (LDH) assay

The activity of LDH in the supernatant was used as a marker of cellular injury. Cells were grown for 24 hours in a 24-well plate before undergoing sham (control) or sIR conditions. At the end of each experimental condition, ischaemia buffer or culture media was collected and LDH content assessed according to manufacturer's protocol (Thermo Scientific™ Pierce™ LDH Cytotoxicity Assay Kit). Briefly, 50 µL of the ischaemia-mimetic buffer or culture media was added to a 96-well plate. Equal volume of the reaction mixture was added into each well and incubated at room temperature (~22°C) for 30 minutes. The reaction was terminated by adding 50 µL of the stop solution. Absorbance was assessed with spectrophotometer at 490 and 680 nm. LDH activity was determined by subtracting the 680 nm absorbance value from the 490 nm absorbance value. Cells in the sham conditions were exposed to lysis buffer to quantify maximal LDH release. Data was normalised to maximal LDH conditions.

3.13 Statistical Analysis

Experiments were performed in duplicates and repeated at least five times. Data are expressed as the mean ± Standard Error of the Mean (SEM). Statistical significance was determined by Student's *t* test or one-way analysis of variance (ANOVA) plus Bonferroni *post hoc* tests, as indicated, with $P<0.05$ denoting significance. GraphPad Prism 8.1 was used to fit the data to the specified nonlinear relationships and for the statistical analyses. In all cases, kinetic data fit best statistically (F-test, $P<0.05$) to a one-phase profile (versus 2-phase association). In efflux studies, initial rates of flux were estimated by extrapolation of the fitted time course profiles to a 10 seconds time point, unless indicate otherwise.

4. Results

4.1 Characterisation of ENT4 activity as a nucleoside transporter

As ENT4 has mostly been investigated as a monoamine transporter, we wanted to further investigate ENT4 as a nucleoside transporter. Of importance, we wanted to investigate whether ENT4 is capable of mediating nucleoside efflux due to its potential implications in cardiac IRI (see section 1.5). To eliminate any confounding influences from other NTs found in endogenous cell systems, we need to study ENT4 in an isolated system such as in a cell line that does not exhibit any endogenous NT activity.

4.1.1 Expression of ENT4 in PK15 NTD cells

PK15-NTD cells have been used as a null-background model to assess the activity of recombinant ENT1 and ENT2 (Tang *et al.*, 2016). To confirm that PK15-NTD cells may be used similarly for ENT4, we investigated whether PK15-NTD cells have any residual acidic pH-sensitive uptake of [^{3}H]2CADO (Figure 4.1). Figure 4.1A shows that PK15-NTD cells exhibit a trend for an acidic pH-sensitive 2-CADO uptake over 15 minutes but did not reach statistical significance (rate constants of 0.080 ± 0.006 and 0.062 ± 0.005 min^{-1} at pH 6.0 and 7.5 respectively). This was supported by the observation that there was no difference in 2CADO uptake in the presence or absence of ENT4 inhibitor, D22, in PK15-NTD cells (Fig 4.1C). Figure 4.1B shows that PK15-NTD cells do not have any sodium-dependent 2CADO uptake over 15 minutes suggesting that CNTs will not be a confounding factor when using the PK15-NTD cells to study ENT4.

It was also shown that PK15-NTD do not express SLC29A4 mRNA (Figure 4.2A). This was supported by functional data where they also do not appear to have any acidic pH-sensitive adenosine (Figure 4.3B) or 5-HT (Figure 4.4B) uptake over 15 minutes, which would have been expected if there was endogenous ENT4.

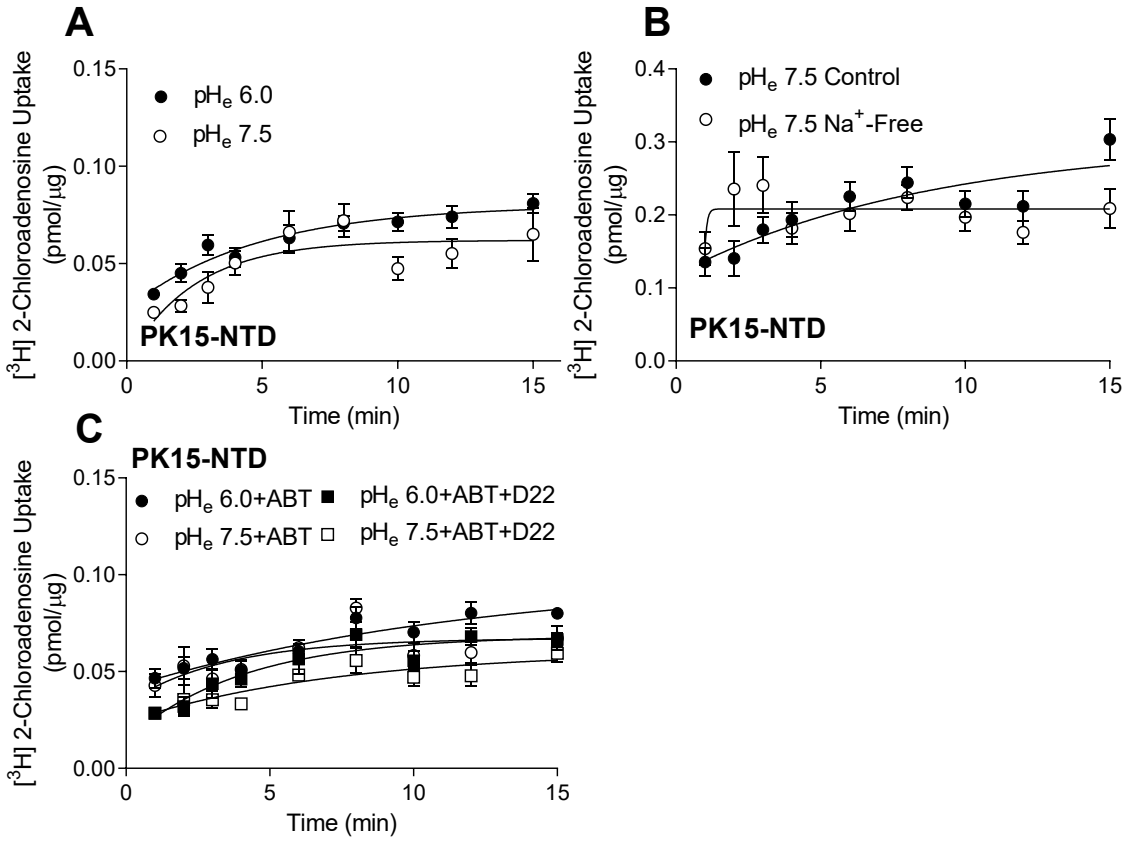

Figure 4.1. [^{3}H]2-chloroadenosine uptake in PK15-NTD cells

A: PK15-NTD cells were exposed to 30 µM [^{3}H]2-chloroadenosine for up to 15 minutes in transport buffer, extracellular pH (pH_e) 6.0 and 7.5. B: PK15-NTD cells were exposed to 100 µM [^{3}H]2-chloroadenosine for up to 15 minutes in the presence or absence of sodium. C: PK15-NTD cells were exposed to 30 µM [^{3}H]2-chloroadenosine and 50 nM ABT-702 for up to 15 minutes in transport buffer, pH 6.0 and 7.5, in the presence or absence of 10 µM D22. Results were expressed as the mean ± SEM, n=5. A one-phase association curve was fitted to these data.

4.1.2 PK15 ENT4 cells exhibit an acidic pH-sensitive 5-HT and adenosine uptake

The null-background PK15-NTD cell model was stably transfected with human SLC29A4 which resulted in the PK15-hENT4 cell line (*Accession number*: NM_001040661.1; as described in methods). The presence of SLC29A4 and the encoded ENT4 was confirmed with PCR and immunoblot analysis respectively (Figure 4.2). Human SLC29A4 transcripts were present in the transfected cell line, but not in the base cell line (Figure 4.2A). Similarly, the myc-tagged human ENT4 was present in the transfected cell line but not in the PK15-NTD cells (Figure 4.2B). An ENT4 antibody was not used due to the lack of an antibody selective for ENT4. With the ENT4 antibody (SA-18, sc101295 Lot #B1513; Santa Cruz Biotechnology, Canada), multiple bands at ~55 kDa were observed in the hearts of both WT and ENT4 KO animals (data not shown). With the monoclonal anti-SLC29A4 (data not shown; Clone 6B6, WH0222962M3, Lot #H7211-6B6; Sigma, Canada), a molecular mass of ~60 kDa was observed with a higher intensity in PK15-NTD cells (no ENT4), compared to hENT4-transfected cells.

The PK15-hENT4 cells exhibited an acidic pH-sensitive uptake of 10 µM 5-HT (Fig 4.3A) and 30 µM adenosine (Fig 4.4A) that was absent in the PK15-NTD cells (Fig 4.3B and 4.4B). Acidic pH-sensitive ENT4-mediated uptake, defined by subtracting the pH 7.5 curve from the pH 6.0 curve, was absent in PK15-NTD cells (Fig 4.3 and 4.4). Rate constants of 0.072 ± 0.040 (Fig 4.3A) and 0.019 ± 0.013 sec^{-1} (Fig 4.4A) for the acidic pH-sensitive uptake of 5-HT and adenosine, respectively, were observed in PK15-hENT4 cells. ENT4-mediated adenosine uptake also did not plateau over the 15 minute uptake period, suggesting that [^{3}H]adenosine was being metabolised intracellularly to impermeable [^{3}H]nucleotides which maintains an inward [^{3}H]adenosine concentration gradient.

Using 1 µM adenosine as a substrate, we investigated how known inhibitors of other ENT affect ENT4. Fig 4.5A shows that except for DY, which significantly inhibited ENT4 by 32 ± 5% at 1 µM, the ENT inhibitors dilazep, soluflazine, draflazine, and NBMPR affected ENT4 only at 10 µM (45 ± 13% for dilazep, 39 ± 6% for soluflazine, 60 ± 10 % for draflazine, and 45 ± 3% for NBMPR).

How D22, a known ENT4 inhibitor, affected ENT4-mediated adenosine uptake in this model was also investigated. ENT4 was significantly inhibited by 1 µM D22 (69 ± 7%; Fig 4.5B), providing further evidence that the SLC29A4-transfected PK15-NTD cells are expressing ENT4. We then wanted to investigate whether 2CADO is recognised by ENT4. Fig 4.5B shows that 2CADO is able to inhibit ENT4-mediated adenosine uptake in a concentration dependent manner (30 ± 5% at 0.1 mM, 60 ± 4% at 0.5 mM, and 68 ± 4% at 1 mM).

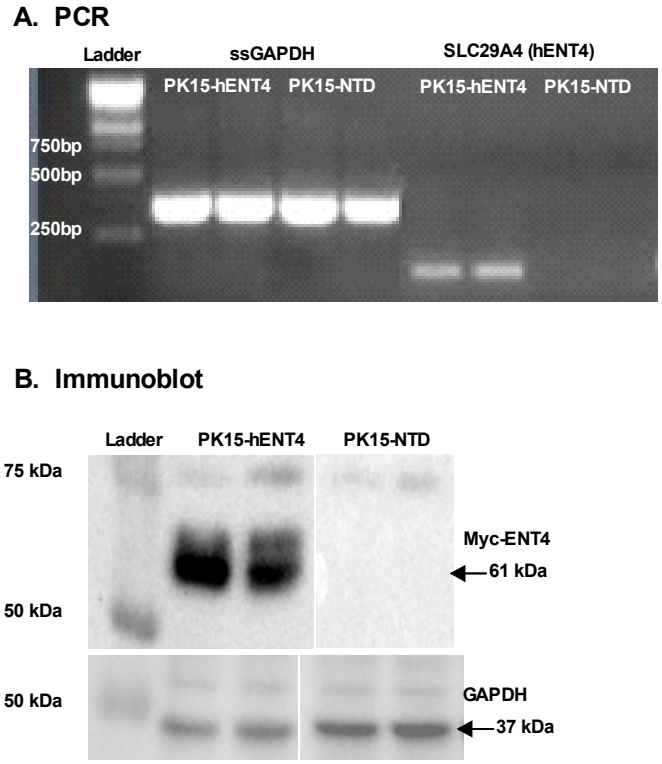

Figure 4.2. ENT4 protein expression in PK15-NTD cells and SLC29A4 transfected PK15-NTD cells.

A: cDNA prepared from total RNA isolated from PK15-NTD and hENT4 transfected PK15-NTD cells were probed for SLC29A4 transcripts. Membranes were prepared from PK15-NTD and hENT4 transfected PK15-NTD cells. B: Samples were resolved on SDS-PAGE gels, transferred to polyvinyl membranes and probed with anti-myc and anti-GAPDH antibodies to detect myc-tagged hENT4 and GAPDH (loading control), respectively. Acknowledgements: G Vilas performed the transfection of SLC29A4 into PK15-NTD cells.

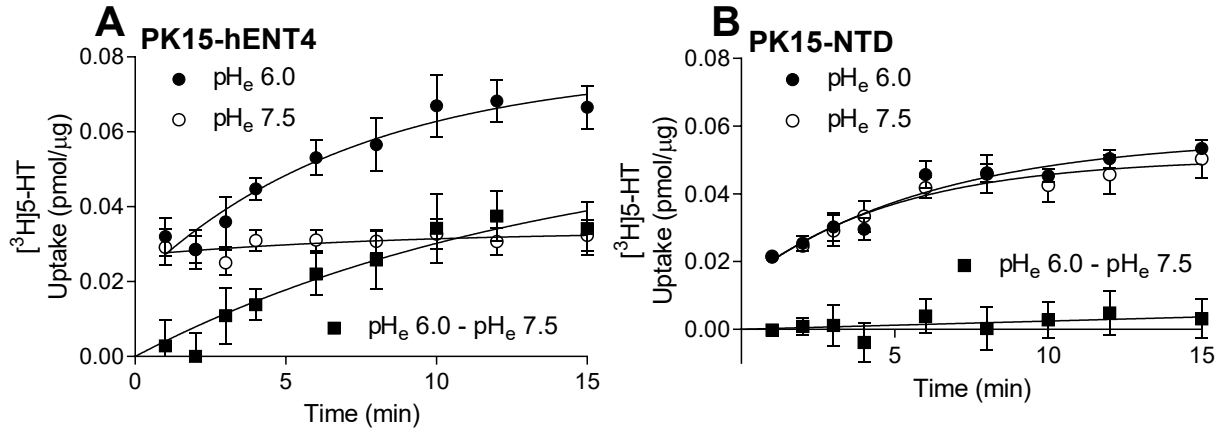

Figure 4.3. [^{3}H]5-HT uptake in ENT4 transfected PK15-NTD and untransfected PK15-NTD cells

A & B: ENT4 transfected PK15-NTD (PK15-hENT4; A) and PK15-NTD (B) cells were exposed to 10 µM [^{3}H]5-HT, 50 µM 2-PCPA, 20 µM corticosterone and 50 µM clomipramine for up to 15 minutes in transport buffer, pH_e 6.0 and 7.5. Acidic pH-sensitive uptake was obtained by subtracting the pH 7.5 curve from the pH 6.0 curve. Results are expressed as the mean ± SEM, n=5. A one-phase association curve was fitted to these data.

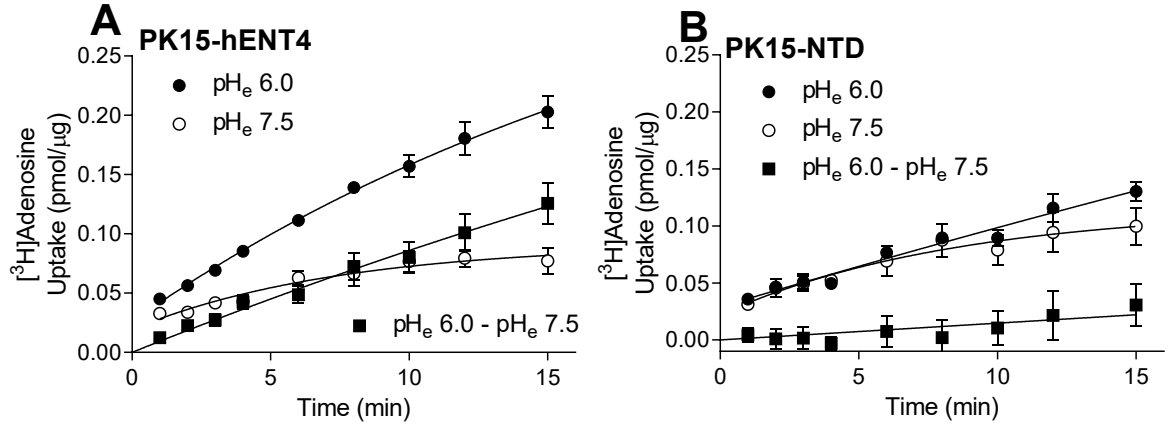

Figure 4.4. [^{3}H]Adenosine uptake in ENT4 transfected PK15-NTD and untransfected PK15-NTD cells

A & B: ENT4-transfected PK15-NTD (PK15-hENT4; A) and PK15-NTD (B) cells were exposed to 30 µM [^{3}H]adenosine, 100 nM EHNA and 50 nM ABT-702 for up to 15 minutes in transport buffer, pH_e 6.0 and 7.5. Acidic pH-sensitive uptake was obtained by subtracting the pH 7.5 curve from the pH 6.0 curve. Results are expressed as the mean ± SEM, n=5. A one-phase association curve was fitted to these data.

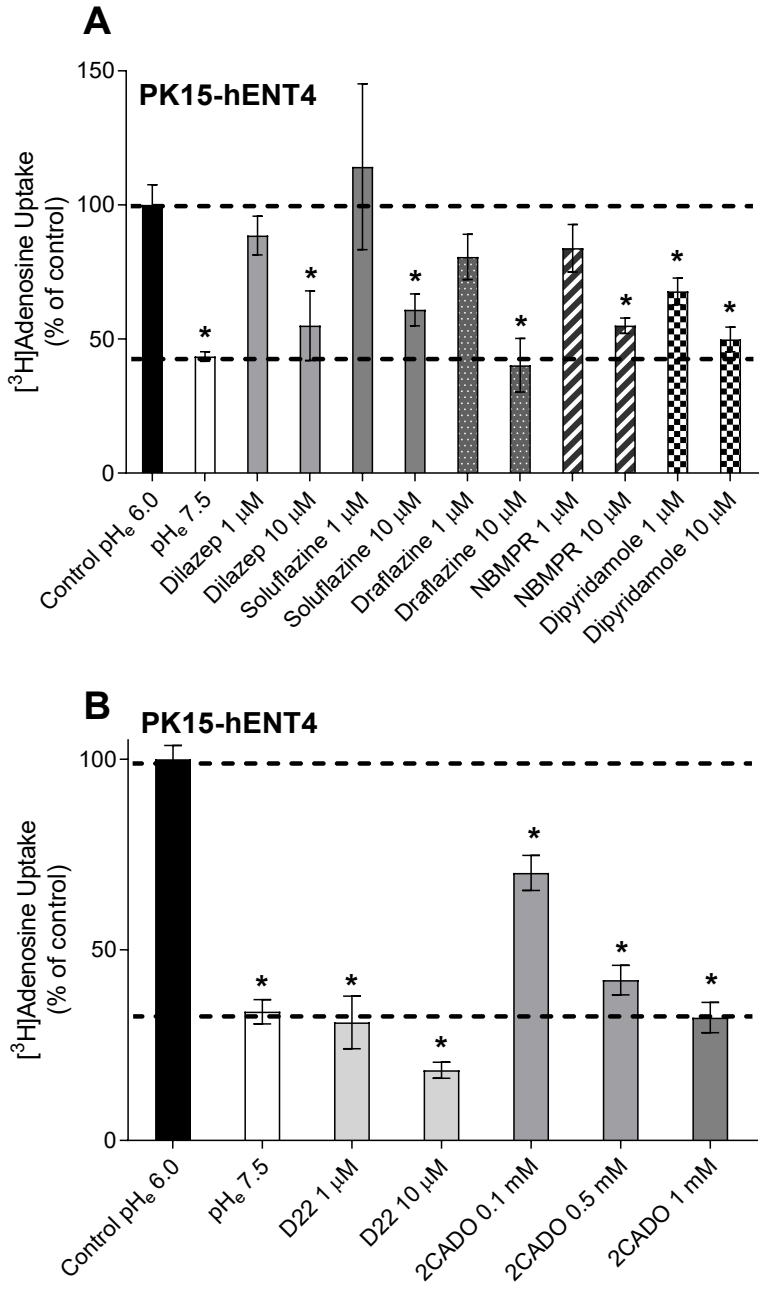

Figure 4.5. Inhibition of [^{3}H]adenosine uptake in ENT4 transfected PK15-NTD cells

A: PK15-hENT4 cells were exposed to 1 µM [^{3}H] adenosine for 6 minutes in transport buffer, pH_e 6.0 and 7.5, in the presence or absence of ENT inhibitors at the indicated concentration. B: (A) was repeated in the presence or absence of D22 and 2CADO. Results are expressed as the mean ± SEM, n=5. Dashed lines represent uptake at pH_e 6.0 (100%) and 7.5 (44 ± 2 % for A and 34 ± 3% for B). $^*p<0.05$ vs pH 6.0 as determined by one-way ANOVA plus Bonferroni *post hoc* tests. Acknowledgements: With the exception of 2CADO, which I conducted, these experiments were performed by G Vilas.

4.1.3 The adenosine analogue, 2-chloroadenosine, is a substrate for ENT4

Fig 4.6 shows that accumulation of 30 μM [^{3}H]2CADO was faster under acidic conditions compared to neutral pH with a rate constant of 0.112 ± 0.025 sec^{-1} in the PK15-hENT4 cells. The rate constant and plateau were calculated from the acidic pH-sensitive uptake curves (Fig 4.6B). Since this pH sensitivity was not observed in the PK15-NTD cells (Fig 4.1C), this suggests that this acidic pH-sensitive accumulation observed in PK15-hENT4 cells is ENT4-mediated.

Like that seen for [^{3}H]adenosine, accumulation of [^{3}H]2CADO under acidic conditions was not saturable over the 15 minute time course when done in the absence of ABT-702, an adenosine kinase inhibitor. In the presence of 50 nM ABT-702, 2CADO accumulation was saturable with a maximal accumulation that was significantly lower than in the absence of ABT-702 (0.148 ± 0.019 and 0.075 ± 0.019 pmol/μg in the absence and presence of 50 nM ABT-702 respectively; $p<0.05$ as determined by Student's t-test). ABT-702, however, had no effect on the initial rate of accumulation of [^{3}H]CADO (0.112 ± 0.025 and 0.169 ± 0.097 min^{-1} in the absence and presence of 50 nM ABT-702 respectively).

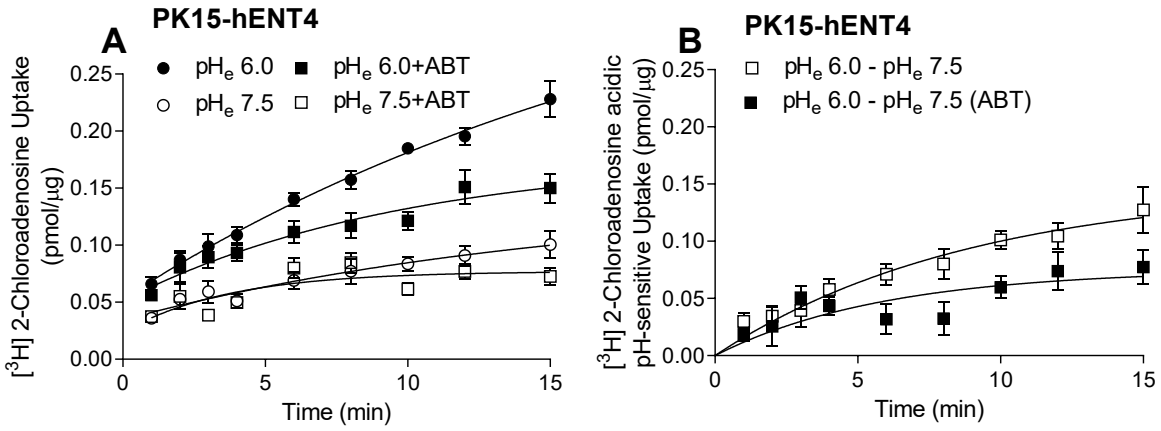

Figure 4.6. [^{3}H]2-chloroadenosine uptake in PK15-hENT4 cells

A: PK15-hENT4 were exposed to 30 µM [^{3}H]2-chloroadenosine for up to 15 minutes in transport buffer, pH_e 6.0 and 7.5, in the presence or absence of 50 nM ABT-702. B: Acidic pH-sensitive uptake was obtained by subtracting the pH_e 7.5 curve from the pH_e 6.0 curve. Results were expressed as the mean ± SEM, n=5. A one-phase association curve was fitted to these data.

The uptake of a range of concentrations of [^{3}H]2CADO up to 3 mM (aqueous solubility limit), in the presence of 50 nM ABT-702, was then assessed using a 4 minute incubation period to assess approximate initial rates of influx. 2CADO initial rates of uptake were higher under acidic conditions in the PK15-hENT4 cells, compared with that seen at neutral pH in the PK15-hENT4 cells and at both pH 6.0 and 7.5 in the PK15-NTD cells (Figure 4.7A). 2CADO accumulation by the PK15-NTD cells was linear with increasing concentrations, indicative of a non-mediated process, and there was no significant difference in uptake between pH 6.0 and 7.5 in the PK15-NTD cells. Therefore, to elucidate the total ENT4-mediated transport, rates of 2CADO influx at pH 6.0 in PK15-hENT4 cells were subtracted against pH 6.0 in PK15-NTD cells. Total ENT4-mediated 2CADO uptake demonstrated a maximum rate of transport (V_{max}) of 821 ± 161 nmol/μg/min and a K_m of 1522 ± 606 μM (Fig 4.7B).

In addition to the enhanced uptake at pH 6.0 in PK15-hENT4 cells, a greater uptake at pH 7.5 in PK15-hENT4 cells compared to PK15-NTD cells was observed, particularly when using the higher concentrations of 2CADO (>750 μM). The datasets were consequently analysed to dissect out the differences between ENT4-mediated acidic pH-sensitive (Fig 4.7C) and neutral pH-mediated (Fig 4.7D) transport. The former was analysed by subtracting the rate of 2CADO influx at pH 6.0 against pH 7.5 in PK15-hENT4 cells whilst the latter was analysed by subtracting the rate of 2CADO influx at pH 7.5 in PK15-hENT4 cells against pH 7.5 in PK15-NTD cells. Approximately half of the total uptake occurred in an acidic pH-sensitive manner with a V_{max} of 505 ± 91 nmol/μg/min (Fig 4.7C), with the other half not requiring an acidic pH with a V_{max} of 493 ± 120 nmol/μg/min (Fig 4.7D). The K_m for both transport systems were not different from one another, with K_m values of 1306 ± 471 μM and 1740 ± 752 μM, respectively. Both K_m values were also not different from the K_m of total ENT4 mediated, suggesting that it was the same transport system (ENT4).

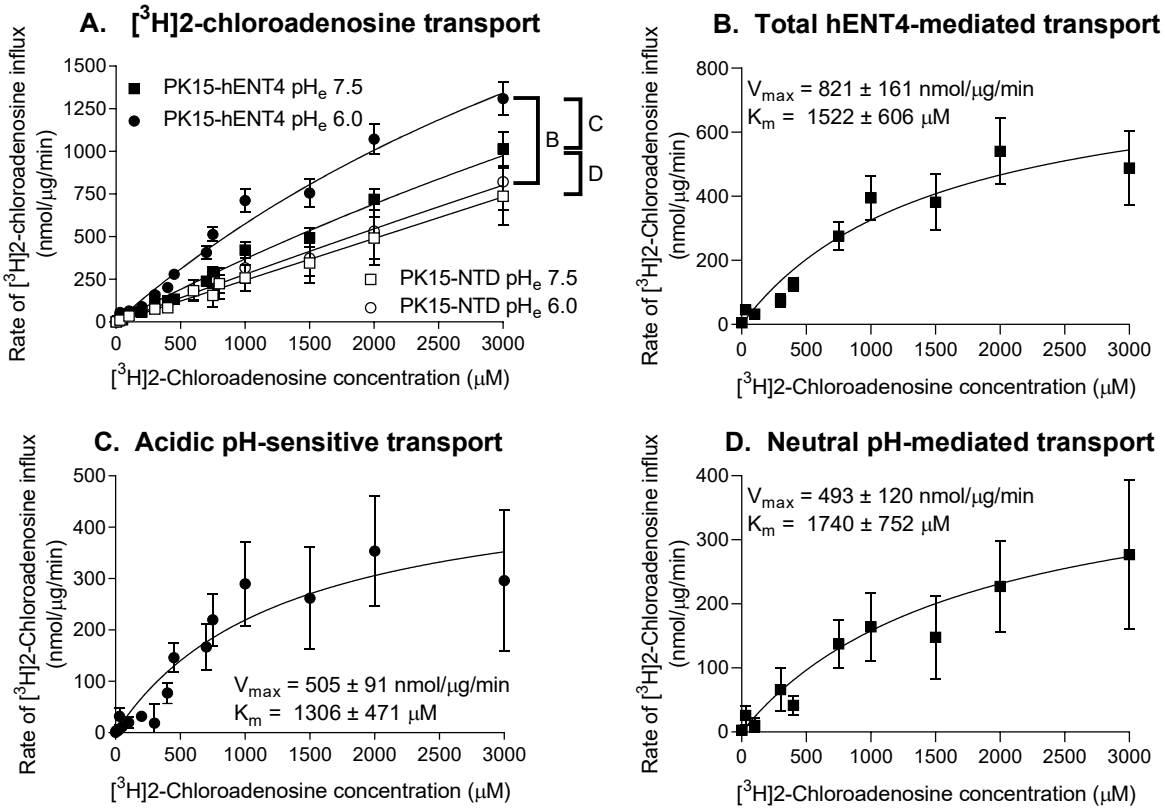

Figure 4.7. Concentration-dependence of [^{3}H]2-chloroadenosine uptake

A: PK15-NTD and PK15-hENT4 cells were exposed to increasing concentrations of [^{3}H]2-chloroadenosine for 4 minutes in transport buffer, pH_e 6.0 and 7.5, in the presence of 50 nM ABT-702. B: Total hENT4-mediated transport was obtained by subtracting the PK15-NTD pH_e 6.0 curve from the PK15-hENT4 pH_e 6.0 curve. C: Acidic pH-sensitive transport was obtained by subtracting the PK15-hENT4 pH_e 7.5 from PK15-hENT4 pH_e 6.0 curve. D: Neutral pH-mediated transport was obtained by subtracting the PK15-NTD pH_e 7.5 from PK15-hENT4 pH_e 7.5 curve. Results were expressed as the mean ± SEM, n=5. A Michaelis–Menten curve was fitted to these data.

4.1.4 Inhibition of ENT4-mediated 2-chloroadenosine uptake

We next investigated the inhibition characteristics of ENT4 inhibitors, D22 and TC-T6000, and a known ENT4 substrate, MPP^+, in the PK15-hENT4 cells. There were two sub-aims, and we first determined whether there was any difference in the ability of D22 and TC-T6000 to inhibit ENT4 if they were added at the same time as [^{3}H]2CADO, or if the cells were pre-incubated with the inhibitors prior to the uptake assay. This was necessary as we were unable to pre-incubate ENT4 inhibitors and concurrently load 2CADO (via ENT4) into PK15-hENT4 cells for our efflux studies (see below). Secondly, we looked at the inhibition profile of ENT4-mediated 2CADO uptake by D22, TC-T6000, and MPP^+ in a concentration dependent manner.

Figure 4.8A and B show that 2 µM D22 and 1 µM TC-T6000 inhibited ENT4 in a similar manner with or without pre-incubation over 15 minutes. Acidic pH-sensitive uptake was obtained by subtracting the pH 6.0 curve from the pH 7.5 curve to estimate rate constants and plateau and shown in Figure 4.8C and D and Table 4.1.

D22 and TC-T6000 were also able to inhibit ENT4 in a concentration dependent manner. They are likely to inhibit both the acidic pH-sensitive and neutral pH-mediated transport. However, these data need to be interpreted with caution as an inhibition plateau was not observed even when the highest concentration was used (solubility limit) (Fig 4.8G). Given this limitation, we can predict from the results in Fig 4.7A that the acidic pH-sensitive component constitutes about 55% of the total ENT4-mediated 2CADO uptake. Therefore, complete inhibition of ENT4 should plateau at about -82% in Fig 4.8G, assuming that 45% of the total ENT4-mediated 2CADO uptake is acidic pH-insensitive. With a constrained plateau analysis to -82%, D22 and TC-T6000, respectively, had an IC_{50} of 2.29 µM ($logIC_{50}$= -5.64 ± 0.05) and 2.34 µM ($logIC_{50}$= -5.63 ± 0.04). Using the estimated K_m of 1.52 mM previously determined for 2CADO (Fig 4.7B), this led to the calculation of a K_i of 2.24 µM for D22 and 2.30 µM for TC-T6000.

Conversely, MPP^+ only appeared to inhibit the acidic pH-sensitive component of ENT4-mediated 30 µM 2CADO uptake with an IC_{50} of 218 µM ($log\ IC_{50}$= -3.66 ± 0.11), leading to the calculation of

a K_i of 215 µM using the estimated K_m of 1.52 mM previously determined for 2CADO (Fig 4.7B). Fig 4.8E & F show that 0.5 mM MPP^+ also significantly reduced total accumulation of 30 µM 2CADO (Table 4.1).

When the cells were pre-incubated with inhibitors, a trend for inhibition below the neutral pH levels was observed, with maximal accumulation of 0.079 ± 0.010 and 0.073 ± 0.007 pmol/µg in the presence of D22 and TC-T6000 respectively, compared to 0.122 ± 0.032 pmol/µg in the absence of an inhibitor (Fig 4.8A).

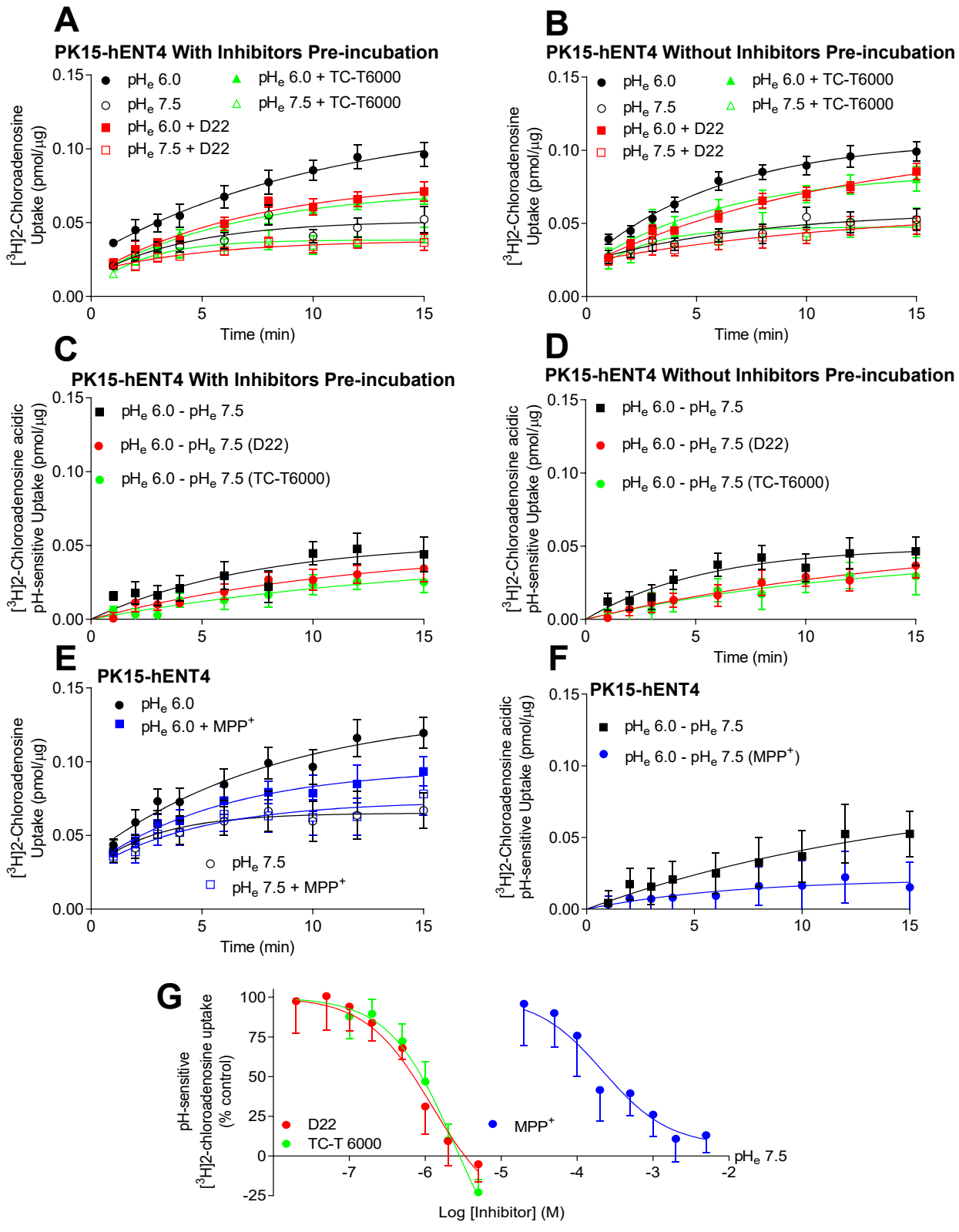
A
PK15-hENT4 With Inhibitors Pre-incubation
pHe 6.0
pHe 7.5
pHe 6.0 + D22
pHe 7.5 + D22
pHe 6.0 + TC-T6000
pHe 7.5 + TC-T6000
[3H]2-Chloroadenosine Uptake (pmol/µg)
Time (min)
B
PK15-hENT4 Without Inhibitors Pre-incubation
C
PK15-hENT4 With Inhibitors Pre-incubation
pHe 6.0 - pHe 7.5
pHe 6.0 - pHe 7.5 (D22)
pHe 6.0 - pHe 7.5 (TC-T6000)
[3H]2-Chloroadenosine acidic pH-sensitive Uptake (pmol/µg)
D
PK15-hENT4 Without Inhibitors Pre-incubation
E
PK15-hENT4
pHe 6.0 + MPP+
pHe 7.5 + MPP+
F
pHe 6.0 - pHe 7.5 (MPP+)
G
pH-sensitive [3H]2-chloroadenosine uptake (% control)
D22
TC-T 6000
MPP+
pHe 7.5
Log [Inhibitor] (M)

Figure 4.8. Inhibition of ENT4-mediated 2-chloroadenosine uptake by D22, TC-T6000, and MPP^+

A & B: PK15-hENT4 cells were incubated with 30 µM [^{3}H]2-chloroadenosine and 50 nM ABT-702 for the specified times in transport buffer, with 1 µM D22 or 2 µM TC-T6000 given competitively or pre-incubated respectively. E: PK15-hENT4 cells were also incubated with 30 µM [^{3}H]2-chloroadenosine, 50 nM ABT-702, and in the presence or absence of 0.5 mM MPP^+ for the specified times in transport buffer. C, D & F: Acidic pH-sensitive uptake was obtained by subtracting the pH_e 7.5 curve from the pH_e 6.0 curve for A, B and E respectively. G: PK15-hENT4 cells were exposed to 30 µM [^{3}H]2-chloroadenosine and 50 nM ABT-702 for 6 minutes with increasing concentrations of D22, TC-T6000 or MPP^+, with apparent uptake at pH 7.5 defined as 0%. Results are expressed as the mean ± SEM, n=5. A one-phase association curve or non-linear regression was fitted to these data.

	Plateau (pmol/µg)	Rate Constant (sec $^{-1}$)
Control (Pre-incubation; Fig 4.8C)	0.053 ± 0.013	0.135 ± 0.065
D22 (Pre-incubation; Fig 4.8C)	0.049 ± 0.011	0.083 ± 0.029
TC-T6000 (Pre-incubation; Fig 4.8C)	0.045 ± 0.021	0.062 ± 0.041
Control (Competition; Fig 4.8D)	0.049 ± 0.005	0.183 ± 0.045
D22 (Competition; Fig 4.8D)	0.057 ± 0.016	0.064 ± 0.025
TC-T6000 (Competition; Fig 4.8D)	0.044 ± 0.012	0.081 ± 0.033
Control (MPP^+; Fig 4.8F)	0.086 ± 0.027	0.065 ± 0.029
MPP^+ (Fig 4.8F)	0.021 ± 0.004 *	0.147 ± 0.064

Table 4.1. Data analysis from Figure 4.8

Maximal accumulation (plateau) of 30 µM 2CADO and rate constant estimates from Fig 4.8. Specific graphs where they were derived from is indicated. $^*p<0.05$ vs respective control as determined by Student's t-test.

Uridine has affinity for all known nucleoside transporters (except for the intracellularly expressed ENT3) in the micromolar range (Young *et al.*, 2013), with the highest K_m being approximately 0.2 mM for ENT1 and ENT2, and CNTs having at least 10 fold higher affinity. 3 mM uridine did not inhibit ENT4-mediated 2CADO uptake, with similar rate constants observed under control conditions (0.062 ± 0.043 min^{-1}) and in the presence of uridine (0.134 ± 0.029 min^{-1}) (Fig 4.9B).

Figure 4.10A shows that 10 mM adenosine reduced maximal accumulation of 2CADO by ENT4 below the neutral pH levels in PK15-hENT4, 0.147 ± 0.276 pmol/µg in the presence of 10 mM adenosine, compared to 0.393 ± 0.144 pmol/µg under control conditions (Fig 4.10A). In addition

to adenosine, a nucleobase (adenine) and a nucleobase analogue (6-mercaptopurine; 6-MP) also reduced the observed maximal accumulation. Figure 4.10B shows that maximal accumulation in the presence of 10 mM adenine and 300 µM 6-MP is 0.059 ± 0.004 pmol/µg and 0.106 ± 0.018 pmol/µg respectively, compared to 0.126 ± 0.010 pmol/µg under control conditions. Likewise, 10 mM adenosine significantly reduced maximal accumulation of 2CADO in PK15-NTD and only a trend for reduction was observed in the presence of 10 mM adenine (Fig 4.10C and D and Table 4.2).

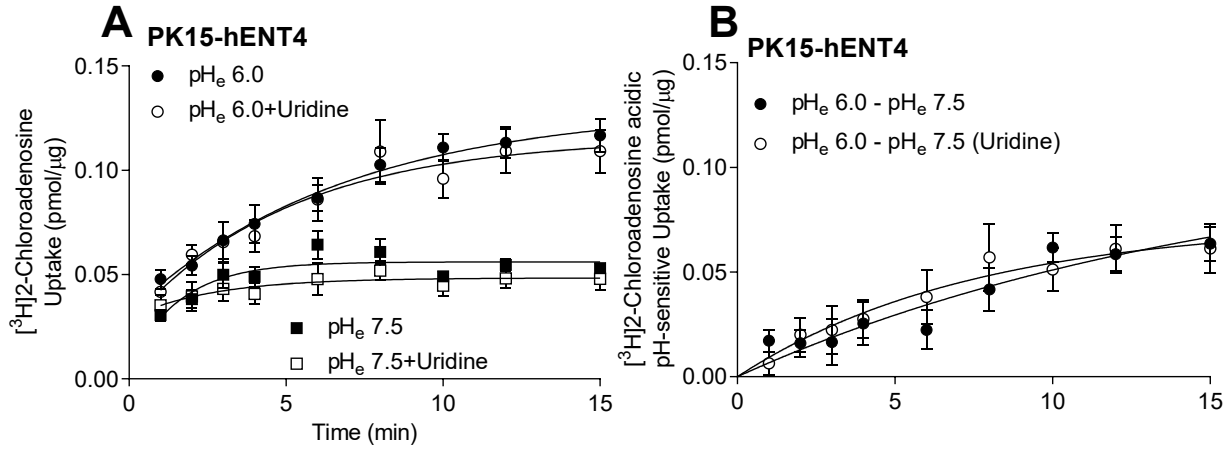

Figure 4.9. Uridine does not inhibit ENT4

A: PK15-hENT4 cells were incubated with 30 µM [^{3}H]2-chloroadenosine and 50 nM ABT-702 for the specified times in the presence or absence of 3 mM uridine. B: Acidic pH-sensitive uptake was obtained by subtracting the pH_e 7.5 curve from the pH_e 6.0 curve. Results were expressed as the mean ± SEM, n=5. A one-phase association curve was fitted to these data.

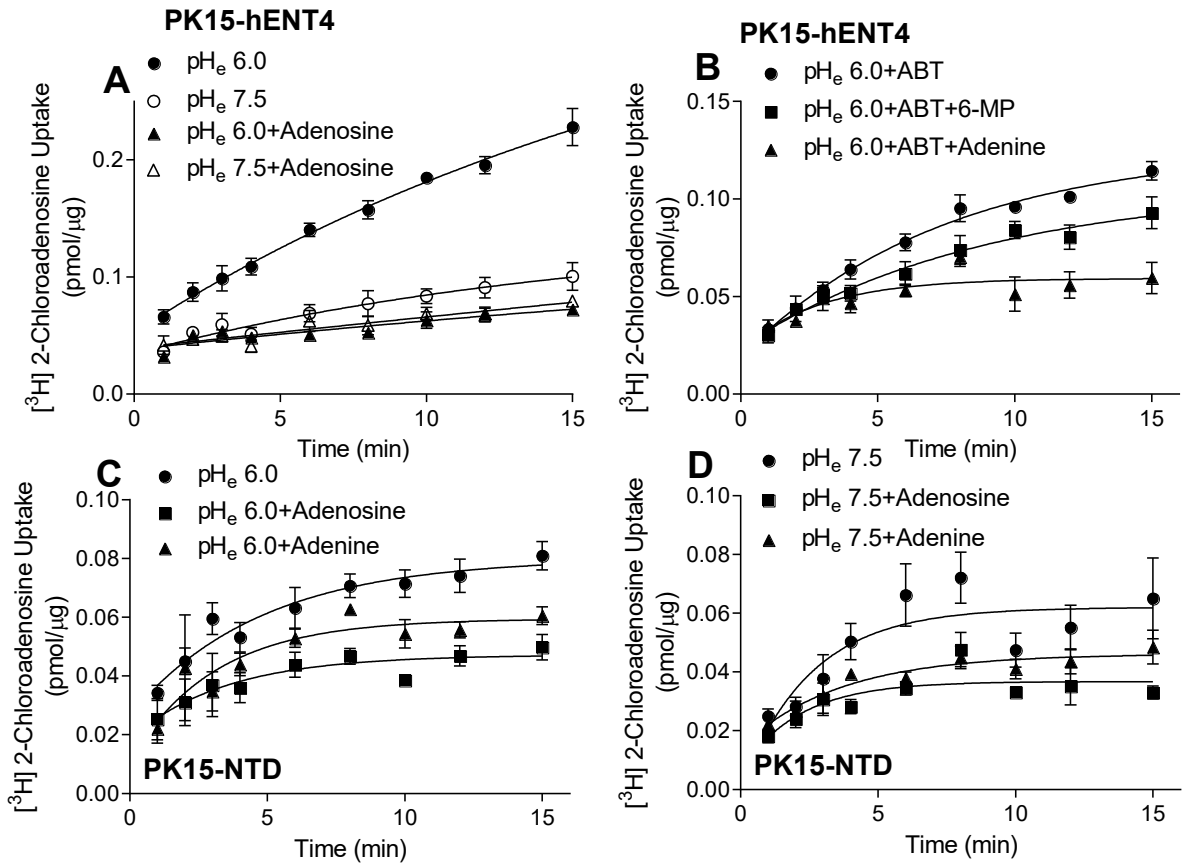

Figure 4.10. Inhibition of ENT4-mediated 2-chloroadenosine uptake by nucleoside and nucleobases

A & B: PK15-hENT4 cells were incubated with 30 µM [^{3}H]2-chloroadenosine for the specified times in transport buffer, with 10 mM adenosine (A) or with 50 nM ABT-702 and 300 µM 6-MP, or 10 mM adenine (B). C & D: PK15-NTD cells were exposed to 30 µM [^{3}H]2-chloroadenosine for up to 15 minutes in transport buffer, pH_e 6.0 and 7.5, in the presence or absence of 10 mM adenosine and 10 mM adenine. Results are expressed as the mean ± SEM, n=5. A one-phase association curve was fitted to these data.

	Plateau (pmol/µg)
pH_e 6.0	0.080 ± 0.006
pH_e 6.0 + 10 mM adenosine	0.047 ± 0.005*
pH_e 6.0 + 10 mM adenine	0.059 ± 0.005
pH_e 7.5	0.062 ± 0.005
pH_e 7.5 + 10 mM adenosine	0.037 ± 0.002#
pH_e 7.5 + 10 mM adenine	0.046 ± 0.003

Table 4.2. Data analysis from Figure 4.10C and D

Maximal accumulation (plateau) of 30 µM 2CADO estimates from Fig 4.10C and D. *$p<0.05$ vs pH_e 6.0 or #$p<0.05$ vs pH_e 7.5 as determined by one-way ANOVA plus Bonferroni *post hoc* tests.

4.1.5 Nucleoside efflux by ENT4 is also acidic pH-sensitive

To investigate ENT4-mediated nucleoside efflux, cells were loaded with [^{3}H]2CADO in the presence of the adenosine kinase inhibitor ABT-702, and then the rate of release of [^{3}H] was assessed under different extracellular pH conditions. Efflux was significantly faster when extracellular pH was acidic, compared to pH 7.5 and 8.2 (Fig 4.11A). Initial rate of efflux, used as an estimate of transport (ENT4) activity, was significantly higher at pH 6.0 (1.1 ± 0.1 pmol/mg/10 secs), versus that measured at pH 7.5 or 8.2; one-way ANOVA plus Bonferroni *post hoc* tests (Fig 4.11B).

The efflux study was then repeated with longer time-points, to allow time for a plateau to be attained, in the presence of D22 and TC-T6000. An acidic pH-sensitive efflux was also observed where a plateau was reached faster than at pH 7.5 or 8.2 (Fig 4.11C). This enhanced efflux when extracellular pH is acidic was significantly inhibited in the presence of 2 µM D22 (0.48 ± 0.07 pmol/µg/10 secs), but only a trend in the same direction was observed with 1 µM TC-T6000 (0.55 ± 0.10 pmol/µg/10 secs; Fig 4.11D). 1 µM TC-T6000 did not further reduce the observed 2CADO efflux at pH 7.5.

An alkaline pH of 8.2 has been shown to abolish ENT4-mediated MPP^+ influx in ENT4 transfected MDCK cells, with comparable uptake to that observed in untransfected MDCK cells (Xia *et al.*, 2007). In the PK15-hENT4 cells, there was no difference in efflux between the extracellular pH 7.5 and 8.2 conditions (Fig 4.11).

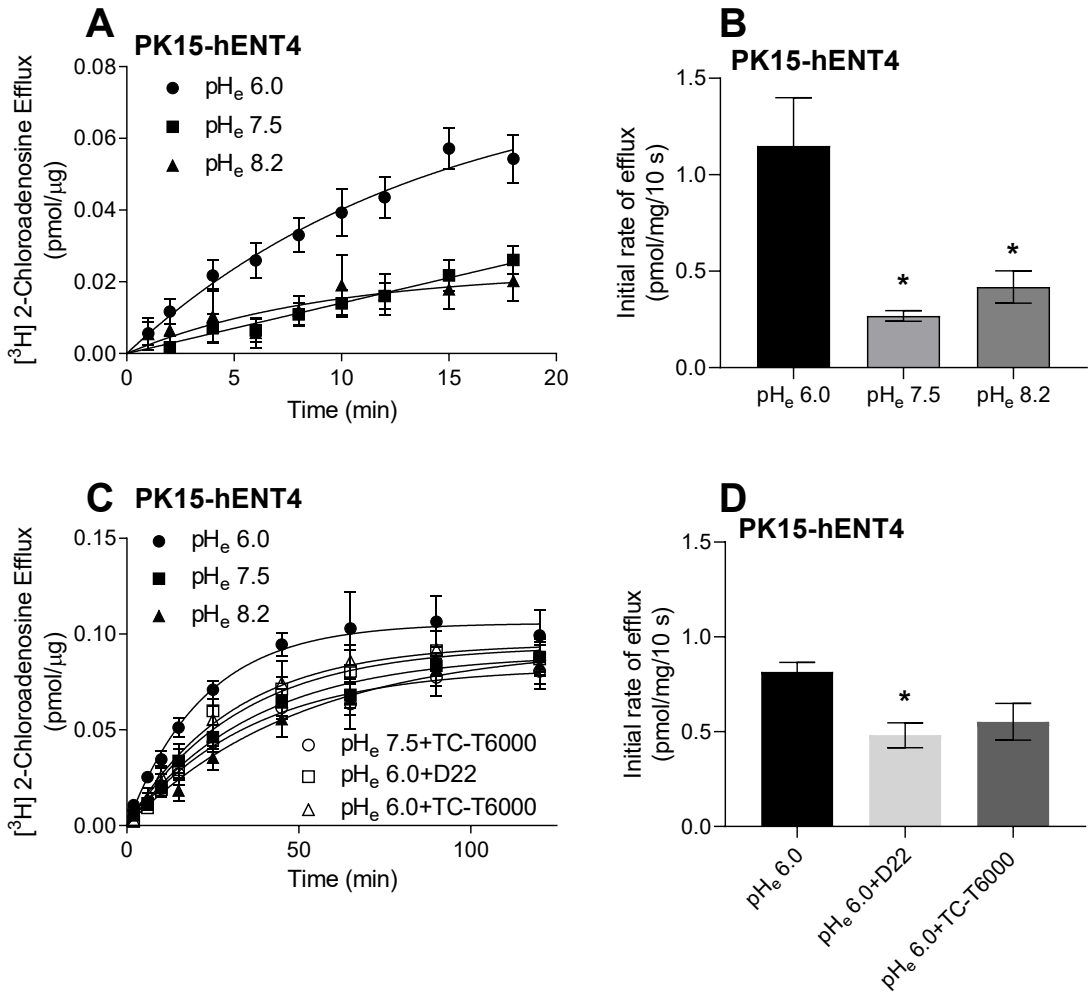

Figure 4.11. ENT4 mediates 2-chloroadenosine efflux

PK15-hENT4 cells were loaded with 30 µM [^{3}H]2-chloroadenosine and 50 nM ABT-702 for 12 minutes in transport buffer, and efflux initiated by exposure to a substrate-free buffer. Efflux was estimated by measuring the accumulation of [^{3}H]2-chloroadenosine in the substrate-free buffer for the specified times in the absence and presence of 1 µM TC-T6000 and 2 µM D22. Values obtained at t=0 were used as background. B & D: Initial rates were assessed by extrapolation of the one phase association curves fitted to the data shown in A & C respectively. Results are expressed as the mean ± SEM, n=5. $^*p<0.05$ vs respective controls as determined by one-way ANOVA plus Bonferroni *post hoc* tests.

4.1.6 Effects of nigericin on ENT4 function

To further investigate the acidic pH sensitivity of ENT4, nigericin (a proton/potassium ionophore) was used to clamp intracellular pH to extracellular pH (see Fig 4.13B). As nigericin will affect the homeostasis of potassium ions, it was necessary to perform the assay in a high KCl buffer which matched the intracellular concentration of potassium. As ENT4 activity is known to be sensitive to membrane potential changes, how these changes in ionic composition might affect ENT4-mediated 2CADO uptake was assessed. Figure 4.12A and C indicates a trend towards an increased maximal accumulation of 2CADO and an increased rate constant, from 0.054 ± 0.014 pmol/µg and 0.059 ± 0.022 min^{-1} under control conditions, to 0.090 ± 0.039 pmol/µg and 0.077 ± 0.051 min^{-1} in a high KCl buffer. In addition, the acidic pH-sensitive component was reduced in the presence of 1 µM TC-T6000 and, albeit not significant, there was also a reduced rate constant (0.041 ± 0.028 and 0.016 ± 0.049 min^{-1} for control and TC-T6000, respectively; Fig 4.12B and D).

Although it remains unclear how the conditions of high KCl alone affects ENT4, a high KCl buffer in the presence of 10 µM nigericin did not affect 2CADO uptake at neutral pH (Fig 4.12E). Therefore, how 10 µM nigericin (in the presence of a high KCl buffer) affected the acidic pH-sensitive component of ENT4 was tested. Nigericin reduced the total accumulation of 2CADO, compared to the absence of nigericin (0.029 ± 0.002 and 0.061 ± 0.004 pmol/µg with and without nigericin respectively; $^{*}p<0.05$ as determined by Student's t-test) without affecting the rate of uptake (0.364 ± 0.103 and 0.202 ± 0.034 min^{-1}) (Fig 4.12 E – F).

4.1.7 Measurement of intracellular pH in PK15-hENT4 cells

Changes in intracellular pH (pH_i) within the time frame used to measure transport kinetics, 15 minutes of pre-incubation plus 15 minutes of substrate uptake/efflux, was quantified using the BECEF-AM dye. It was found that the initial proton gradient across the plasma membrane was not maintained for more than 5 minutes when incubated with an extracellular buffer of pH 6.0 or 8.2 (Fig 4.13A). This suggests that a proton gradient was not maintained during the time used to estimate transport kinetics.

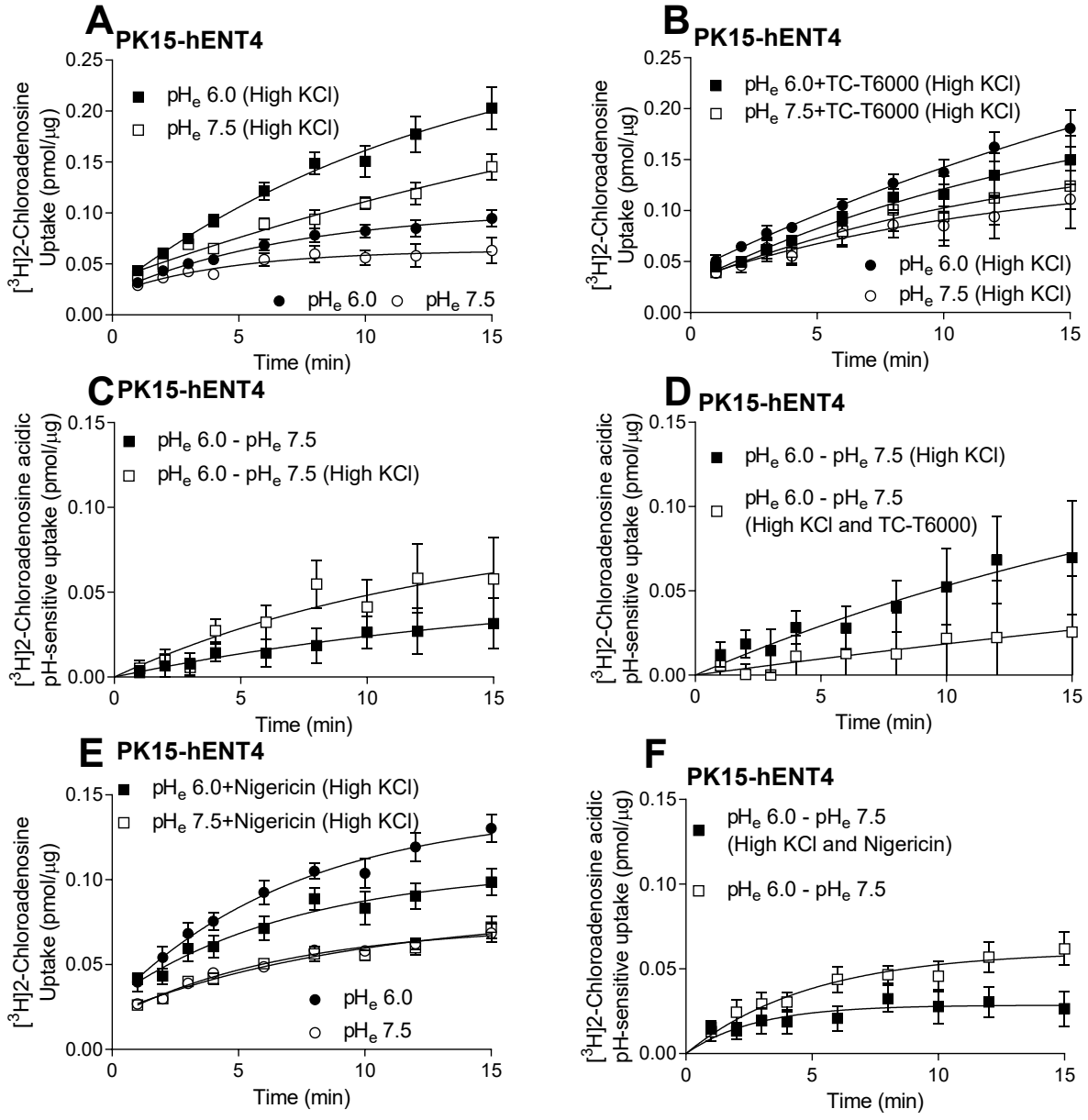

Figure 4.12. ENT4 pH sensitivity is not dependent on a proton gradient

A, B, & E: PK15-hENT4 cells were exposed to 30 µM [^{3}H]2-Chloroadenosine and 50 nM ABT-702 for up to 15 minutes in regular transport buffer or high KCl transporter buffer, pH_e 6.0 and 7.5, in the presence of 1 µM TC-T6000 or 10 µM nigericin. C, D, & F: Acidic pH-sensitive uptake was obtained by subtracting the pH_e 7.5 curve from the pH_e 6.0 curve for A, B, & E respectively. A one-phase association curve was fitted to these data. Results were expressed as the mean ± SEM, n=5.

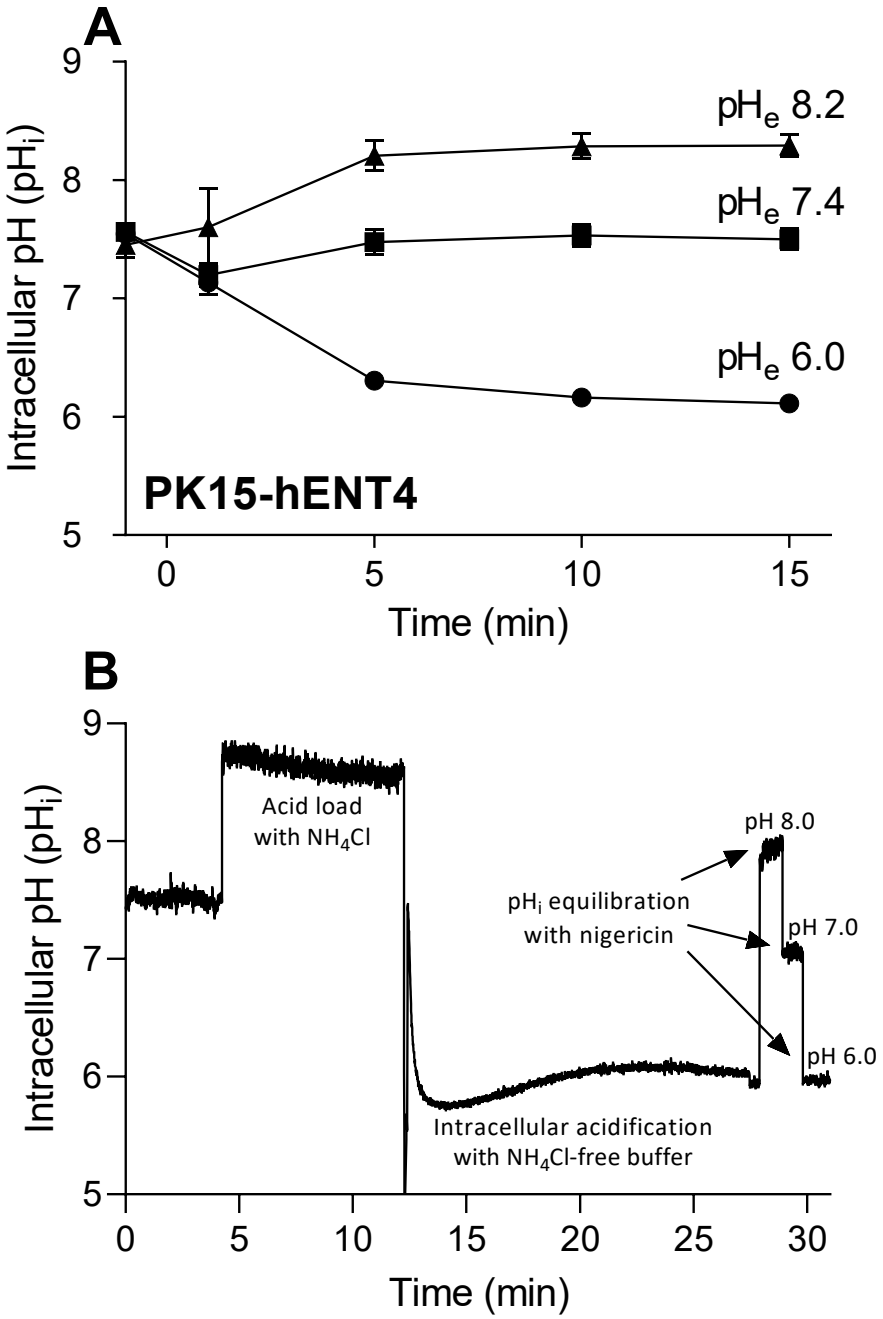

Figure 4.13. Intracellular pH measurements in PK15-hENT4 cells

A: Intracellular pH changes in PK15-hENT4 cells during the time used to determine transport kinetics was measured using BECEF-AM. Results were expressed as the mean ± SEM, n=5. B: PK15-hENT4 cells were exposed to a 50 mM NH_4Cl acid load for the indicated time on the x-axis before being exposed to a NH_4Cl free buffer to induce acidification. Cells were also incubated in the presence of 10 μM nigericin to equilibrate intracellular pH levels to that seen at the extracellular site. Y-axis indicates intracellular pH levels.

4.1.8 Effects of modifying intracellular pH with ammonium chloride (NH_4Cl) on ENT4 activity

Intracellular acidification due to anaerobic glycolysis (Finegan *et al.*, 1996) precedes the extracellular acidification that occurs during cardiac IRI. Therefore, it was of interest to determine how intracellular acidification directly affects ENT4 activity. It was shown previously that cytosolic acidification by NH_4Cl is dependent on both the concentration used (Chen *et al.*, 1998) and the duration of exposure to NH_4Cl (Fraser *et al.*, 2005). The highest concentration of NH_4Cl was, therefore, used and how different periods of NH_4Cl incubation affected ENT4-mediated 2-CADO uptake was investigated (see Fig 4.13B for a representative acid load trace). A gradual decrease in ENT4 activity was observed with increasing incubation periods of NH_4Cl (Fig 4.14A). Although this might suggest that a proton gradient is important for ENT4 activity, a similar reduction was observed when NH_4Cl was replaced with NMG^+ over the 12 minute incubation period (Figure 4.14B).

The observed decrease in ENT4 activity might be due to the alkalisation of the extracellular buffer as a result of NH_3 efflux from the cells after an acid load (Fig 3.1C). Therefore, as an attempt to remove this variable, cells were exposed to a sodium-free (NMG^+) buffer for a minute after an acid load. In the absence of sodium, the sodium hydrogen exchanger is inactive and this will allow NH_3 efflux and yet trapping H^+ ions in the intracellular space. This will maintain intracellular acidification before initiating uptake in the sodium containing (transport) buffer. However, we were unable to assess uptake as ENT4 is sensitive to changes in membrane potential (in the sodium-free [NMG^+] buffer when sodium is absent), and did not observe any acidic pH-sensitive uptake even in the absence of NH_4Cl incubation (Fig 4.14C).

Furthermore, Fig 4.15D indicates that the solution pH was unchanged, and that there was no general alkalisation of the uptake buffer mixture which might have been caused by NH_3 efflux. It was also confirmed that there was an acid load and initial alkalisation followed by intracellular acidification with NH_4Cl incubation, confirming that the model works in the PK15-hENT4 cells (Fig 4.13B and 4.15C).

Another possibility for this loss in ENT4 activity with increasing NH_4Cl incubation, is a loss in membrane potential; ENT4 activity has been shown to be reduced upon depolarisation (Engel *et al.*, 2004). To examine this, changes in membrane potential in our different experimental conditions was assessed using $DiBAC_4(3)$ dye. Using a high KCl buffer as a positive control for depolarisation, we showed that membrane potential was unchanged with the NH_4Cl and NMG^+ incubations. Therefore, the loss of ENT4 activity was not due to cellular depolarisation (Fig 4.15).

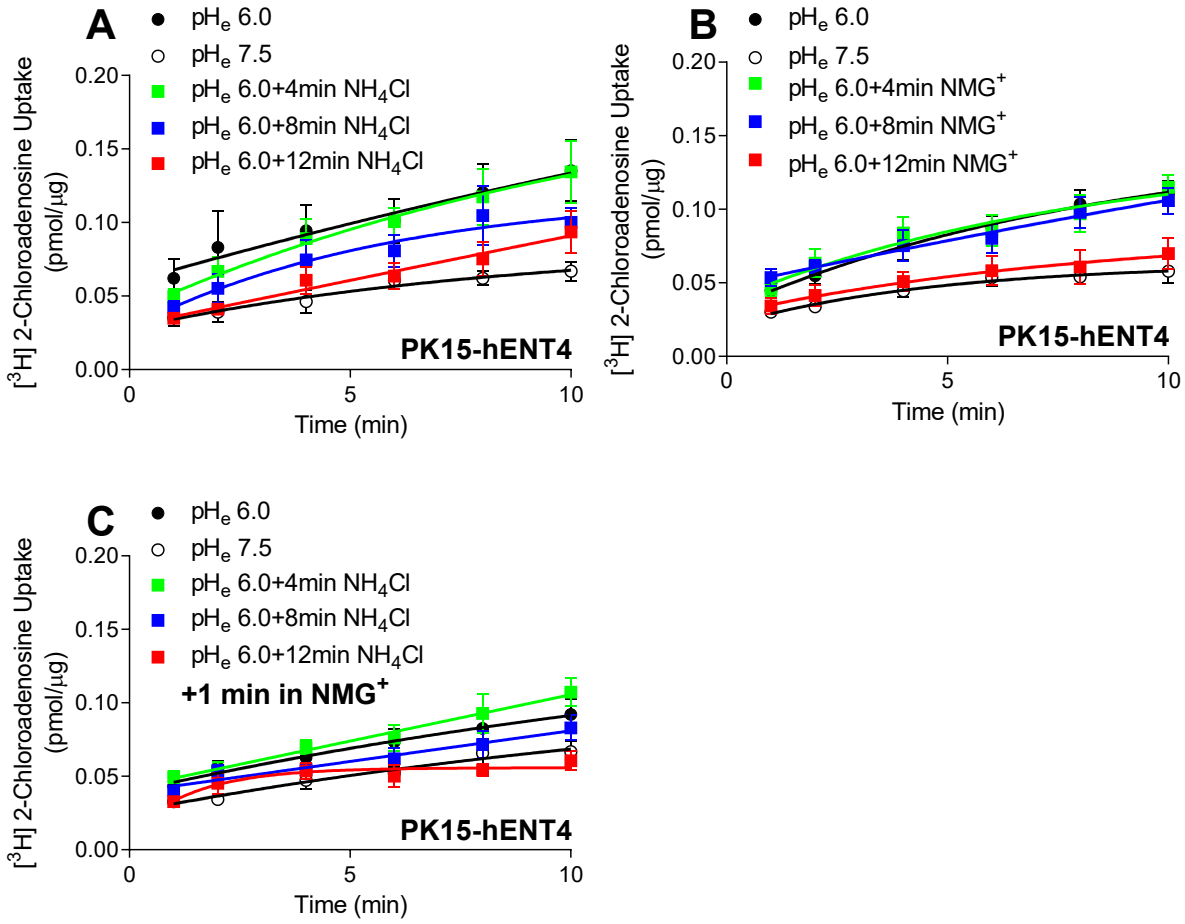

Figure 4.14. Effects of NH_4Cl and NMG^+ on ENT4 activity

A & B: PK15-hENT4 cells were pre-incubated with 50 mM NH_4Cl or 50 mM NMG^+ transport buffer before being exposed to 30 µM [^{3}H]2-chloroadenosine and 50 nM ABT-702 for up to 10 minutes in a NH_4Cl-free transport buffer, pH_e 6.0 or 7.5. C: Experimental condition in (A) was repeated but had an additional incubation in a sodium-free buffer (NMG^+) for a minute before exposure to a NH_4Cl-free buffer. Results were expressed as the mean ± SEM, n=5. A one-phase association curve was fitted to these data.

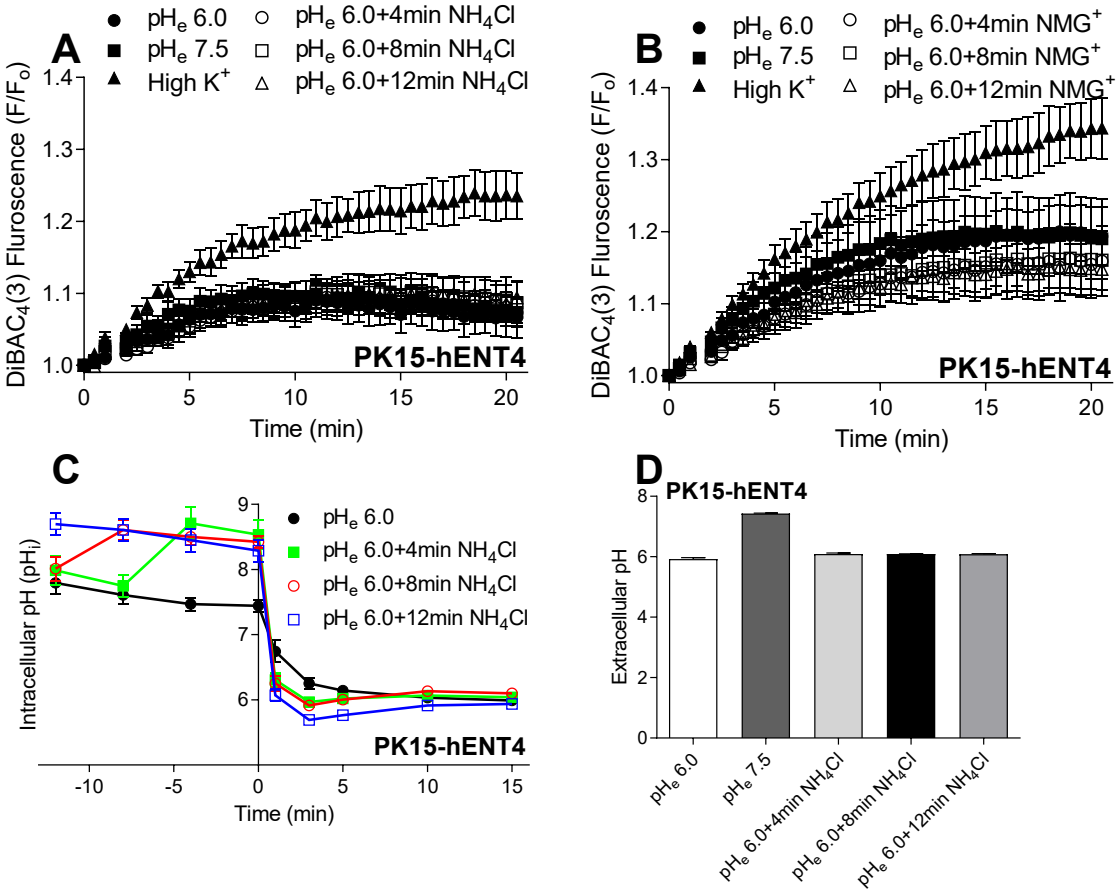

Figure 4.15. Effects of NH_4Cl and NMG^+ on membrane potential and pH in PK15-hENT4 cells

A & B: PK15-hENT4 cells were pre-incubated with 50 mM NH_4Cl or 50 mM NMG^+ transport buffer and 2 µM $DiBAC_4(3)$ before being exposed to 30 µM 2-chloroadenosine, 50 nM ABT-702 and 2 µM $DiBAC_4(3)$ in a NH_4Cl-free transport buffer, pH_e 6.0 or 7.5. A high K^+ buffer was used as a positive control. $DiBAC_4(3)$ fluorescence was measured every 30 seconds for 20 minutes. C & D: PK15-hENT4 cells were pre-incubated with 50 mM NH_4Cl transport buffer, pH_e 7.5, for the indicated time before being exposed to a NH_4Cl-free transport buffer. Changes in intracellular and extracellular pH was measured using BECEF-AM dye and a pH meter respectively. Results were expressed as the mean ± SEM, n=5.

To investigate whether intracellular acidification alone is sufficient to mediate ENT4 acidic pH-sensitive 2CADO uptake, intracellular acidification was induced using ammonium chloride, as above, but with a neutral extracellular pH. No acidic pH-sensitive 2CADO uptake was observed with the pre-incubation of NH_4Cl (Fig 4.16A). Though the longest period of NH_4Cl incubation

induced intracellular acidification, it was not maintained beyond 5 minutes in the PK15-hENT4 cells (Fig 4.16B).

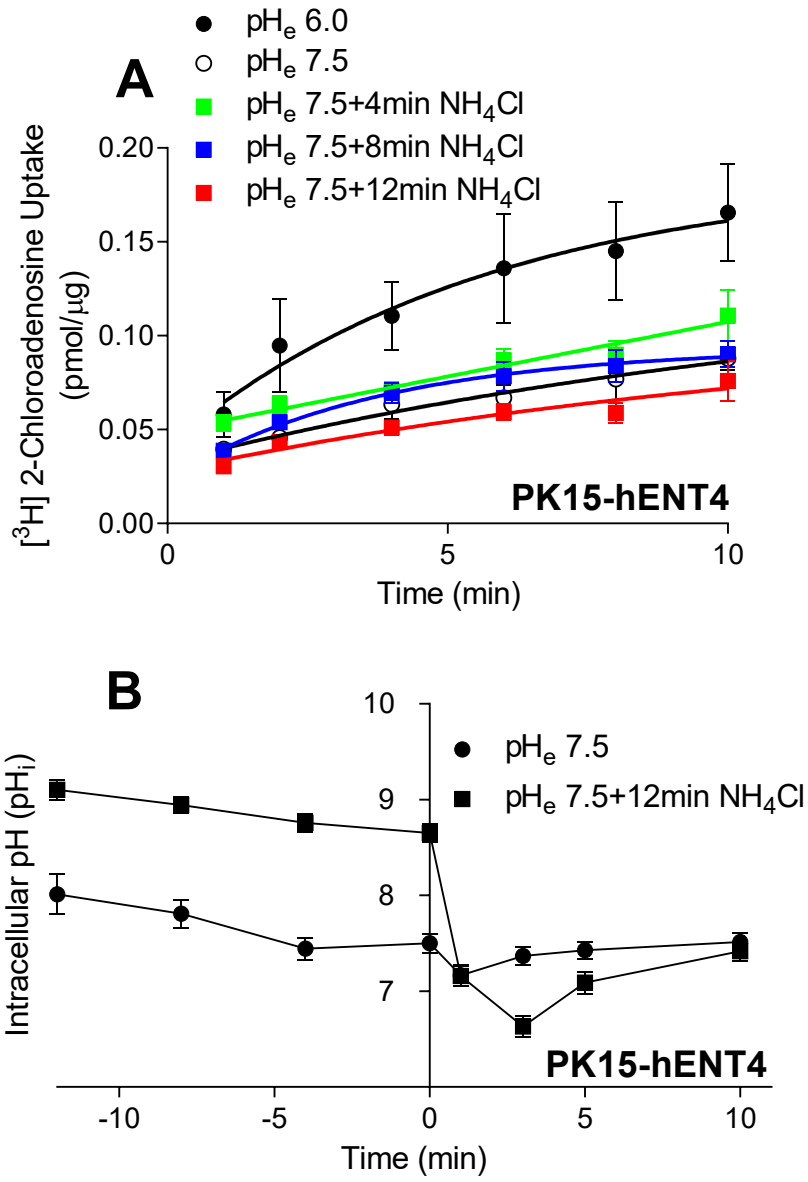

Figure 4.16. Effects of NH_4Cl on ENT4 activity and intracellular pH in PK15-hENT4 cells

A: PK15-hENT4 cells were pre-incubated with 50 mM NH_4Cl transport buffer before being exposed to 30 µM [^{3}H]2-chloroadenosine and 50 nM ABT-702 for up to 10 minutes in a NH_4Cl-free transport buffer, pH_e 6.0 or 7.5. B: Changes in intracellular pH under the indicated experimental condition observed in (A) were measured using BECEF-AM dye. Results are expressed as the mean ± SEM, n=5. A: A one-phase association curve was fitted to these data.

4.1.9 Assessment of HEK293 cells as a potential cell model for studying ENT4

Although the PK15-NTD cells remain a useful model to study ENT4 or other nucleoside transporters in isolation, they are not a human-based cell line and thus are not suitable for studies on the cellular regulation of human transporters (due to species differences in intracellular regulatory factors). We therefore investigated whether a commonly used human cell line, HEK293, exhibited ENT4-mediated nucleoside flux. HEK293 cells are known to have both ENT1 and ENT2 activity. ENT1 can be blocked with the specific inhibitor NBMPR, and we showed previously that NBMPR does not inhibit ENT4 at concentrations that completely block ENT1 (Figure 4.5A). This just leaves ENT2, which does not have any selective inhibitors, as a problem. In collaboration with Dr Basil Hubbard (Department of Pharmacology, University of Alberta), the CRISPR/Cas9 system was used to delete ENT2 from HEK293 cells, creating a HEK293-ENT2KO cell line. A null background HEK293 cell line, with genetic deletion of ENT1 and ENT2, was also created subsequent to these studies.

[^{3}H]2CADO uptake in the HEK293-ENT2KO cells exhibited a trend towards increased maximal accumulation at pH 6.0, 1.336 ± 0.212 pmol/µg, compared to 0.867 ± 0.127 pmol/µg at pH 7.5. The rate constants of 0.105 ± 0.050 and 0.150 ± 0.136 sec^{-1} at acidic and neutral pH, respectively, were not significantly different (Fig 4.17). As this was performed in the absence of NBMPR in a sodium-containing buffer, ENT1 and CNTs would contribute to the observed uptake. In the presence of 100 nM NBMPR, which would inhibit ENT1 completely, 2CADO uptake was reduced at both pH 6.0 and 7.5 (Fig 4.17). The influence of CNTs was also removed by conducting assays in a sodium-free (NMG^+) buffer. CNTs might indirectly have acidic pH-sensitivity due to its sodium dependence and therefore proton dependence as sodium and proton homeostasis is connected via the NHE system. There was no difference in NBMPR-insensitive uptake between sodium-containing and sodium-free (NMG^+) buffer (rate constant of 0.051 ± 0.044 sec^{-1} in the presence of sodium versus 0.057 ± 0.048 sec^{-1} in the absence of sodium under acidic conditions), suggesting that the contribution of CNTs to 2CADO uptake over 15 minutes is negligible. There was also no difference in rate constant at pH 6.0 (0.051 ± 0.044 sec^{-1}) or 7.5 (0.020 ± 0.063 sec^{-1}) in a sodium

containing buffer. Overall, most of the 2CADO uptake in HEK293-ENT2KO cells is mediated by ENT1 while the contribution of CNTs and ENT4 is minimal.

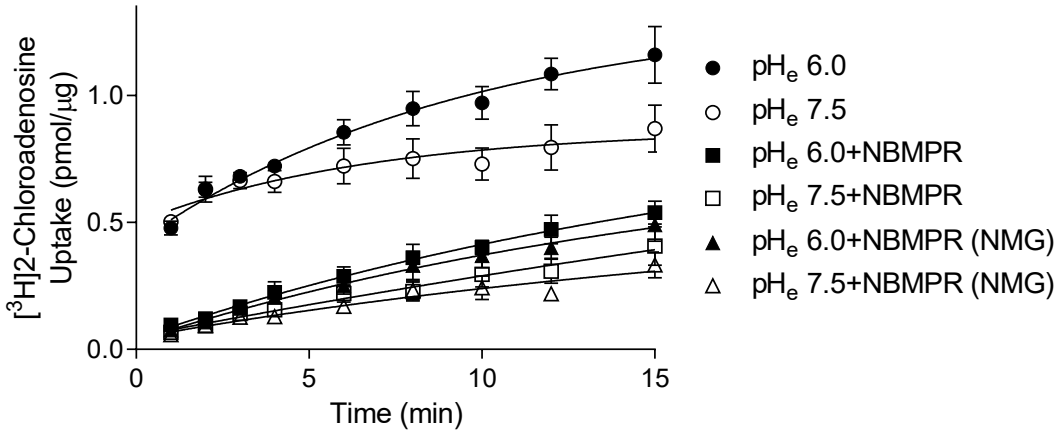

Figure 4.17. [^{3}H]2-chloroadenosine uptake in HEK293-ENT2KO cells

HEK293 cells with ENT2 deletion by CRISPR/Cas9 system were exposed to 30 μM [^{3}H]2-chloroadenosine and 50 nM ABT-702 for up to 15 minutes in sodium-containing or sodium-free (NMG^+) transport buffer, pH_e 6.0 and 7.5, in the presence or absence of 100 nM NBMPR. A one-phase association curve was fitted to these data. Results were expressed as the mean ± SEM, n=5.

4.2 Investigating how ENT4 activity changes following simulated ischaemia-reperfusion injury

We wanted to investigate how endogenous ENT4 activity changed following cardiac IRI. Regulation of other ENTs by hypoxia, a component of an ischaemic insult, has been shown to be regulated transcriptionally (Eltzschig *et al.*, 2005; Morote-Garcia *et al.*, 2009). If ENT4 is also transcriptionally regulated, this would not be observed in the PK15-hENT4 model which only has the coding region of ENT4 present (without the promoter region). Since ENT4 has been reported to be expressed in vascular endothelial cells and cardiomyocytes (Barnes *et al.*, 2006), we looked at whether immortalised human microvascular endothelial (HMEC-1) cells and mouse cardiomyocytes HL-1 exhibited acidic pH-sensitive nucleoside uptake mediated by ENT4.

4.2.1 Characterisation of nucleoside transporters present in HMEC-1 cells

[^{3}H]2CADO uptake by HMEC-1 cells in a sodium-containing buffer resulted in a maximal accumulation of 2.339 ± 4.783 pmol/μg at pH 6.0 which is ~5-fold higher than that seen using a sodium-free (NMG^+) buffer (maximal accumulation of 0.481 ± 0.091 pmol/μg at pH 6.0; Fig 4.18A). This suggests the operation of a concentrative pH-sensitive transport system. To eliminate the potential contribution of ENT1 and ENT2 in our uptake assays, 500 nM DY was included. Rather than a reduced uptake, an unexpected increase in the maximal accumulation of 2CADO at pH 6.0 (2.344 ± 0.486 pmol/μg at pH 6.0 compared to 1.100 ± 0.115 pmol/μg at pH 7.5; Fig 4.18B) was observed. This phenomenon was not observed when studies were performed in a sodium-free (NMG^+) buffer (maximal accumulation of 1.605 ± 1.239 pmol/μg at pH 6.0 compared to 0.808 ± 0.125 pmol/μg at pH 7.5), again suggesting that CNTs play a major role here. There were also no acidic pH-sensitive changes in the rate constant, 0.149 ± 0.087 and 0.341 ± 0.198 min^{-1} in transport buffer and in the presence of DY at pH 6.0 and 7.5 respectively (no difference as determined by Student's t-test). This suggests that ENT4 is not present functionally. Accumulation of 2CADO was completely abolished in the presence of 10 mM adenosine when (0.051 ± 0.004 pmol/μg; Fig 4.18B), indicating that the process was purine transporter mediated.

We then investigated how sIR affected HMEC-1 cell viability (Fig 4.19). Fig 4.19 shows that after 2 hr of simulated ischaemia and 1, 2, and 4 hr of reperfusion, 71 ± 3 %, 78 ± 3%, and 85 ± 2% of cells remained viable respectively. 3 hr of simulated ischaemia and 1, 2, and 4 hr of reperfusion resulted in 51 ± 5%, 54 ± 5%, and 67 ± 8% cell viability respectively. To model a sIR stress before conducting uptake studies, 3 hr of simulated ischaemia and 1 hr of reperfusion was used in HMEC-1. In the presence of 3 mM uridine which does not inhibit ENT4 (Fig 4.9) but does block all other nucleoside transporters, 3hr sI/1hr R caused no difference in 2CADO uptake compared to sham controls (Fig 4.18C). Given the confounding contribution of CNTs in this cell line, and the relatively low level of ENT4 activity, HMEC-1 cells were deemed unsuitable for the intended purpose.

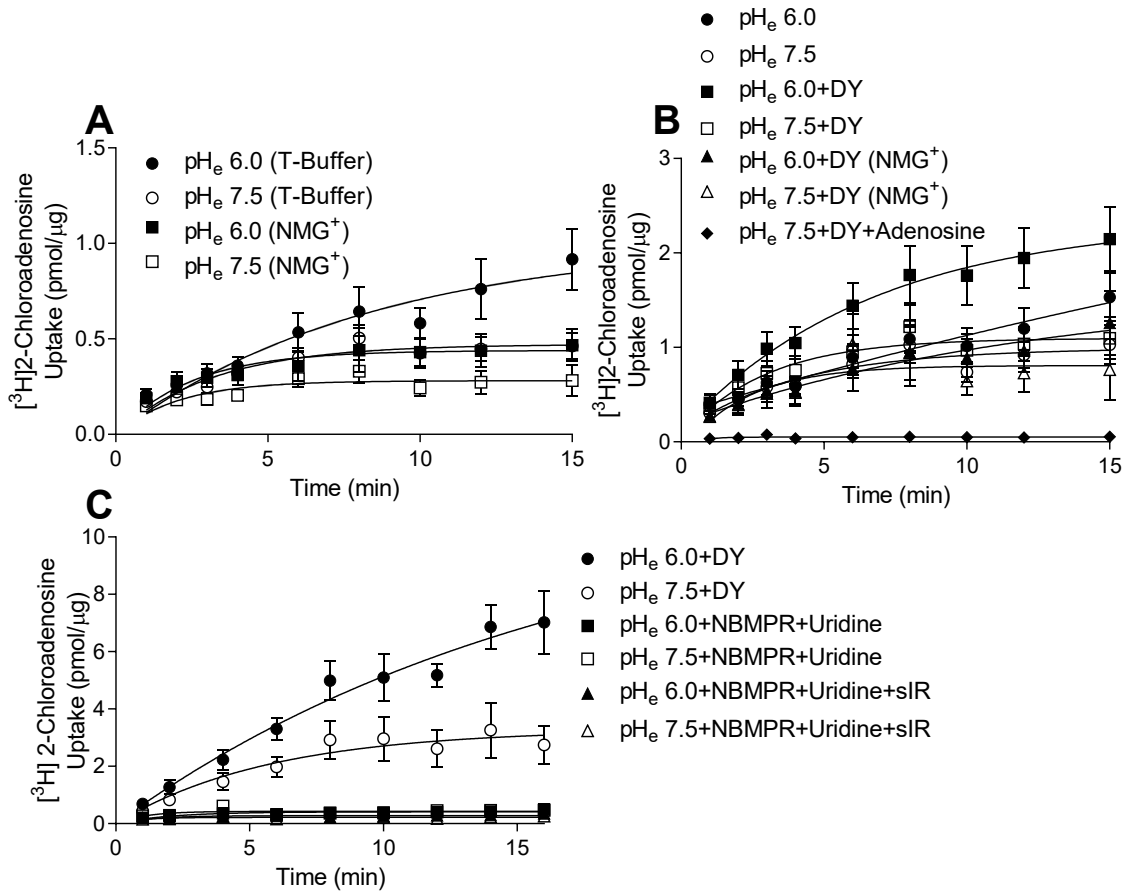

Figure 4.18. [^{3}H]2-chloroadenosine uptake in HMEC-1 cells

A & B: Immortalised human microvascular endothelial (HMEC-1) cells were exposed to 10 µM [^{3}H]2-chloroadenosine and 50 nM ABT-702 for the specified times in sodium-containing (transport) buffer or sodium-free (NMG^+) buffer (Na^+-free), pH_e 6.0 and 7.5, with or without 500 nM DY, and 10 mM adenosine. C: HMEC-1 were also subjected to 3hr simulated ischaemia and 2hr reperfusion before exposing them to 10 µM [^{3}H]2-chloroadenosine in the presence of 100 nM NBMPR and 3 mM uridine. A one-phase association curve was fitted to these data. Results are expressed as the mean ± SEM, n=5.

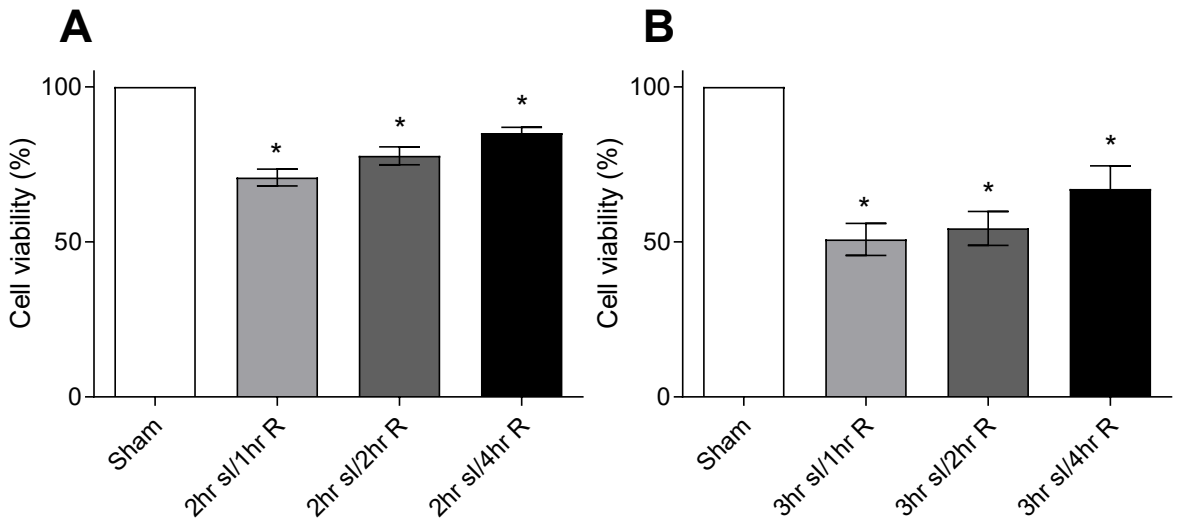

Figure 4.19. Simulated ischaemia-reperfusion induced cell death in HMEC-1 cells

A & B: Immortalised human microvascular endothelial (HMEC-1) cells were exposed to 2 (A) or 3 (B) hours of simulated ischaemia and 1-4 hours of reperfusion. Cell viability was assessed using MTT. Results were expressed as the mean ± SEM, n=3 for (A) and 6 for (B). $^{*}p<0.05$ vs respective controls as determined by one-way ANOVA plus Bonferroni *post hoc* tests.

4.2.2 HL-1 cardiomyocytes exhibit an acidic pH-sensitive nucleoside uptake

HL-1 cardiomyocytes have been shown previously to express ENT4 protein (Barnes *et al.*, 2006), but whether they exhibit an acidic pH-sensitive purine nucleoside uptake has not been addressed. Our data show that HL-1 cardiomyocytes exhibit an acidic pH-sensitive 2CADO uptake in the presence of 100 nM NBMPR to inhibit ENT1 (maximal accumulations of 0.224 ± 0.029 and 0.124 ± 0.006 pmol/µg at pH 6.0 and 7.5 respectively; Fig 4.20A). As other nucleoside transporters are still capable of mediating 2CADO flux under these conditions, 2CADO uptake in the presence of 1 mM uridine which can suppress all endogenous nucleoside transporters except ENT4 was also performed. An acidic pH-sensitive 2CADO uptake with a maximal accumulation of 0.070 ± 0.010 pmol/µg and rate constant of 0.218 ± 0.185 min^{-1} at pH 6.0, and no uptake at pH 7.5 was observed in the presence of 1 mM uridine. This pH sensitive uptake was completely inhibited with 10 µM D22 (Fig 4.20B).

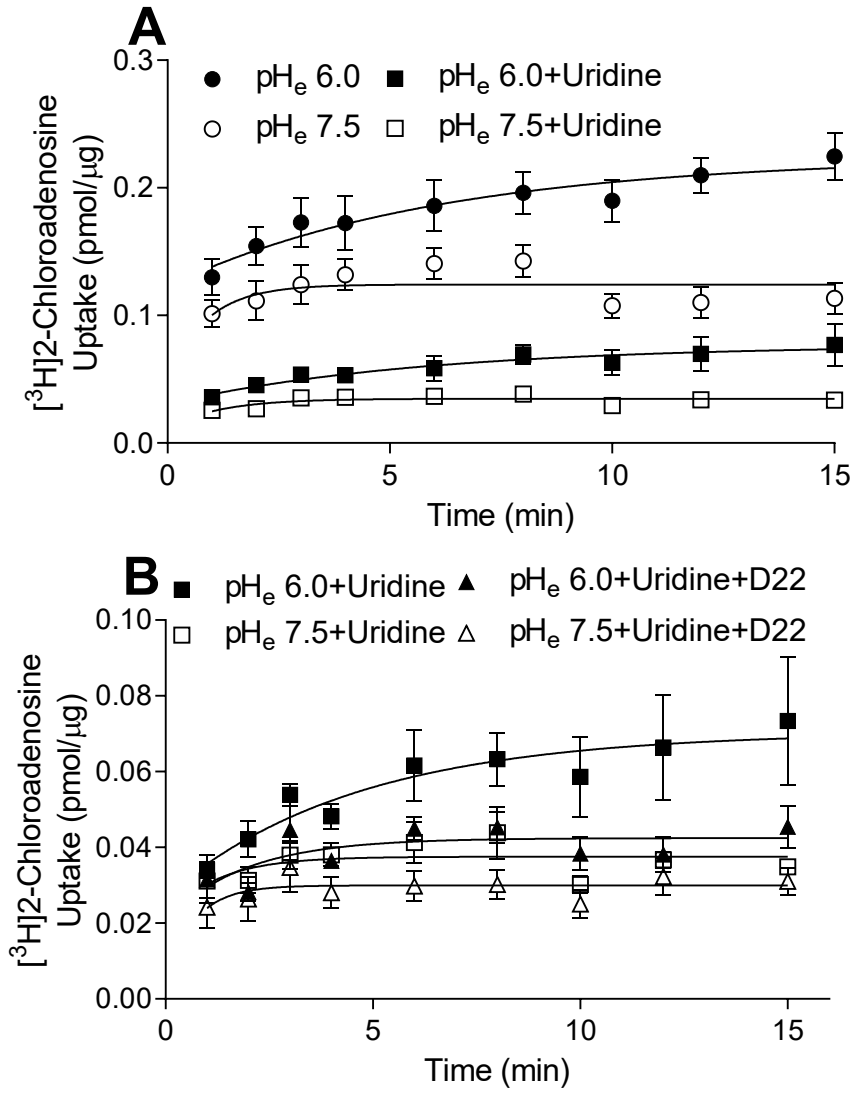

Figure 4.20. HL-1 cardiomyocytes exhibit pH-sensitive [^{3}H]2-chloroadenosine uptake

A: HL-1 cells were exposed to 10 µM [^{3}H]2-chloroadenosine, 50 nM ABT-702, and 100 nM NBMPR for up to 15 minutes in transport buffer, pH_e 6.0 and 7.5, in the presence or absence of 1 mM uridine. B: Uptake was performed as with (A), with 1 mM uridine, and in the presence or absence of 10 µM D22. Results are expressed as the mean ± SEM, n=5. A one-phase association curve was fitted to these data.

4.2.3 ENT4 activity was suppressed following simulated ischaemia stress

As HL-1 cardiomyocytes express ENT4 functionally, they may be an appropriate model to study how ischaemia-reperfusion affects ENT4. To simulate this, HL-1 cells were exposed to 2-5 hr of simulated ischaemia followed by 1-2 hr of reperfusion. Using LDH and MTT as markers for cell death and viability, respectively, 4hr sI/2hr R resulted in 78 ± 2% cell viability and is supported by the cellular release of 12 ± 2% of maximal LDH (Fig 4.21). These conditions define a level of cellular stress that is significant but not too severe such that there are still sufficient viable cells to quantify ENT4 activity.

Although HL-1 cardiomyocytes exhibited an acidic pH-sensitive uptake of 2CADO, it was not particularly robust, while the uptake of adenosine was more consistent with a better signal:noise ratio (Fig 4.22A and B). This possibly reflects a difference in 2CADO affinity between the human and mouse ENT4. Hence, adenosine was used (in the presence of EHNA and ABT-702, adenosine deaminase and adenosine kinase inhibitors respectively) instead for subsequent experiments using HL-1 cells. Despite the presence of the aforementioned enzyme inhibitors to minimise metabolism of adenosine and trapping of the [^{3}H] signalling, adenosine was still clearly metabolised as we observed a linear relationship with time (Fig 4.22C and D). While clearly not ideal for assessing transport kinetics, linear regression analysis showed a significant reduction in the rate of uptake in the presence of 10 µM D22 (0.064 ± 0.006 VS 0.013 ± 0.001 min^{-1}) or 10 µM TC-T6000 (0.057 ± 0.003 VS 0.009 ± 0.002 min^{-1}), $^{*}p<0.05$ as determined by Student's t-test. This shows that an acidic pH-sensitive uptake of adenosine was present in HL-1 cardiomyocytes and was reduced in the presence of D22 or TC-T6000 (Fig 4.22C and D). ENT4-mediated acidic pH-sensitive adenosine uptake was reduced following 4hr sI but was restored after 2hr R (Fig 4.22E). On the other hand, ENT4-mediated adenosine uptake at neutral pH was unaffected (Fig 4.22F).

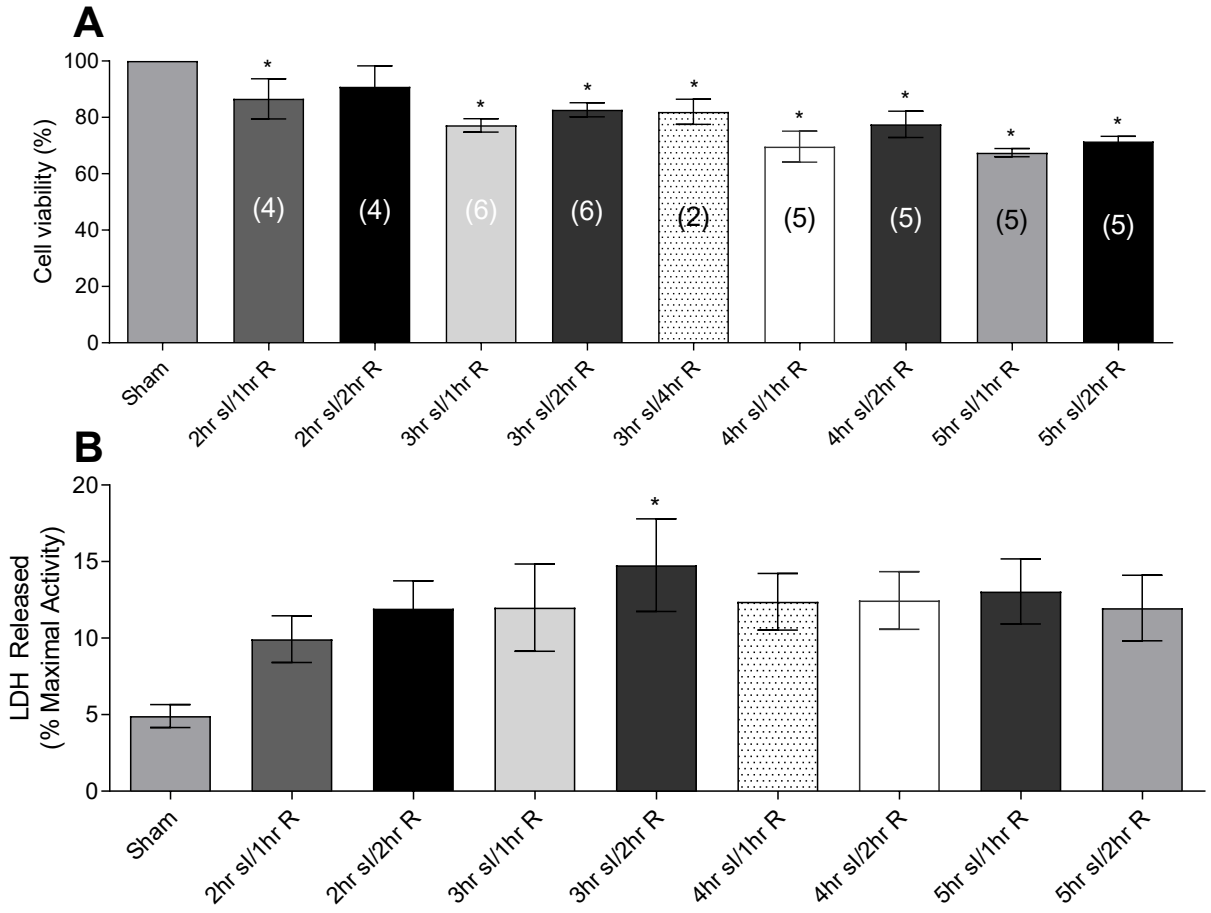

Figure 4.21. Simulated ischaemia-reperfusion induced cell death in HL-1 cells

A & B: HL-1 cells were exposed to 2-5 hours of simulated ischaemia and 1-2 hours of reperfusion. Cell viability (A) and cell death (B) were assessed using MTT and LDH respectively. Results expressed as the mean ± SEM, n=2-6 for (A) and 5 for (B). $^{*}p<0.05$ vs respective controls as determined by one-way ANOVA plus Bonferroni *post hoc* tests.

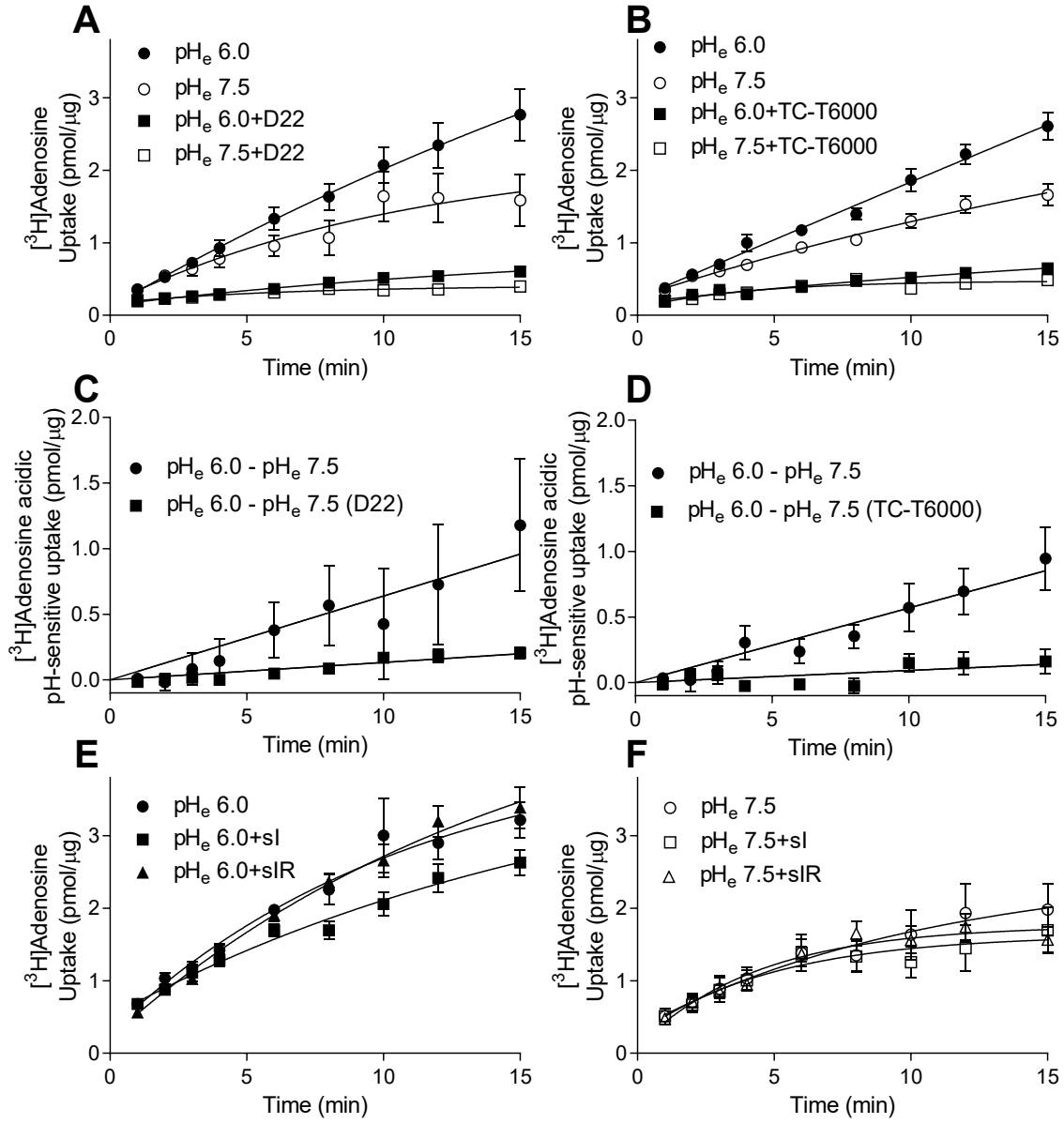

Figure 4.22. Reduced ENT4 activity following sIR

A & B: HL-1 cells were exposed to 100 µM [^{3}H]adenosine, 50 nM ABT-702, 100 nM NBMPR, and 1 mM uridine for up to 15 minutes in transport buffer, pH_e 6.0 and 7.5, in the presence and absence of 10 µM D22 (A) or 10 µM TC-T6000 (B). C & D: Acidic pH-sensitive uptake was obtained by subtracting the pH_e 7.5 curve from the pH_e 6.0 curve for A & B respectively. E & F: Cells were subjected to 4hr sI/2hr R before initiating uptake at pH_e 6.0 (E) or pH_e 7.5 (F). Results were expressed as the mean ± SEM, n=5. A one-phase association curve (A, B, E, F) or linear regression (C, D) was fitted to these data.

A similar reduction in Slc29a4 was observed following 4 hr of sI but this suppression was maintained even after 2 hr of reperfusion (Fig 4.23A), compared to that seen for the adenosine uptake (Fig 4.22E). As hypoxia-inducible factor 1α (HIF-1α) and inflammation and oxidative stress are known to play a role in IRI (Verma *et al.*, 2002), we screened initially for changes in these mRNA transcripts. A trend for increase in Hif1a was observed in our ischaemic conditions but this was reduced after reperfusion (Fig 4.23B). With sIR, there was a significant increase in pro-inflammatory Tnf and a trend for increased Ccl2, and Il-6, but not for Icam1 and Nfkbib (Fig 4.23C – F and 4.24F). Oxidative stress markers remained unchanged (Fig 4.24A – C, E). There was also an increased Parp1, a marker of cell death (Fig 4.24D), after 4 hr of sI, consistent with the MTT and LDH results described previously (Fig 4.21).

HL-1 cells were also exposed to sIR in the presence of 10 μM TC-T6000 to investigate any potential protection exerted by ENT4 inhibition. TC-T6000 did not significantly inhibit the increased Tnf observed with sIR (Fig 4.25C). sIR did not affect the other markers of inflammation or oxidative stress and neither did TC-T6000 affect those markers (Fig 4.25 and 4.26). Although the expression of Gpx1, an anti-oxidant marker, was unchanged with sIR, there was a significant reduction in the presence of TC-T6000 (Fig 4.26A), and that Gpx1 expression was suppressed below its basal level.

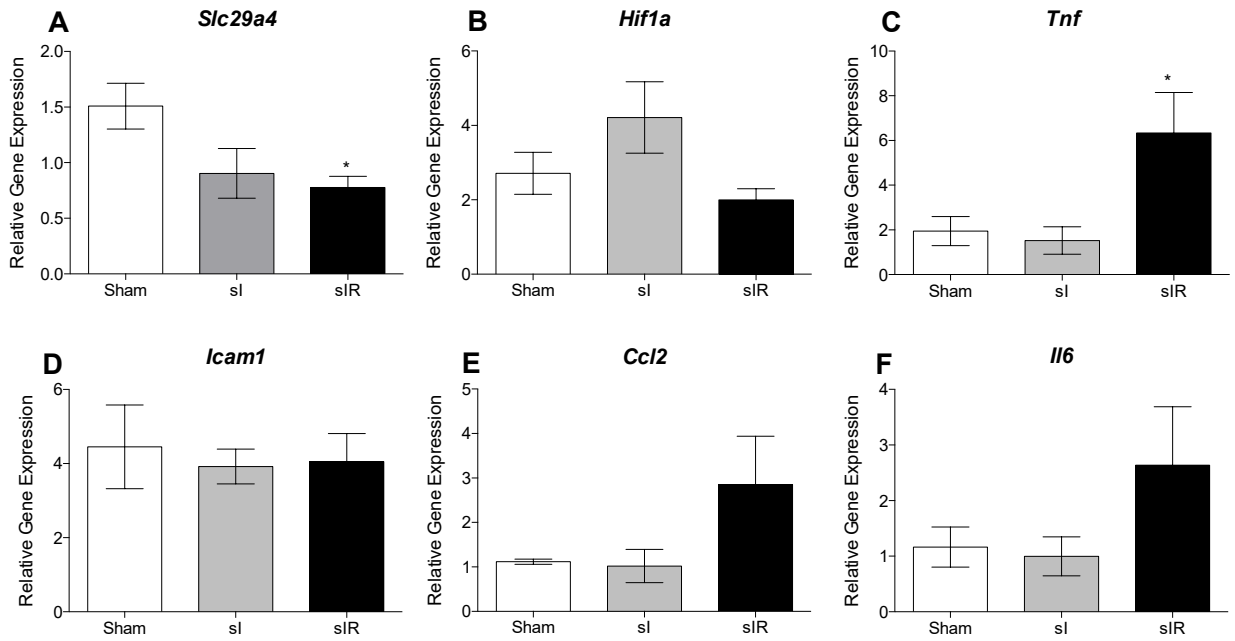

Figure 4.23. Gene expression of inflammation and hypoxia markers after simulated ischaemia

qPCR analysis in HL-1 cells of ENT4, hypoxia, and inflammatory markers following 4 hours of simulated ischaemia or 4 hours of simulated ischaemia and 2 hours of reperfusion. GAPDH, β-actin and α-tubulin were used as reference gene and their geometric mean was used to calculate a normalisation index. Results were expressed as the mean ± SEM, n=6. *p<0.05 vs sham as determined by one-way ANOVA plus Bonferroni *post hoc* tests. Experiments were performed by undergraduate research project student M. Ntiamoah.

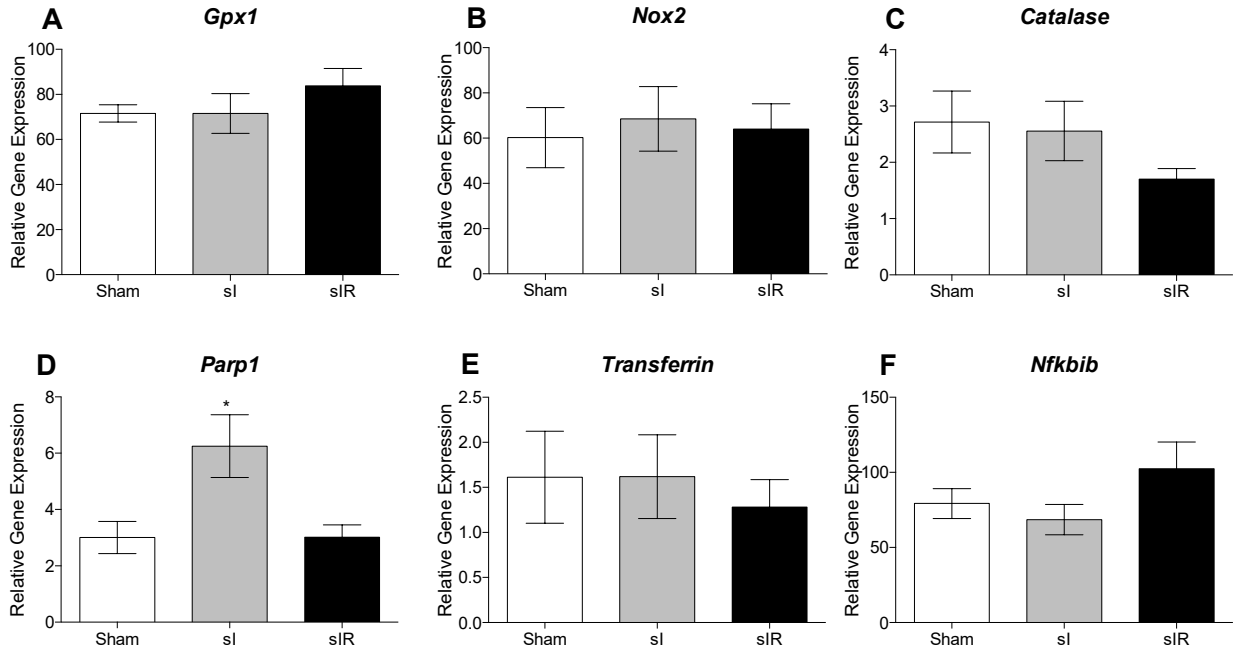

Figure 4.24. Gene expression of oxidative stress and cell death markers after simulated ischaemia

qPCR analysis in HL-1 cells of oxidative stress, antioxidant, and cell death markers following 4 hours of simulated ischaemia or 4 hours of simulated ischaemia and 2 hours of reperfusion. GAPDH, β-actin and α-tubulin were used as reference gene and their geometric mean was used to calculate a normalisation index. Results were expressed as the mean ± SEM, n=6. *p<0.05 vs sham as determined by one-way ANOVA plus Bonferroni *post hoc* tests. Experiments were performed by undergraduate research project student M. Ntiamoah.

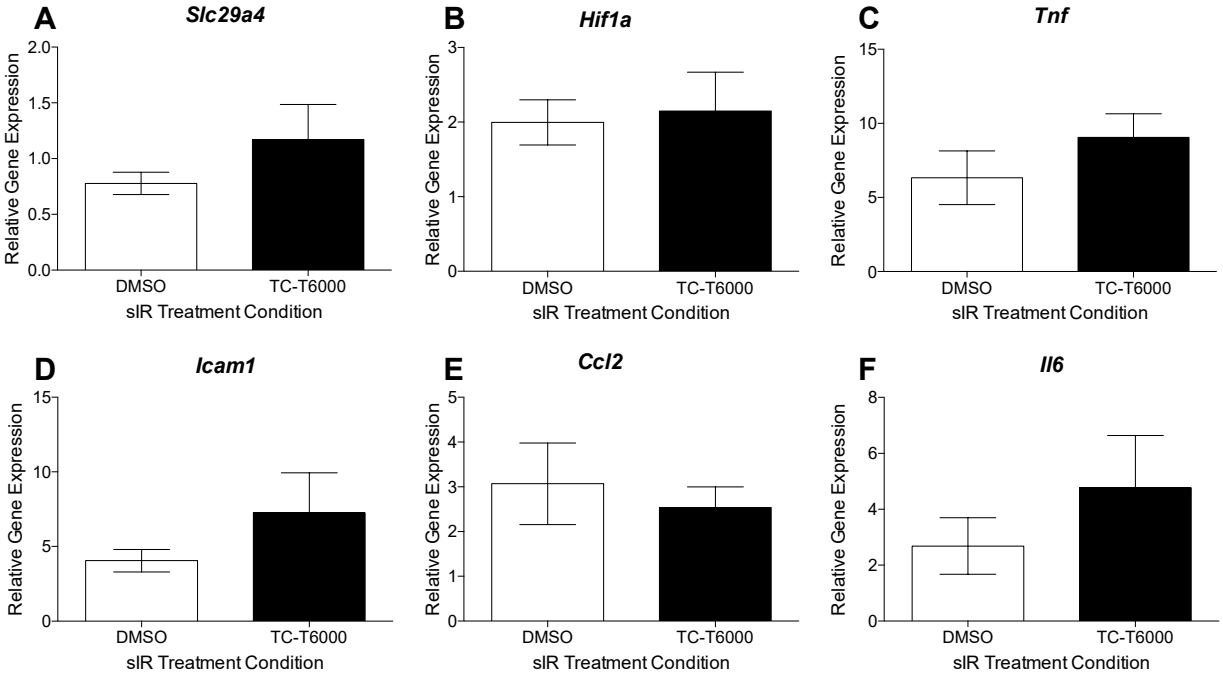

Figure 4.25. Gene expression of inflammation and hypoxia markers after simulated ischaemia in the presence of TC-T6000

qPCR analysis in HL-1 cells of ENT4, hypoxia, and inflammatory markers following 4 hours of simulated ischaemia and 2 hours of reperfusion in the presence or absence of 10 µM TC-T6000. GAPDH, β-actin and α-tubulin were used as reference gene and their geometric mean was used to calculate a normalisation index. Results were expressed as the mean ± SEM, n=6. No significant differences were observed, as determined by Student's t-test. Experiments were performed by undergraduate research project student M. Ntiamoah.

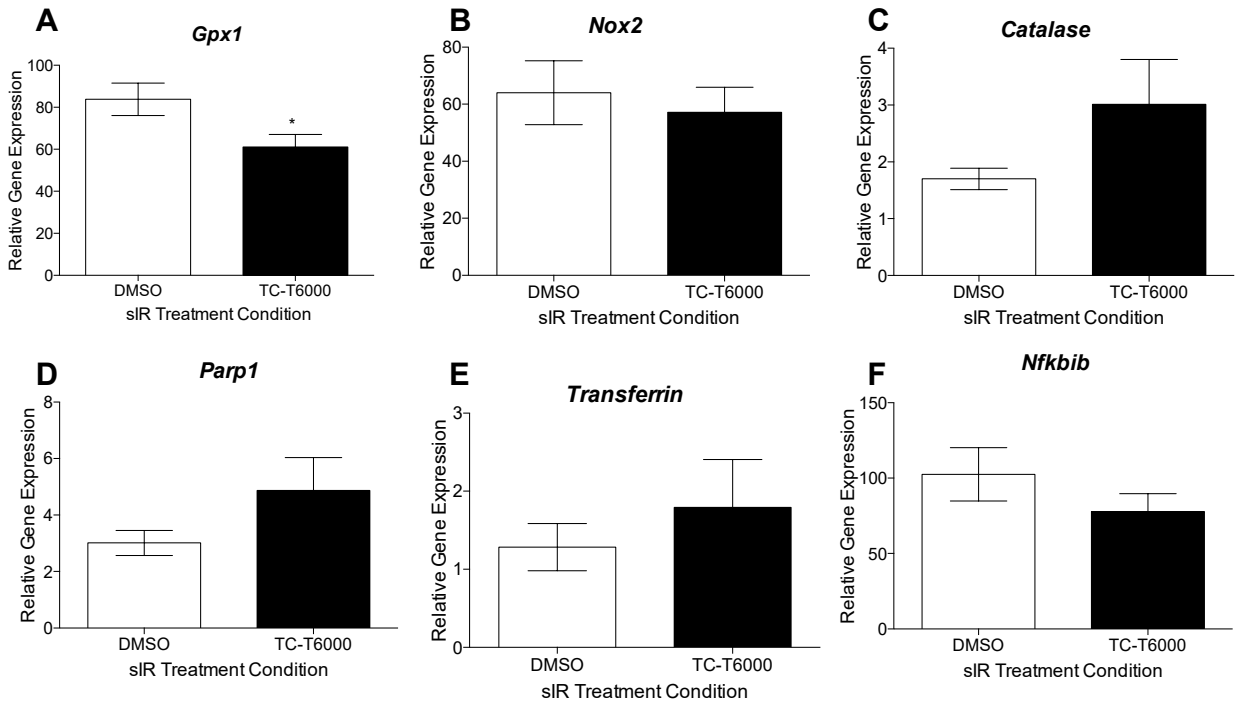

Figure 4.26. Gene expression of oxidative stress and cell death markers after simulated ischaemia in the presence of TC-T6000

qPCR analysis in HL-1 cells of oxidative stress, antioxidant, and cell death markers following 4 hours of simulated ischaemia and 2 hours of reperfusion in the presence or absence of 10 µM TC-T6000. GAPDH, β-actin and α-tubulin were used as reference gene and their geometric mean was used to calculate a normalisation index. Results were expressed as the mean ± SEM, n=6. *$p<0.05$ vs DMSO as determined by Student's t-test. Experiments were performed by undergraduate research project student M. Ntiamoah.

4.3 Exploring compensatory changes in mice with a global deletion of ENT4 (ENT4 KO)

Ex vivo and *in vivo* experiments concerning changes in cardiac and vascular function in ENT4 KO (global knockout) mice were conducted concurrently with this thesis work in collaboration with Drs Plane, Lopaschuk, and Bourque. To assist with the interpretation of data collected using these mice, potential compensatory changes that may occur with the loss of ENT4 were assessed. Three month old mice were used for *ex vivo* mesenteric vascular and *in vivo* haemodynamics studies while six month old mice were used for *ex vivo* heart perfusion studies. Therefore, gene expression analyses of mesenteric arteries were done from three month old male and female mice while gene expression analyses of the hearts were done from six month old male and female mice.

4.3.1 ENT1 protein expression remained unchanged in the hearts of ENT4 KO mice

To determine whether genetic deletion of ENT4 affected ENT1 protein expression in the heart (the major ENT in this tissue), [^{3}H]NBMPR binding, a compound selective for ENT1 at low nanomolar concentrations, was used to assess ENT1 levels. Experiments were paired between WT and KO animals and therefore potential sex- and age-related differences were not compared due to confounding factors between experimental conditions, including differences in heart sizes and thus total protein content between male and females and 3-month and 6-month animals.

There was no change in total ENT1 protein expression in the 3-month and 6-month male and female ENT4 KO hearts, as defined by the maximum specific binding (B_{max}) of NBMPR, compared to WT (Figures 4.27 and 4.28 and Table 4.3). A similar K_D (Table 4.3) across all our experiments suggests that there was consistency across different experiments and this affinity of the NBMPR binding site matched that reported previously for ENT1 (Bone *et al.*, 2010), indicating that we were indeed probing for ENT1.

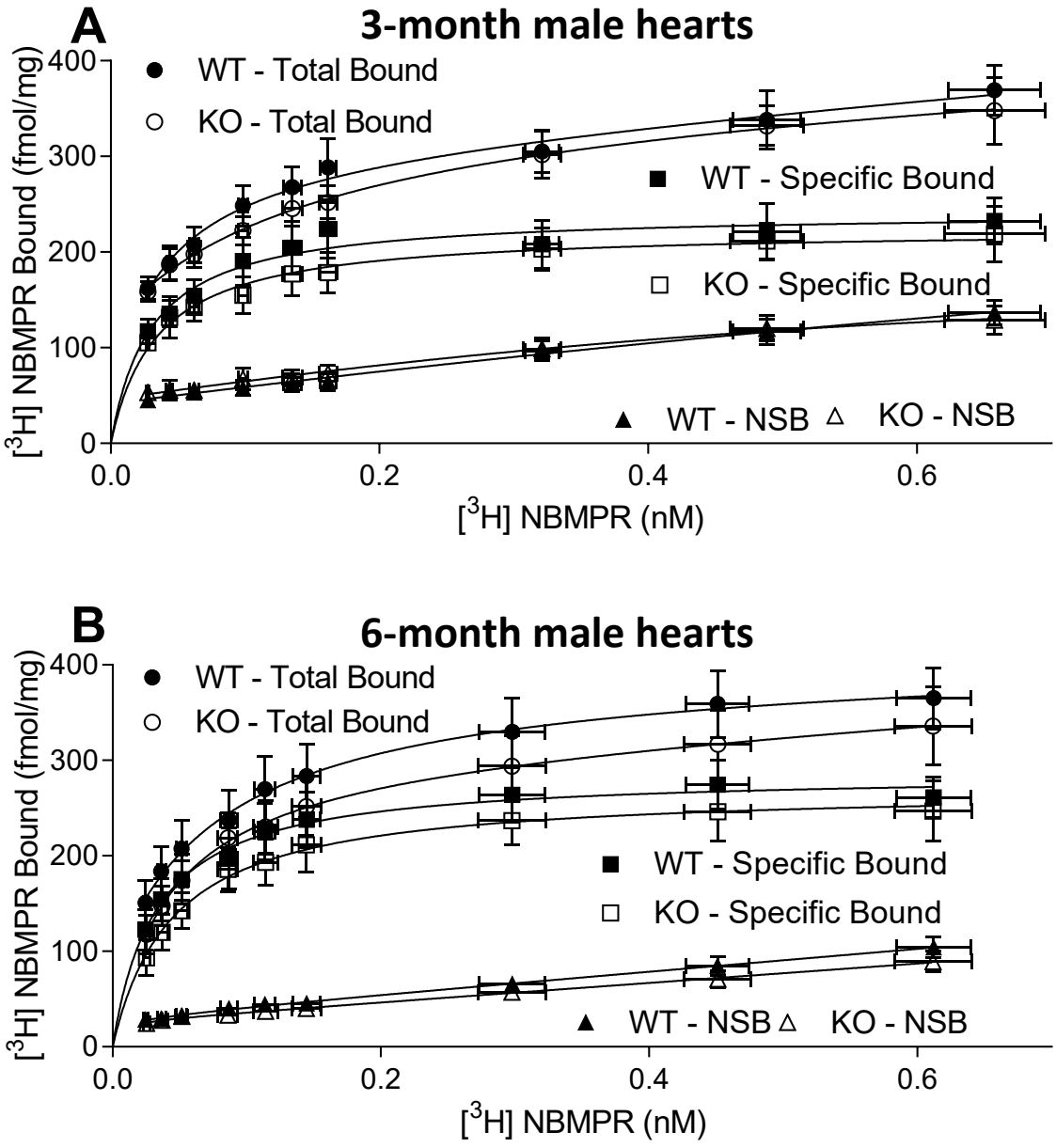

Figure 4.27. [^{3}H]NBMPR binding in male ENT4 WT and KO hearts

A & B: Crude membrane homogenates from the hearts of 3-month (A) and 6-month (B) male ENT4 WT and KO animals, respectively, were incubated with a range of concentrations of [^{3}H]NBMPR for 45 minutes to obtain total binding. 10 μM DY was added to obtain non-specific binding (NSB). Specific binding was obtained by subtracting NSB from total binding. Results were expressed as the mean ± SEM, n=6. A one-site binding model (rectangular hyperbola) was fitted to these data. No significances differences were observed, as defined by Student's t-test ($P<0.05$).

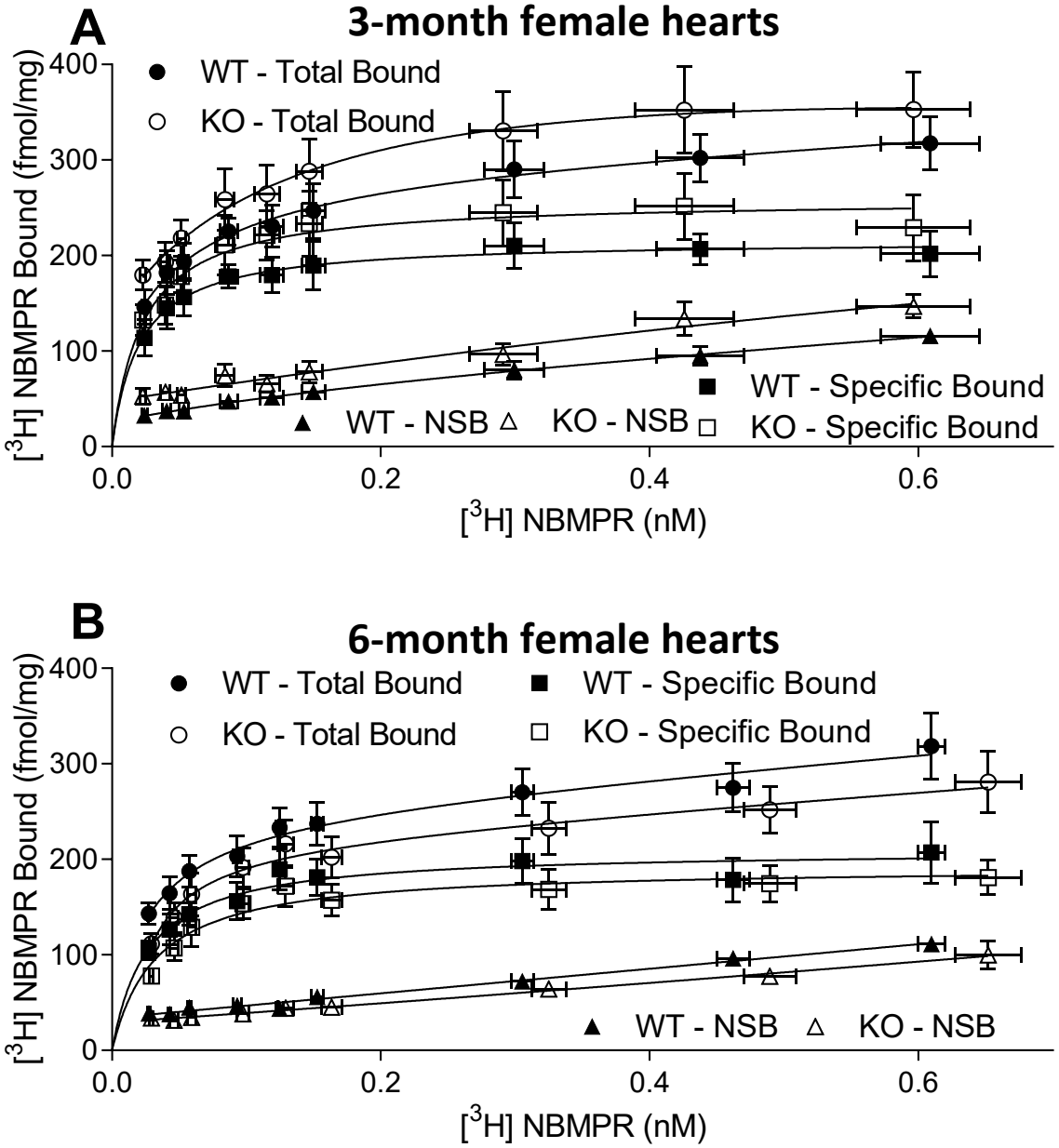

Figure 4.28. [^{3}H]NBMPR binding in female ENT4 WT and KO hearts

A & B: Crude membrane homogenates from the hearts of 3-month (A) and 6-month (B) female ENT4 WT and KO animals, respectively, were incubated with a range of concentrations of [^{3}H]NBMPR for 45 minutes to obtain total binding. 10 µM DY was added to obtain non-specific binding (NSB). Specific binding was obtained by subtracting NSB from total binding. Results were expressed as the mean ± SEM, n=6. A one-site binding model (rectangular hyperbola) was fitted to these data. No significances differences were observed, as defined by Student's t-test ($P<0.05$).

	B_{max} (fmol/mg)	K_D (nM)
3-month male WT	261.3 ± 27.9	0.034 ± 0.002
3-month male KO	223.7 ± 28.5	0.030 ± 0.003
6-month male WT	290.2 ± 21.9	0.043 ± 0.014
6-month male KO	269.6 ± 30.1	0.046 ± 0.006
3-month female WT	215.5 ± 20.1	0.022 ± 0.003
3-month female KO	259.0 ± 36.1	0.024 ± 0.005
6-month female WT	211.6 ± 27.4	0.027 ± 0.007
6-month female KO	192.4 ± 20.8	0.033 ± 0.003

Table 4.3. Data analysis from Figure 4.27 and 4.28

Maximum specific binding (B_{max}) of NBMPR and binding affinity (K_D) from each individual experiment was estimated from the specific binding data and expressed as the mean ± SEM, n=6. No significances differences compared to WT were observed, as defined by Student's t-test ($P<0.05$).

4.3.2 Characterising potential compensatory changes in expression of purinergic and serotonergic system components in hearts from ENT4 KO mice

qPCR was conducted to further investigate any compensatory changes in the expression of transporters, receptors and enzymes involved in 5-HT and adenosine metabolism/actions. Except for the increased Maob expression in 6-month male hearts, there was no differences in 5-HT related genes between the hearts from WT and ENT4 KO mice. On the other hand, hearts from ENT4 KO mice had significantly increased transcript levels for Adora2a (in 3-month females), Adora1 and Slc29a2 (in 6-month females), and Adk and Adora2b (in 6-month males) relative to hearts from age-matched WT mice (Fig 4.29, 4.30, 4.32). The unchanged Slc29a1 expression in the heart, regardless of sex and age, was consistent with our NBMPR binding data.

Interestingly, a differential regulation of Slc22a1 transcripts in the female hearts was observed, with increased expression at 3-months, but reduced expression at 6-months (Fig 4.29A and 4.30A). At 3-months old, there was a sex-dependent regulation of Slc22a3 in the heart, with reduced transcript expression in females, but increased expression in males (Fig 4.29A and 4.31A).

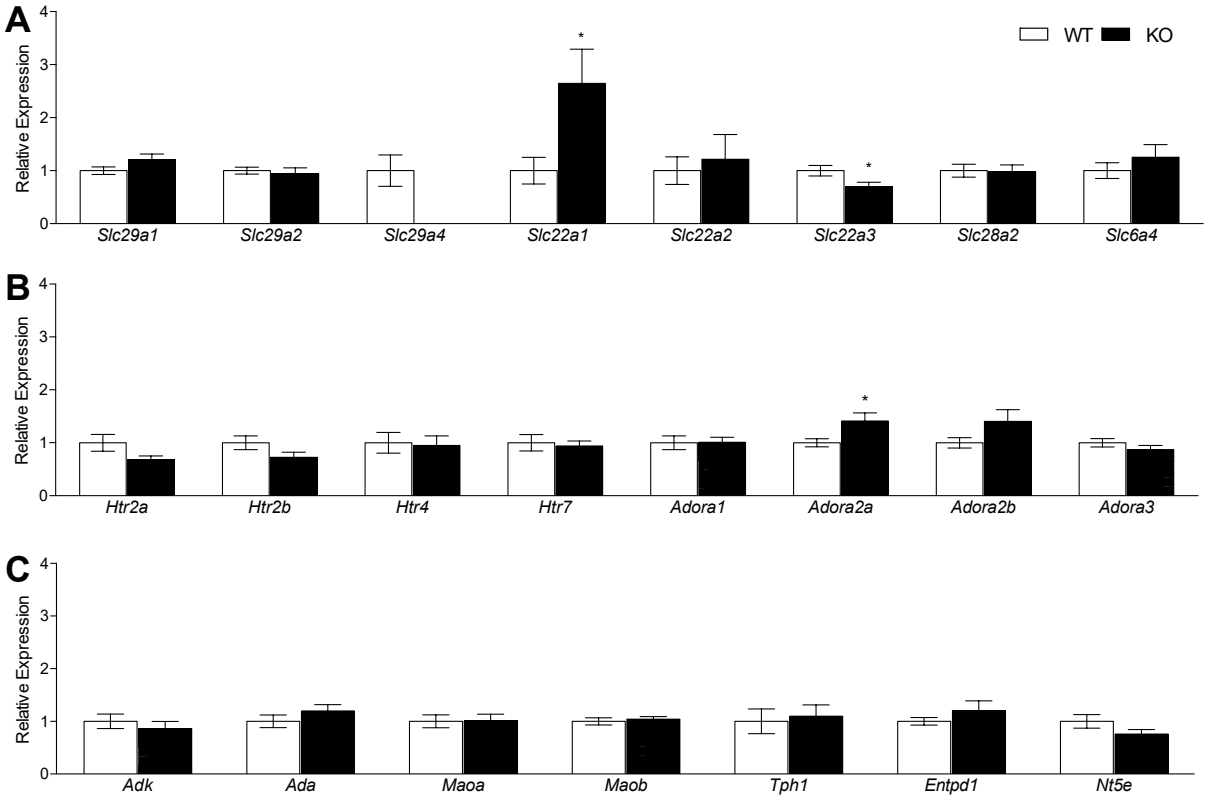

Figure 4.29. mRNA expression profile of 3-month female ENT4 WT and KO hearts

qPCR analysis of 3-month female ENT4 WT and KO heart; A: relevant transporters, B: 5-HT and adenosine receptors, and C: 5-HT and adenosine metabolising enzymes. Gene expression were normalised to GAPDH and analysed relative to expression in WT mice. Results are expressed as the mean ± SEM, n=7-8. $^{*}p<0.05$ vs WT as determined by Student's t-test.

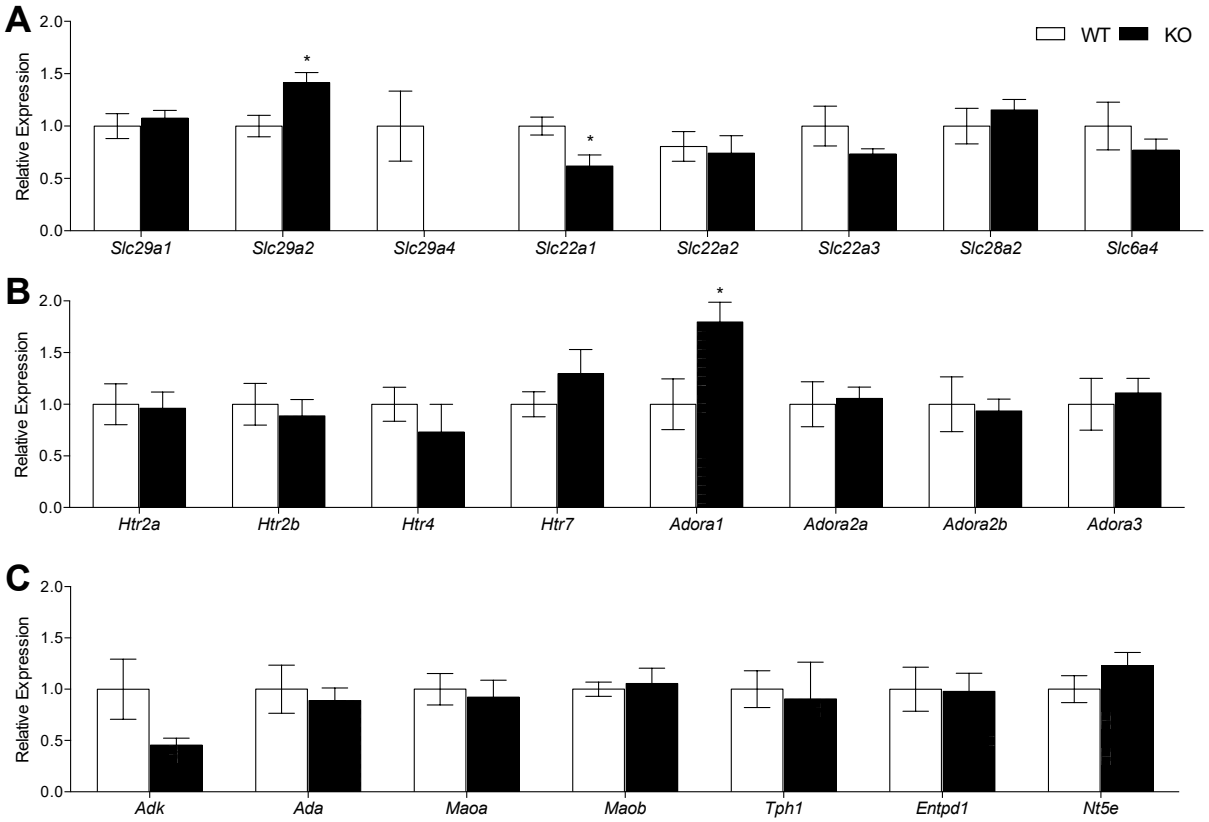

Figure 4.30. mRNA expression profile of 6-month female ENT4 WT and KO hearts

qPCR analysis of 6-month female ENT4 WT and KO heart; A: relevant transporters, B: 5-HT and adenosine receptors, and C: 5-HT and adenosine metabolising enzymes. Gene expression were normalised to GAPDH and analysed relative to expression in WT mice. Results were expressed as the mean ± SEM, n=8-9. $^{*}p<0.05$ vs WT as determined by Student's t-test.

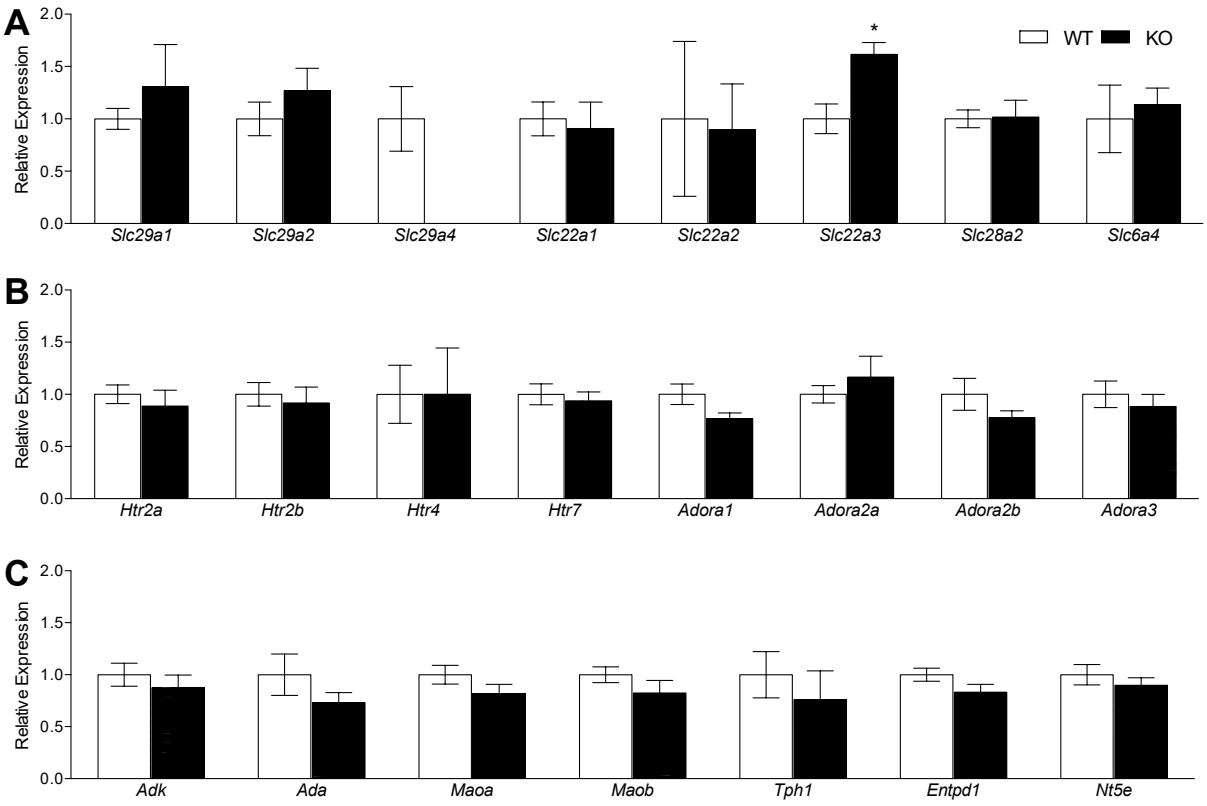

Figure 4.31. mRNA expression profile of 3-month male ENT4 WT and KO hearts

qPCR analysis of 3-month male ENT4 WT and KO heart; A: relevant transporters, B: 5-HT and adenosine receptors, and C: 5-HT and adenosine metabolising enzymes. Gene expression were normalised to GAPDH and analysed relative to expression in WT mice. Results were expressed as the mean ± SEM, n=7-8. $^{*}p<0.05$ vs WT as determined by Student's t-test.

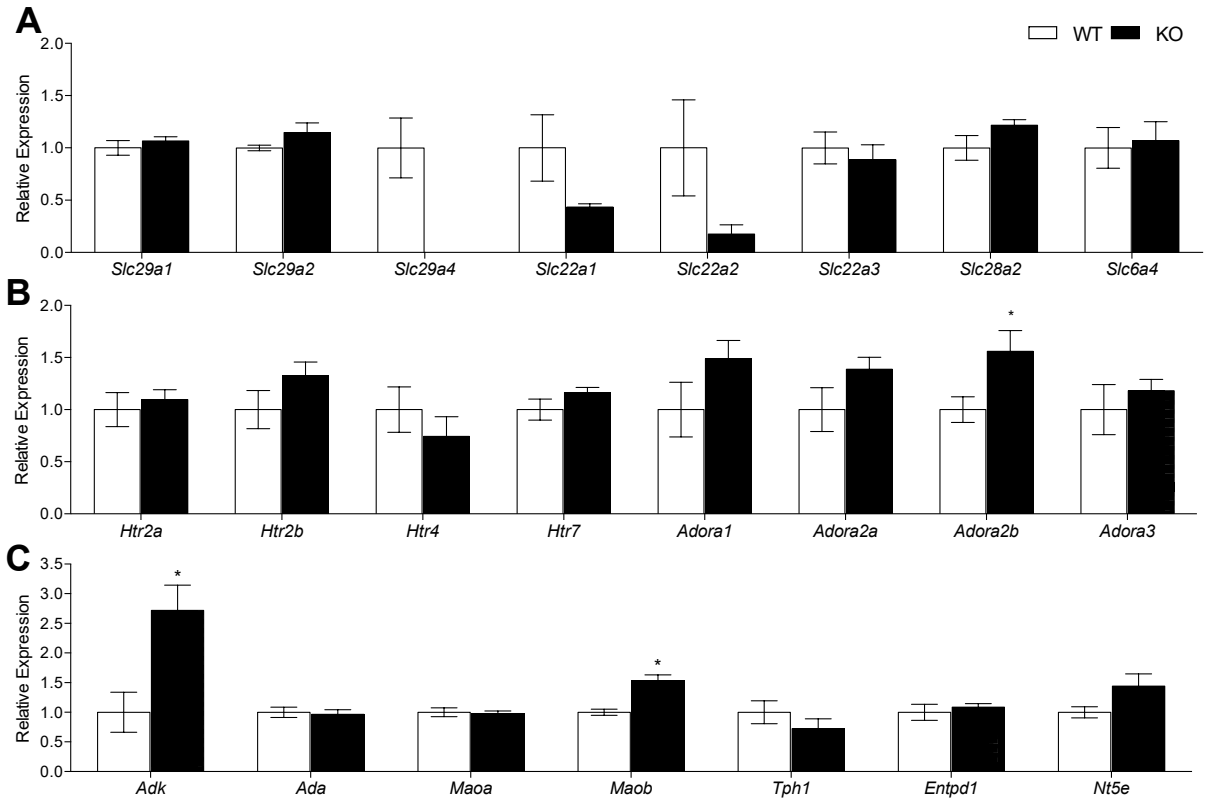

Figure 4.32. mRNA expression profile of 6-month male ENT4 WT and KO hearts

qPCR analysis of 6-month male ENT4 WT and KO heart; A: relevant transporters, B: 5-HT and adenosine receptors, and C: 5-HT and adenosine metabolising enzymes. Gene expression were normalised to GAPDH and analysed relative to expression in WT mice. Results were expressed as the mean ± SEM, n=7-8. $^{*}p<0.05$ vs WT as determined by Student's t-test.

4.3.3 Characterising potential compensatory changes in expression of purinergic and serotonergic system components in the mesenteric vessels from ENT4 KO mice

To complement functional studies being performed on the mesenteric vessels in ENT4 WT and KO mice, we investigated compensatory changes in the expression of transporters, receptors and enzymes involved in 5-HT and adenosine metabolism/actions from mesenteric arteries isolated from WT and ENT4 KO mice. Interestingly, no changes in 5-HT related genes (Fig 4.33 and 4.34) was observed, suggesting that the observed phenotype in our functional studies is unlikely to be due to the actions of 5-HT. Differential regulation of adenosine related genes in the mesenteric vessels was observed, with reduced expression of Slc28a2 in females and increased expression of Slc28a2 in males (Fig 4.33A and 4.34A). In addition, an increase of Adora2a in female mesenteric arteries, and reduced of Adora2b in the male mesenteric arteries from ENT4 KO mice, relative to those from WT mice was observed (Fig 4.33B and 4.34B). On the other hand, Slc22a2 were similarly reduced in both male and female in the ENT4 KO animal.

In the mesenteric arteries from male ENT4 KO mice, an increased expression of Ada and Slc29a2 was also observed (Fig 4.36A & C), suggesting that ENT4 may play a role in regulating adenosine flux and that adenosine deaminase and ENT2 compensated for the loss of ENT4 activity. There is also an increase in the expression of Nos2 and reduced Ptgs2 (Fig 4.36D) in the male ENT4 KO mesenteric arteries, suggesting potential changes in vascular regulation in the ENT4 KO mice.

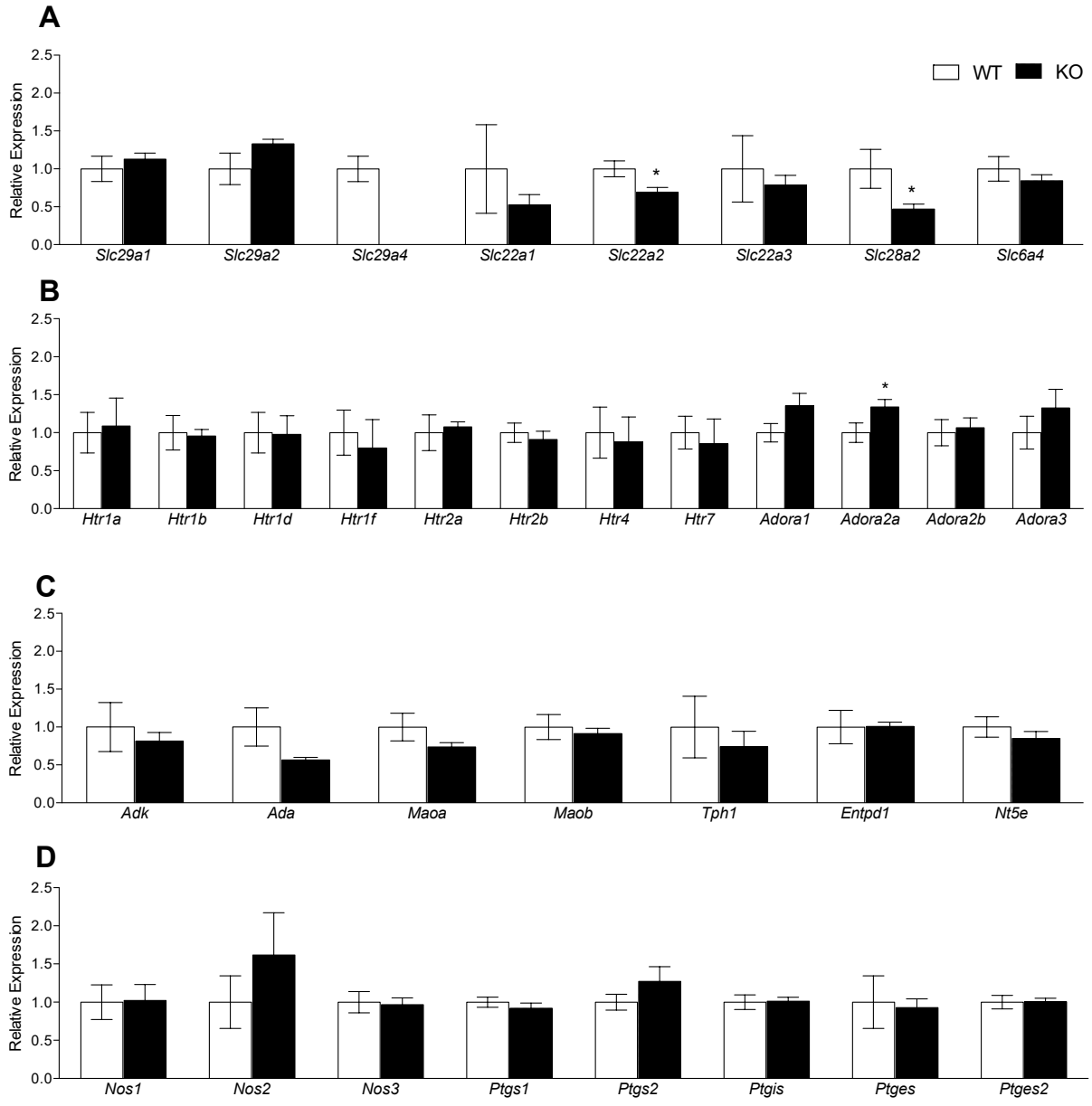

Figure 4.33. mRNA expression profile of 3-month female ENT4 WT and KO mesenteric vessels

qPCR analysis of 3-month female ENT4 WT and KO mesenteric vessels; A: relevant transporters, B: 5-HT and adenosine receptors, C: 5-HT and adenosine metabolising enzymes, and D: enzymes involved in regulation of vascular function. Gene expression were normalised to GAPDH and analysed relative to expression in WT mice. Results were expressed as the mean ± SEM, n=6-8. $^{*}p<0.05$ vs WT as determined by Student's t-test.

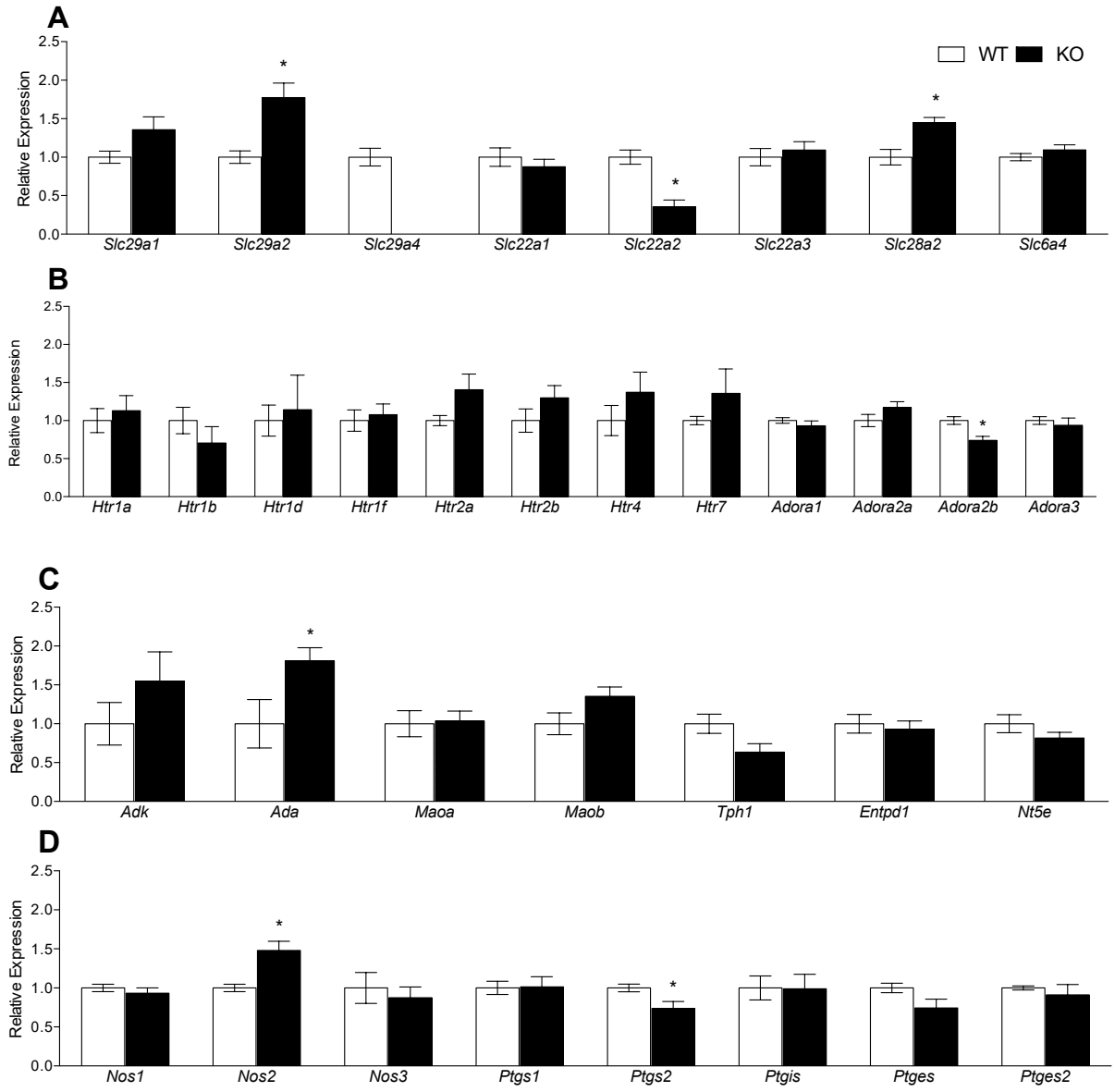

Figure 4.34. mRNA expression profile of 3-month male ENT4 WT and KO mesenteric vessels

qPCR analysis of 3-month male ENT4 WT and KO mesenteric vessels; A: relevant transporters, B: 5-HT and adenosine receptors, C: 5-HT and adenosine metabolising enzymes, and D: enzymes involved in regulation of vascular function. Gene expression were normalised to GAPDH and analysed relative to expression in WT mice. Results were expressed as the mean ± SEM, n=8-9. $^{*}p<0.05$ vs WT as determined by Student's t-test.

5. Discussion

5.1 PK15-NTD as a model to study ENT4

The overarching goal of this project was to better characterise ENT4 as a nucleoside transporter and determine whether it might potentially be a novel therapeutic target for cardiac IRI. Before we were able to study ENT4, we had to characterise a cell model to study ENT4 in isolation and without any confounding factors that comes with the presence of other nucleoside transporters. Past studies have used both MDCK cells (Engel *et al.*, 2004) and *Xenopus oocytes* (Barnes *et al.*, 2006). However, they are not an ideal model as the former has endogenous ENT1 whilst the latter has a large filling volume and a hydrophobic intracellular yolk mass that can complicate the time required to reach transport equilibrium and kinetic analyses. We have previously used the PK15-NTD model to study the main nucleoside transporter, ENT1 (Hughes *et al.*, 2015). Although PK15-NTD has been characterised as a null-background cell model, the time used to assess transport kinetics has been in seconds. ENT4 has a much slower transport kinetics, up to 15 minutes, and it may not have been detected in previous studies on PK15-NTD cells. Therefore, whether PK15-NTD is truly nucleoside transport deficient over 15 minutes was assessed.

PK15-NTD cells do not have any functional acidic pH-sensitive nucleoside or 5-HT uptake which would have been suggestive of the presence of ENT4. Though devoid of known NTs (CNTs & ENTs), accumulation of 2CADO was modestly reduced in the presence of supra-physiological levels of adenosine and adenine under neutral and acidic conditions (Fig 4.10). This suggests that, albeit slow and insignificant, 2CADO is getting into PK15-NTDs. This can potentially be diffusion or another NT that is either expressed at low levels in PK15-NTDs or has a low affinity for nucleosides/nucleobases. This might be the SLC43A3-encoded equilibrative nucleobase transporter 1 (ENBT1) that was inhibited by 1 mM 2CADO (Furukawa *et al.*, 2015; Ruel *et al.*, 2019) and was found to be present in the PK15-NTD cells (Bone *et al.*, 2007). The apparent accumulation of 5-HT over 15 minutes in the PK15-NTD cells that is not acidic pH sensitive (Fig 4.3) also suggests the presence of a different 5-HT transporter, especially since the PK15-NTDs were selected for their deficiency of nucleoside transporters, not 5-HT transporters. As the observed uptake was not sensitive to acidic pH, it is unlikely to be SERT. Sodium dependent transporters are inherently

pH sensitive as the homeostasis of sodium and hydrogen ions are linked by the NHE system. With an inward proton gradient across the plasma membrane, this would create a larger inward sodium gradient as H^+ ions are exchanged for Na^+ via the NHE system. In peripheral tissues, SERT also mainly functions in platelets (Watts, 2005), and making it less likely to be found in PK15s.

The other known transporter is OCT3 which has been shown to have a K_m of 988 ± 264 µM for 5-HT in *Homo sapiens* (Duan *et al.*, 2010) and is a sodium independent transporter. OCT3 have also been shown to be expressed in mammalian kidneys (Wu *et al.*, 2000) and is not acidic pH-sensitive (Massmann *et al.*, 2014). Although there have not been any investigations on the expression of OCT3 in PK15-NTD cells, it's likely that the 5-HT uptake observed in PK15-NTD is mediated by OCT3. 20 µM corticosterone was included in the assay to suppress any endogenous activity of OCT3, but this was assuming that there were negligible species differences between *Homo sapiens* and *Sus scrofa*. Corticosterone was shown to inhibit human OCT3 with an IC_{50} of 0.29 ± 0.04 µM and a 100-fold selectivity over other OCTs (Hayer-Zillgen *et al.*, 2002). Human OCT1 have also been shown to be capable of mediating 5-HT uptake, with a K_m of 197 ± 42 µM (Boxberger *et al.*, 2014). As OCT1 has been found to be expressed in kidneys (Koepsell, 2004), it is plausible that both OCT 1 and 3 contributed to the observed 5-HT uptake in PK15-NTD cells.

A nominally sodium-free (NMG^+) buffer where sodium is replaced with either NMG^+ or choline chloride is commonly used when studying recombinant ENT function to eliminate any potential contribution by the sodium-dependent CNTs (Ward *et al.*, 2000; Endres *et al.*, 2005; Hughes *et al.*, 2015). However, ENT4 is sensitive to membrane potential (Engel *et al.*, 2004) and therefore we would need to use a regular sodium-containing physiological buffer. Figure 4.1B shows that PK15-NTD cells do not have any sodium-dependent 2CADO uptake over 15 minutes suggesting that CNTs will not be a confounding factor when we are using the PK15-NTD cells to study ENT4. Therefore, the PK15-NTD cells were stably transfected with SLC29A4, creating the PK15-hENT4 cells.

5.2 2-Chloroadenosine as a substrate for ENT4

Consistent with the literature (Engel *et al.*, 2004; Barnes *et al.*, 2006), though in a different cell model, an acidic pH-sensitive 5-HT (Fig 4.3A) and adenosine (Fig 4.4A) uptake was demonstrated in the PK15-hENT4 cells. This provides the functional data, in addition to mRNA and protein expression, that we have a cell model where we can study human ENT4 in isolation. We further showed that the uptake of adenosine is inhibited by 2CADO in a concentration dependent manner in PK15-hENT4 cells. This suggests that 2CADO may be a substrate for ENT4, and we did further transport kinetic experiments to confirm this. Previous work by different groups assessing ENT4 function as a nucleoside transporter have made use of adenosine (Barnes *et al.*, 2006; Zhou *et al.*, 2010; Wang *et al.*, 2013), a compound that is rapidly metabolised intracellularly, giving it an exceptionally short half-life of approximately 10 seconds (Conti, 1991). Using the PK15-hENT4 cells, we showed that 2-CADO, a more suitable experimental tool for defining nucleoside transport kinetics, is a substrate of ENT4 and can be used as an alternative to study ENT4 as a nucleoside transporter. To minimise metabolism and trapping of [^{3}H], however, it was still found to be necessary to conduct the assays in the presence of ABT-702, an adenosine kinase inhibitor. While 2CADO has previously been described as being a weaker substrate for adenosine kinase than adenosine (a 2-fold lower affinity) (Lin *et al.*, 1988), it can still be phosphorylated and thereby 'trapped' in cells as phosphorylated metabolites, and this became a significant factor in this work due to the slow kinetics of ENT4 flux. ABT-702 did not affect 2CADO initial rate but did affect the total accumulation of 2CADO, suggesting that it minimised 2CADO metabolism and did not inhibit ENT4 directly. It also did not affect ENT4-mediated 5-HT uptake (Fig 4.3A), providing further evidence that ABT-702 does not directly inhibit ENT4.

While some studies have shown that ENT4 transports nucleosides only under acidic pH conditions (Barnes *et al.*, 2006), others have shown that there is some ENT4-mediated flux of adenosine at neutral pH in some models (Zhou *et al.*, 2010). Consistent with the latter study, a component of the ENT4-mediated uptake of 2CADO did occur at neutral pH in the PK15-hENT4 cells. This was supported not only by the K_m/V_{max} data, where mediated uptake at neutral pH became apparent at higher 2CADO concentrations (Fig 4.7A), but also the inhibition data by D22 and TC-T6000 (Fig

4.8G). Together with the trend where 10 µM D22 (though not significant) inhibited ENT4-mediated adenosine uptake below levels measured at pH 7.5 (Fig 4.5B), this further suggests that ENT4 transport nucleosides at both acidic and neutral pH, like that described for monoamines. In addition, the HL-1 data show that ENT4 exhibits a neutral pH-mediated uptake for adenosine. In the presence of D22 and TC-T6000, this uptake was completely abolished and below the levels observed at neutral pH (Fig 4.22A & B). Interestingly, while our data suggests that D22 and TC-T6000 are likely capable of inhibiting both the acidic pH-sensitive and neutral pH-mediated component of ENT4, MPP^+ may selectively inhibit the acidic pH-sensitive component (Fig 4.8). Therefore, MPP^+, as a charged molecule, might only be competing with 2CADO for the acidic pH-sensitive component in ENT4.

Together with ENT4 kinetic data demonstrated by 2 different groups using adenosine (Barnes *et al.*, 2006; Zhou *et al.*, 2010), the kinetics of 2CADO transport also suggests that ENT4 functions as a low-affinity, high capacity nucleoside transporter (Fig 4.7). Though ENT4 has an approximately 20-fold lower affinity for adenosine than ENT1, we are hypothesising that ENT4 plays a pathophysiological role under conditions where adenosine concentrations are markedly elevated. Despite having a low affinity (relatively higher K_m compared to other NTs) for adenosine or 2CADO, a time-course analysis showed that ENT4 is still capable of mediating nucleoside transport at substrate concentrations as low as 1 µM (Fig 4.5) and 10 µM (Fig 4.20), suggesting that it remains a relevant transport system *in vivo*, especially under pathophysiological conditions. ENT4 is also a unique transporter within the nucleoside transporter family whereby it has much slower transport kinetics (in minutes), compared to other NTs such as ENT1 where equilibrium is reached within seconds (Hughes *et al.*, 2015).

Most of the known inhibitors ENT1 and ENT2 inhibited ENT4 only at concentrations in excess of 1 µM (more than 100-fold higher than their K_i values for ENT1 and ENT2). The exception was DY which significantly inhibited ENT4 at 1 µM. This suggests that although DY can be used experimentally to suppress endogenous nucleoside transport activity (ENT1 and 2), it also affects ENT4 and cannot be used to isolate ENT4 in an endogenous cell line. Uridine, on the other hand,

does not affect ENT4 even at concentrations as high as 3 mM (Fig 4.9). This amount of uridine would be expected to inhibit all other NTs, so uridine can be used to inhibit all non-ENT4-mediated purine flux in endogenous cell models that expresses multiple nucleoside transporter subtypes.

Interestingly, a reduced accumulation of 2CADO (mediated by ENT4) in the presence of 10 mM adenine was observed, and a similar trend was seen for 300 µM 6-MP (Fig 4.10). Catalysed by adenine phosphoribosyltransferase, adenine can be converted to AMP (Pedley *et al.*, 2017) and thereby affect intracellular adenosine-AMP homeostasis. Adenosine can be metabolised to inosine and eventually hypoxanthine. Hypoxanthine is in turn metabolised to xanthine and uric acid by xanthine oxidase (XO) (Marro *et al.*, 1997). 6-MP might minimise adenosine metabolism (to a lesser extent than adenine) by competing for XO as 6-MP is metabolised by XO to 6-thiouric acid (Cuffari *et al.*, 1996).

The PK15-NTD cells are suitable to perform functional studies for nucleoside transporters in isolation and therefore we transfected human ENT4, creating the PK15-hENT4. Since they are not a human-based cell model and might not be suitable for future studies looking at regulation of ENT4, HEK239 cells were looked at as a possibility for this purpose. As there is no selective inhibitor for ENT2, we first deleted ENT2 by the CRISPR/Cas9 system. A null background HEK293 cell line, lacking both ENT1 and ENT2, was created subsequent to these studies. As there is no sodium-dependent uptake over 15 minutes, CNTs do not have to be knocked out. There was also no acidic pH-sensitive 2CADO uptake in the HEK293-ENT2KO cells, which would have been characteristic of endogenous ENT4. This suggests that HEK293 can be used as a base cell to study ENT4 after knocking out ENT1 and ENT2.

5.3 ENT4-mediated nucleoside efflux: Potential implications in cardiac ischaemia-reperfusion injury

After establishing that 2CADO is a substrate for ENT4, 2CADO was used as a substrate to study nucleoside efflux by ENT4. Adenosine was not used for efflux studies as it is rapidly metabolised

and thus deemed unsuitable for efflux studies. Engel *et al.* 2005 showed that ENT4 is capable of mediating MPP^+ efflux but did not investigate how pH affects this. We, therefore, investigated this and showed that 2CADO efflux was enhanced under acidic conditions (Fig 4.11). D22, but not TC-T6000, significantly inhibited the enhanced efflux observed at pH 6.0. As ENT4 inhibitors could not be pre-incubated as 2CADO was loaded into PK15-hENT4 cells for our efflux studies, we looked at whether D22 and TC-T6000 were capable of inhibiting ENT4 when given concurrently with 2CADO (without any pre-incubation). ENT4-mediated 2CADO uptake was inhibited to the same extent, with and without pre-incubation with these inhibitors.

The efflux data further suggests that ENT4 might play a pathophysiological role in mediating the efflux of intracellular adenosine pools that accumulated during ischaemia, and thus worsening recovery of cardiac function during reperfusion. As ENT4 is more active under acidic conditions, this indicates that ENT4 may be more active and contributing to this efflux during the early stages of reperfusion before the recovery of acidic conditions in the heart. It would therefore be interesting to investigate whether inhibition of ENT4 solely during reperfusion is able to afford any cardio-protection. Intracellular nucleotide pools can be quantified following an IRI in the presence or absence of an ENT4 inhibitor in an *ex vivo* isolated heart perfusion model. If it preserves intracellular nucleotide pools and improves recovery, this will have clinical translation potential; one may be unable to predict an ischaemic insult but it's clinically feasible to inhibit ENT4 during reperfusion.

5.4 Protonation of ENT4, not a proton gradient, is likely responsible for enhancement of ENT4 activity at acidic pH

Enhanced transport activity at acidic pH may reflect either proton-coupled substrate transport, or amino acid protonation leading to conformational changes in the transporter. If it is due to proton-coupled transport, influx and efflux via ENT4 should be differentially affected by changing extracellular pH. However, 2CADO efflux, like influx, was enhanced with an extracellular acidic pH. This suggests that ENT4 acidic pH sensitivity is not dependent on a proton gradient across the plasma membrane. If it was proton gradient driven, efflux would have been reduced when

extracellular pH is acidic and enhanced when extracellular pH is basic. The concept that ENT4 is not proton coupled is also supported by the finding that a proton gradient across the plasma membrane is not maintained during the time course used to assess both influx and efflux, and that ENT4-mediated 2CADO uptake is still present even in the presence of nigericin (where a proton concentration gradient across the plasma membrane is absent). Therefore, the acidic pH sensitivity may reflect protonation of transporter amino acids. Interestingly, the pH sensitivity of another member of the ENT family, ENT3, has recently been shown to be due to protonation of two amino acids (Asp-219 and Glu-447) (Rahman *et al.*, 2017). Performing a protein sequence alignment of human ENT3 with ENT4 using Clustal Omega (Sievers *et al.*, 2011), Glu-447 in ENT3 matched with Glu-481 in ENT4 (Fig 5.1). Although Asp-219 did not have a matching amino acid in ENT4, Asp-226 in ENT4 (matching with Asp-225 in ENT3) remains a potential candidate. Asp-225 in ENT3, however, was shown to not be involved in its pH dependence. In ENT4, Glu-448 is a likely candidate and whether Asp-226 is also involved remain to be investigated. The protonation of these residues of ENT4 may result in a conformational change that increases its transport efficiency. As the V_{max} is affected under acidic conditions (Engel *et al.*, 2004; Engel *et al.*, 2005), it remains plausible that conformational change resulted in the opening of an acidic pH-sensitive permeation pathway, in addition to a permeation pathway under neutral conditions. It is also possible that ENT4 undergoes a post-translational modification and regulation under acidic conditions that increases the amount of active ENT4 on the surface of membranes. Further site-directed mutagenesis studies on ENT4, starting with Glu-448 and Asp-226, will have to be performed to test this hypothesis, and to provide direct evidence.

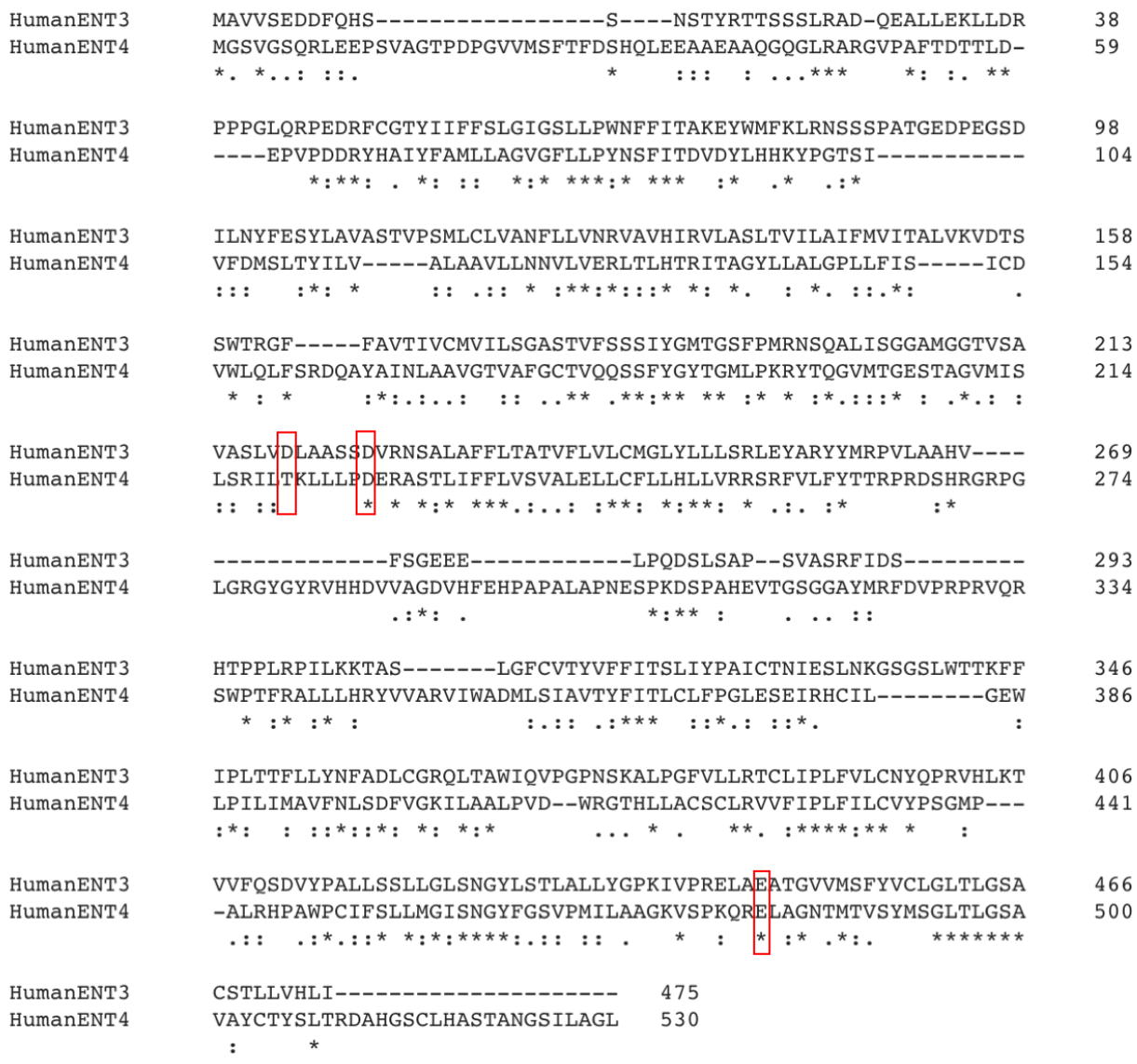

Figure 5.1 Protein sequence alignment of hENT3 and hENT4

hENT3 (*Accession number*: NP_060814.4) protein sequence was aligned to hENT4 (*Accession number*: NP_001035751.1) using Clustal Omega (Sievers *et al.*, 2011). Asp-219 and Glu-447 in hENT3 is involved in its acidic pH-sensitivity, and was matched to Thr-220 and Glu-481 in hENT4 respectively. Although Asp-225 in hENT3 was shown to not be involved in its acidic pH-sensitivity (Rahman *et al.*, 2017), it was aligned with Asp-226 in hENT4 (the closest match to Asp-219 in hENT3). When hENT3 is aligned to hENT4, only 24% of the amino acids are identical to hENT4. Only 21% of the amino acids in hENT4 are identical to the sequence in hENT3. * (asterisk) represents a fully conserved residue, . (period) represents conserved residues with weakly similar properties and : (colon) represents conserved residues with weakly similar properties.

The NH_4Cl method of intracellular acidification was used to test whether decreasing intracellular pH affected ENT4-mediated 2CADO uptake. This acidification will hypothetically reduce ENT4 uptake if it is dependent on a proton gradient. ENT4 activity was reduced with increasing incubation NH_4Cl periods (4, 8 and 12 minutes; Fig 4.14A), but this was not due to an increasing severity of acidification (Fig 4.15C). This suggests that the reduced ENT4 activity was not due to the severity of acidification observed or the gradual loss of the proton gradient, but rather due to the increasing time of incubation with NH_4Cl itself.

The above-mentioned observation was similarly observed when NH_4Cl was replaced with NMG^+ (Fig 4.14B). This further suggests that the observed decrease in ENT4 function is not due to changes in intracellular pH. NMG^+ is a membrane impermeable compound used to maintain ionic balance in sodium-free (NMG^+) buffers and therefore is unlikely to have caused intracellular acidification. Figure 4.15A and B also showed that this decrease in ENT4 function when pre-incubated with NH_4Cl or NMG^+ buffers is not due to changes in membrane depolarisation which would have reduced ENT4 activity (Engel *et al.*, 2004).

Another possibility for the decrease in ENT4 activity is the alkalisation of the extracellular buffer due to the efflux of 50 mM NH_3 into the medium (Fig 3.1) as ENT4 activity is acidic pH-sensitive. Although the overall pH of the extracellular buffer remained unchanged (Fig 4.15D), it remains possible that the localised pH environment of the transporter was alkaline due to the local NH_3 efflux. To eliminate this possibility, we incubated the cells in a sodium-free (NMG^+) buffer for 1 minute after incubation with NH_4Cl buffers before initiating uptake. This incubation with NMG^+ buffer will allow NH_3 efflux and be removed and yet trapping H^+ ions and maintaining acidification in the intracellular space as the NHE system is inactive. However, a minute incubation with NMG^+ buffer affected ENT4 activity and therefore we were unable to directly assess the influence of 50 mM NH_3 efflux (Fig 4.14C).

Since there was evidence that protonation of ENT4 is responsible for its enhanced activity at acidic pH, and a proton gradient is not required, we also hypothesise that intracellular acidification

alone will be sufficient to increase ENT4 activity. We investigated this by inducing intracellular acidification using ammonium chloride (Fig 3.1). However, the intracellular acidification induced by NH_4Cl was not maintained beyond 5 minutes in the PK15-hENT4 cells (Fig 4.16B). This is not long enough to assess its effect on ENT4 activity given the relatively slow kinetics of this transporter. An alternative method to induce intracellular acidification might be to inhibit the sodium-hydrogen exchanger using cariporide (Lam *et al.*, 2013). Whether this approach would produce prolonged acidification in PK15 cells remain to be investigated. If intracellular acidification alone, however, is unable to increase ENT4 activity, this strongly suggests that the residue(s) being protonated that is involved in ENT4 pH dependence is on the extracellular face of the protein.

5.5 Investigating *in vitro* cell models for assessment of endogenous ENT4 regulation

An *in vitro* cell model was sought to assess endogenous regulation of ENT4 by cardiac IRI. The PK15-hENT4 cells only have the coding region of ENT4 transfected, and do not contain the promoter region which might be important for transcriptional regulation during ischaemia. Although ENT4 has previously been shown to be expressed in human umbilical vein endothelial cells and HL-1 cardiomyocytes (Barnes *et al.*, 2006), they did not investigate the functional presence of ENT4.

5.5.1 HMEC-1, immortalised human dermal microvascular endothelial cells

HMEC-1 cells were investigated as a potential model to study endogenous ENT4 function. A pH- and sodium-dependent 2CADO uptake was observed, suggesting that CNTs contribute to 2CADO uptake in HMEC-1. Although this might suggest the presence of ENT4, this might also/alternatively be due to the functional presence of other NTs (both ENTs and CNTs). Therefore, 2CADO uptake by ENT1 and 2 was blocked with 500 nM DY. A greater accumulation of 2CADO was unexpectedly observed in the presence of DY, but this accumulation was only seen in the presence, not absence, of sodium. This suggests that under acidic conditions, 2CADO is being taken up by the sodium-dependent CNTs as there is a greater inward sodium gradient that was created by an inward proton gradient (via the NHE system). In the absence of DY, 2CADO exits

the cell via ENT1 and 2 when the intracellular concentration is higher than the extracellular concentration. Therefore, the contribution of CNTs-mediated 2CADO influx was masked and the concentration gradient of 2CADO remains balanced. In the presence of DY, however, ENT1 and 2 is inhibited and would not be able to mediate the efflux of 2CADO that was taken up by CNTs. 2CADO will continue to be taken up by CNTs in a concentrative manner (and stay in the cell) as long as sodium gradient is maintained. This will lead to a greater intracellular 2CADO concentration, relative to extracellular concentration (Fig 4.18B).

To isolate ENT4 activity (if present), 3 mM uridine was used to competitively inhibit ENT1 and 2 and CNTs. The absence of an acidic pH-sensitive 2CADO uptake, however, suggests that ENT4 is not functionally present in HMEC-1 cells under basal conditions (Fig 4.18C). Therefore, these cells are also not suitable as a model to investigate endogenous ENT4 function.

5.5.2 HL-1 cardiomyocytes as a model to study the role of ENT4 in ischaemia reperfusion injury

As HMEC-1 cells do not exhibit ENT4 activity, HL-1 cardiomyocytes were investigated next. HL-1 cardiomyocytes demonstrated an acidic pH-sensitive 2CADO and adenosine uptake that was inhibited by known ENT4 inhibitors. This suggests that ENT4 is functionally present in these cells and can be used as a model to study endogenous regulation of ENT4 by IRI. We showed that mouse ENT4 is functionally suppressed after simulated ischaemia, but recovers upon reperfusion in HL-1 cardiomyocytes (Fig 4.22). A similar decrease in Slc29a4 expression was observed after simulated ischaemia, but this remained even after reperfusion (Fig 4.23C). This suggests the involvement of both post-translational and transcriptional processes in the down-regulation of ENT4 activity in these simulated ischaemia and reperfusion conditions.

These data do not directly support our hypothesis that ENT4 activity and its contribution to adenosine flux is increased during ischaemia. However, it does suggest that ENT4 activity is modified (reduced) during ischaemia and this might be a protective mechanism that the heart adopts to minimise the loss of intracellular nucleotide pools. By reducing ENT4 activity during ischaemia, the heart retains the intracellular nucleotide pools that accumulate due to the

breakdown of ATP. This would allow the re-phosphorylation and regeneration of intracellular ATP pools, and improve recovery of contractile function.

It should be investigated whether the further inhibition of ENT4 is cardio-protective and beneficial for the recovery of cardiac function. Since an acidic pH-sensitive 2CADO uptake was still observed during ischaemia, this inhibition will be more selective for ischaemic tissues than ENT1. However, the component that was not sensitive to acidic-pH was not affected by ischaemia. This suggests that ENT4 inhibitors will not be devoid of the coronary steal phenomena but rather a reduced coronary steal phenomena, relative to ENT1 inhibitors.

In the simulated ischaemia-reperfusion model, an increase in Hif1a expression was not observed. This might be due the relatively short hypoxic period as an increase in HIF-1α protein was observed by others after 12 hr of hypoxia (Eltzschig *et al.*, 2005). Hif1a expression is also less representative as expression of HIF-1α protein is constantly degraded under normoxic conditions, but gets stabilised under hypoxic conditions (Dengler *et al.*, 2014) and therefore, looking at HIF-1α activity and/or protein levels would be more relevant. An increased expression of Parp1 after sI, but not sIR, relative to sham conditions was observed (Fig 4.24D). This contrasts with an increase in PARP-1 activity following sIR in cultured adult rat cardiac myocytes (Tao *et al.*, 2010). An increase in Tnf after sIR, but not sI, compared to sham conditions was also observed (Fig 4.23C). This is in contrast to an increase in TNFα following both simulated ischaemia or with reperfusion (Meldrum *et al.*, 2001). Whether these observations are true at the protein level remains to be investigated.

We attempted to investigate the effects of ENT4 inhibition on sIR using TC-T6000, but the data was inconclusive. The concentration of TC-T6000, a DY analogue, used may also be sufficient to inhibit ENT1 and ENT2 (Wang *et al.*, 2013). Also, like DY, TC-T6000 may inhibit phosphodiesterases (Ziegler *et al.*, 1995), which would have cardio-protective effects by virtue of cGMP-PKG signalling (Korkmaz-Icoz *et al.*, 2018). TC-T6000 also caused a significant decrease in Gpx1 expression (Fig 4.24A vs Fig 4.26A) despite this gene not being affected by sIR. Further analysis requires the

identification/development of more selective ENT4 inhibitors, or the use of ENT4 gene silencing approaches.

5.6 Compensatory changes in hearts and mesenteric vessels of ENT4 KO animals

Assessment of changes in mRNA levels in hearts and mesenteric arteries from WT and ENT4-KO mice revealed compensatory changes in purinergic related genes (transporters, receptors & enzymes) in the heart and mesenteric vessels rather than serotonergic related genes (except for MAOB in 6-month male hearts). This suggests that although ENT4 is better known for its serotonin transport, loss of ENT4 may actually be disrupting purine homeostasis in the cardiovascular system more than it impacts the serotonergic system. This was unexpected as ENT4 has a relatively low affinity for adenosine (compared to concentrations found under physiological and pathophysiological conditions). On the other hand, ENT4 transports a wider variety of monoamines and at higher affinities relative to adenosine (or 2CADO). Therefore, we hypothesise that the adenosine transport capability by ENT4 has potential biological relevance and might be integral to the regulation of cardiovascular function.

The compensatory increased Nos2 and decreased Ptgs2 expression in male mouse mesenteric vasculature (Fig 4.34D) also suggests that ENT4 deletion might impact NO and arachidonic acid homeostasis. Though the Nos2-encoded inducible nitric oxide synthase (iNOS) is not the main subtype expressed in the endothelium, it is known to contribute to vascular dysfunction. Of note, it is thought to be a contributor to the pathophysiology of sepsis (Shah, 2000). If iNOS expression is also upregulated at the protein level, it might lead to increased NO production. With more NO being produced, it might explain why an increased sensitivity to acetylcholine mediated (i.e. NOS-dependent) vasodilatation was observed in male ENT4 KO animals (Fig 4.34D). On the other hand, female ENT4 KO animals, which did not have a change in Nos2 expression (Fig 4.33D), had an increased sensitivity to an NO-donor, sodium nitroprusside, in a NOS independent pathway (see appendix, Supplementary Fig 3).

There were also no changes in ENT1 mRNA or protein levels in the heart of ENT4 KO animals. This suggests that chronic inhibition of ENT4 in the heart will be unlikely to affect ENT1, and any essential function ENT1 plays in maintaining physiological homeostasis. On the other hand, a consistent suppression of Slc22a2 (which encodes for OCT2) in the mesenteric vessels of both males and females was observed (Fig 4.33A and 4.34A). As dopamine and MPP^+ are substrates for OCT2 (Grundemann *et al.*, 1999), this decrease might be a compensation for the loss of ENT4 function in the mesenteric vascular bed.

5.7 Limitations of current studies

5.7.1 Complementing *in vitro* with *ex vivo* analyses

This study brings together data from the cell and molecular level, to data produced by other laboratories in *ex vivo* and *in vivo* preparations. We investigated our hypothesis that ENT4 activity changes following an ischaemic stress, by utilising an *in vitro* radio-labelled uptake assay. Changes in activity has a greater significance compared to protein levels as post-translational modifications can result in activity changes without affecting protein levels. Although we measured mRNA levels, these changes (or lack thereof) will not necessarily translate to protein changes, therefore they were only used as an indication for potential changes. Since ENT4 activity can only be measured *in vitro* with the tools currently available, a sIR model was used where cells were subjected to a hypoxic chamber in the presence of an ischaemia-mimetic buffer to mimic IRI.

Although we are able to precisely control the ischaemic conditions with a sIR model, these *in vitro* conditions will not completely recapitulate the cardiac IRI seen in *in vivo* or *ex vivo* models. Despite mimicking certain aspects of IRI, simulated ischaemia does not model the supply-demand mismatch that we observe in an isolated beating heart (for example). Cells do not have an energy demand and therefore are unlikely to have a contractile demand. It is also important to not only produce a hypoxic environment, but also mimic a low-flow condition. This was replicated to a certain extent by using a minimum buffer volume to cover the monolayer cells (800 µL in a six-well plate) and prevent cellular dehydration during the simulated ischaemic period. This minimum

buffer volume, however, is likely to be greater than the interstitial fluid in cardiomyocytes (Tutami *et al.*, 1994) and therefore is unlikely to mimic no-flow conditions observed in severe ischaemia.

In addition, as ENT4 is acidic pH-sensitive, it remains unclear whether sIR resulted in intracellular acidification in HL-1 cardiomyocytes, as pump and exchangers that maintain proton homeostasis are likely to still be functioning under those conditions. Despite these limitations, this model can provide valuable leads to inform the interpretation of data generated in *ex vivo* models. The *ex vivo* preparation being performed in parallel produces distinctive information on whether ENT4 is a viable target, and therefore both datasets complement each other, provide important insights on ENT4, and brings together data from different models ranging from cellular to an organ level.

Though MTT assays have commonly been used to assess cell viability, this might not be the best approach in the current study. MTT measures mitochondrial function and therefore, cells were allowed to recover following simulated ischaemia before measuring MTT where a trend in cell viability recovery with longer reperfusion was observed (Fig 4.21A). They can still be used to measure cell injury as there is a reduced cell viability with increasing periods of simulated ischaemia. LDH release was also measured to substantiate the MTT data and that the sIR produced certain level of cellular stress. As cardiomyocytes viability may not predict changes in infarct size in an intact heart, this limitation can be minimised with animal studies using 2,3,5-triphenyltetrazolium chloride staining to determine myocardial infarction in an isolated working heart model (Fishbein *et al.*, 1981).

5.7.2 Complications of current kinetic analysis studies

In measuring transport kinetics of ENT4, a much longer time-point of minutes was used, rather than a shorter time-point of seconds commonly used for other NTs. This creates a complication involving intracellular substrate metabolism. Despite the inhibition of intracellular enzymes, intracellular metabolism of the substrate which becomes a confounding factor in trying to analyse transport function was observed. This is well illustrated by the adenosine uptake studies in both

PK15-hENT4 and HL-1 cells where a linear relationship in substrate accumulation with time was observed.

In the presence of ABT-702 and EHNA, adenosine was still metabolised, and we were unable to accurately determine rate constants of ENT4-mediated transport. The estimated plateau and rate of uptake from a linear regression analysis in adenosine uptake were used to qualitatively estimate ENT4 activity, especially in HL-1 studies. We recognise that this is not an accurate determination of activity as the total cellular accumulation of substrates (adenosine or 2CADO) is dependent on enzymatic metabolism of substrates as soon as it gets taken up. ADK was shown to have a K_m of 0.15 µM (Yamada *et al.*, 1981), a higher affinity for adenosine than for ADA with a K_m of 65 µM (Hirschhorn *et al.*, 1976). This suggests that adenosine and 2CADO was mainly metabolised by ADK and trapped intracellularly as AMP. This maintains an inward concentration gradient for adenosine or 2CADO, resulting in an increased total accumulation or a linear relationship with time. ADK and ADA is also known to be less active at pH 6.0, compared to pH 7.5 (Yamada *et al.*, 1981; Lindley *et al.*, 1993), and therefore its plausible that the contribution of these enzymes is reduced at pH 6.0. While recognising that these intracellular enzymes contribute to the substrate cellular accumulation, the plateau, i.e. maximal accumulation, can indirectly represent ENT4 activity. The plateau and curve slopes are significantly lower in the presence of D22 or TC-T6000 or at neutral pH compared to acidic pH, especially in HL-1 studies. This suggests that ENT4 contributed to the observed changes in plateau, even if it is minimal compared to ADK and ADA.

Despite being a more stable adenosine analogue, a clear plateau with time even in the presence of ABT-702 was not observed. This was a major limitation in trying to estimate ENT4 function. A similar trend was observed for 2CADO uptake in the absence of NBMPR in HEK293-ENT2KO cells (Fig 4.17). Initial rate of uptake represents transporter function and would have been a better comparison. However, a variable dataset and a low signal-to-noise ratio meant that it would not represent the expected enhanced uptake observed under acidic conditions. For example, a statistically significant increase in initial rate of uptake was not observed at pH 6.0, compared to

pH 7.5, and a significant decrease in initial rate of uptake was not observed at pH 6.0 in the presence of an inhibitor, D22 or TC-T6000, compared to control conditions.

5.7.3 Measurement of membrane potential changes

Although the slow-response $DiBAC_4(3)$ probe remains a useful and relatively inexpensive method to assess changes in membrane potential, the dye might not have been sensitive enough to detect small changes in membrane potential. 120 mM KCl which would have been expected to result in significant cellular depolarisation only resulted in a 20% increase in $DiBAC_4(3)$ fluorescence (Fig 4.15). $DiBAC_4(3)$ was previously shown to have a relatively slow kinetics where changes of fluorescence intensity in response to changes in membrane potential reached a plateau in minutes (Brauner *et al.*, 1984). Changes in fluorescence signal was also shown to be dependent on cell size, with a larger cell have a faster kinetics (and lower rate constant) (Brauner *et al.*, 1984). A relatively slow kinetics observed in the PK15-hENT4 cell line would suggests that it has a relatively small cell size.

5.7.4 Future experiments

Consistent with the literature, qPCR analysis of the heart and mesenteric vessel confirms the expression of ENT4 in the heart and vasculature. Its functional significance, however, will ideally still need to be investigated using primary cell cultures, in addition to *ex vivo* studies. We would also need to study sex dependent cardio-protection (if any) observed with ENT4 inhibition in animals, and since there is a known sex-dependent protection against IRI (Kher *et al.*, 2005). Our collective data also suggests a sex dependent regulation of ENT4 where there was (1) a differential regulation in the heart and mesenteric vessels of male versus female ENT4 KO animals (OCT3 in the heart and CNT2 in the mesenteric vessels), (2) a loss of myogenic tone exclusively in male ENT4 KO animals (see appendix, Supplementary Fig 2), and (3) an increased sensitivity to 5-HT biphasic response exclusively in female ENT4 KO animals (see appendix, Supplementary Fig 5).

As there are limitations associated with mRNA data and since it might not be translated to protein or functional changes, this needs to be verified by measuring corresponding protein levels and

enzyme activities, in particular with respect to the sex and age dependent differential regulation of OCT1 and OCT3. There is, however, a lack of a specific ENT4 antibody (section 4.1.2), which proved to be a major limitation in our current study. Other available ENT4 antibodies can be characterised by testing it in ENT4 WT and KO animals. An antibody that demonstrates a band at ~55kDa (Barnes *et al.*, 2006) only in WT mice, but not in ENT4 KO animals, can be used. It can then be further used to study localisation of ENT4 with immunohistochemistry.

Since ENT4 also transport monoamines (with 5-HT having the highest affinity), how ENT4 inhibition affects the cardiovascular effects of 5-HT should be studied. Although the mRNA data suggests otherwise, whether a 5-HT receptor antagonist might be necessary as an adjuvant therapy to suppress any unwanted harmful effects due to excess accumulation of extracellular 5-HT should be investigated. ENT4 is not the only transporter responsible for 5-HT clearance, and how extracellular 5-HT levels are changed when ENT4 activity is suppressed should be examined. If 5-HT levels are sensitive to ENT4 activity, a significant increase in plasma 5-HT levels when ENT4 is pharmacologically inhibited is expected only in WT mice, but not in ENT4 KO animals.

In conclusion, our data supports our hypothesis that ENT4 is capable of mediating not just adenosine transport, but also that of an adenosine analogue (2CADO), in an acidic pH-sensitive manner. This is the first time that an adenosine analogue has been shown to be a substrate for ENT4. In addition to influx, we showed that ENT4 could mediate 2CADO efflux in an acidic pH-sensitive manner. Our data, however, does not support our hypothesis that ENT4 acidic pH sensitivity is dependent on a proton gradient across the plasma membrane. Rather, we now speculate that protonation of Glu-448 and Asp-226 might be involved in the ENT4 pH sensitivity. Our data also did not support our hypothesis that ENT4 activity is increased during ischaemia under which conditions are acidic. Conversely, we saw a reduction in ENT4 activity. Nevertheless, this change may also be relevant to IRI with respect to protecting cellular adenine nucleotide pools during early reperfusion. Furthermore, qPCR and functional (see appendices) data from our animal studies supported our hypothesis that ENT4 function as a nucleoside transporter plays a significant role in the regulation of the cardiovascular system.

This thesis adds on to our current understanding of ENT4, a transporter that has therapeutic potential for a clinically unmet condition, cardiac IRI, as it is not ubiquitously expressed and has not yet been implicated in a human disorder, unlike the other ENTs. Further studies are clearly warranted to determine the therapeutic benefit of ENT4 inhibition. Considering the role of ENT4 in the brain (Duan *et al.*, 2013), a blood-brain barrier impermeable modulator of ENT4 may be needed for its use in cardiovascular indication.

References

Abd-Elfattah AS, Tuchy GE, Jessen ME, Salter DR, Goldstein JP, Brunsting LA, 3rd, Wechsler AS (2013). Hot shot induction and reperfusion with a specific blocker of the es-ENT1 nucleoside transporter before and after hypothermic cardioplegia abolishes myocardial stunning in acutely ischemic hearts despite metabolic derangement: hot shot drug delivery before hypothermic cardioplegia. *J Thorac Cardiovasc Surg* **146**(4)**:** 961-970 e963.

Abd-Elfattah AS, Wechsler AS (1994). Separation between ischemic and reperfusion injury by site specific entrapment of endogenous adenosine and inosine using NBMPR and EHNA. *J Card Surg* **9**(3 Suppl)**:** 387-396.

Abebe W, Hussain T, Olanrewaju H, Mustafa SJ (1995). Role of nitric oxide in adenosine receptor-mediated relaxation of porcine coronary artery. *Am J Physiol* **269**(5 Pt 2)**:** H1672-1678.

Acimovic Y, Coe IR (2002). Molecular evolution of the equilibrative nucleoside transporter family: identification of novel family members in prokaryotes and eukaryotes. *Mol Biol Evol* **19**(12)**:** 2199-2210.

Amith SR, Wilkinson JM, Fliegel L (2016). KR-33028, a potent inhibitor of the Na(+)/H(+) exchanger NHE1, suppresses metastatic potential of triple-negative breast cancer cells. *Biochemical pharmacology* **118:** 31-39.

Archer RG, Pitelka V, Hammond JR (2004). Nucleoside transporter subtype expression and function in rat skeletal muscle microvascular endothelial cells. *British journal of pharmacology* **143**(1)**:** 202-214.

Armstrong S, Ganote CE (1994). Adenosine receptor specificity in preconditioning of isolated rabbit cardiomyocytes: evidence of A3 receptor involvement. *Cardiovasc Res* **28**(7)**:** 1049-1056.

Avkiran M, Marber MS (2002). Na(+)/H(+) exchange inhibitors for cardioprotective therapy: progress, problems and prospects. *J Am Coll Cardiol* **39**(5)**:** 747-753.

Aymerich I, Duflot S, Fernandez-Veledo S, Guillen-Gomez E, Huber-Ruano I, Casado FJ, Pastor-Anglada M (2005). The concentrative nucleoside transporter family (SLC28): new roles beyond salvage? *Biochemical Society transactions* **33**(Pt 1)**:** 216-219.

Baldwin SA, Yao SY, Hyde RJ, Ng AM, Foppolo S, Barnes K, Ritzel MW, Cass CE, Young JD (2005). Functional characterization of novel human and mouse equilibrative nucleoside transporters (hENT3 and mENT3) located in intracellular membranes. *The Journal of biological chemistry* **280**(16)**:** 15880-15887.

Barnes K, Dobrzynski H, Foppolo S, Beal PR, Ismat F, Scullion ER, Sun L, Tellez J, Ritzel MW, Claycomb WC, Cass CE, Young JD, Billeter-Clark R, Boyett MR, Baldwin SA (2006). Distribution and functional characterization of equilibrative nucleoside transporter-4, a novel cardiac adenosine transporter activated at acidic pH. *Circulation research* **99**(5)**:** 510-519.

Belardinelli L, Shryock JC, Song Y, Wang D, Srinivas M (1995). Ionic basis of the electrophysiological actions of adenosine on cardiomyocytes. *FASEB journal : official publication of the Federation of American Societies for Experimental Biology* **9**(5)**:** 359-365.

Bers DM (2002). Cardiac excitation-contraction coupling. *Nature* **415**(6868)**:** 198-205.

Blomstrom-Lundqvist C, Scheinman MM, Aliot EM, Alpert JS, Calkins H, Camm AJ, Campbell WB, Haines DE, Kuck KH, Lerman BB, Miller DD, Shaeffer CW, Jr., Stevenson WG, Tomaselli GF, Antman EM, Smith SC, Jr., Alpert JS, Faxon DP, Fuster V, Gibbons RJ, Gregoratos G, Hiratzka LF, Hunt SA, Jacobs AK, Russell RO, Jr., Priori SG, Blanc JJ, Budaj A, Burgos EF, Cowie M, Deckers JW, Garcia MA, Klein WW, Lekakis J, Lindahl B, Mazzotta G, Morais JC, Oto A, Smiseth O, Trappe HJ, American College of C, American Heart Association Task Force on Practice G, European Society of Cardiology Committee for Practice Guidelines. Writing Committee to Develop Guidelines for the Management of Patients With Supraventricular A (2003). ACC/AHA/ESC guidelines for the management of patients with supraventricular arrhythmias--executive summary: a report of the American College of Cardiology/American Heart Association Task Force on Practice Guidelines and the European Society of Cardiology Committee for Practice Guidelines (Writing Committee to Develop Guidelines for the Management of Patients With Supraventricular Arrhythmias). *Circulation* **108**(15)**:** 1871-1909.

Bone DB, Choi DS, Coe IR, Hammond JR (2010). Nucleoside/nucleobase transport and metabolism by microvascular endothelial cells isolated from ENT1-/- mice. *American journal of physiology. Heart and circulatory physiology* **299**(3)**:** H847-856.

Bone DB, Hammond JR (2007). Nucleoside and nucleobase transporters of primary human cardiac microvascular endothelial cells: characterization of a novel nucleobase transporter. *American journal of physiology. Heart and circulatory physiology* **293**(6)**:** H3325-3332.

Bonizzoni E, Milani S, Ongini E, Casati C, Monopoli A (1995). Modeling hemodynamic profiles by telemetry in the rat. A study with A1 and A2a adenosine agonists. *Hypertension* **25**(4 Pt 1)**:** 564-569.

Boxberger KH, Hagenbuch B, Lampe JN (2014). Common drugs inhibit human organic cation transporter 1 (OCT1)-mediated neurotransmitter uptake. *Drug metabolism and disposition: the biological fate of chemicals* **42**(6)**:** 990-995.

Brauner T, Hulser DF, Strasser RJ (1984). Comparative measurements of membrane potentials with microelectrodes and voltage-sensitive dyes. *Biochim Biophys Acta* **771**(2)**:** 208-216.

Cairns SP, Borrani F (2015). beta-Adrenergic modulation of skeletal muscle contraction: key role of excitation-contraction coupling. *The Journal of physiology* **593**(21)**:** 4713-4727.

Cerniway RJ, Yang Z, Jacobson MA, Linden J, Matherne GP (2001). Targeted deletion of A(3) adenosine receptors improves tolerance to ischemia-reperfusion injury in mouse myocardium. *American journal of physiology. Heart and circulatory physiology* **281**(4)**:** H1751-1758.

Chaudary N, Naydenova Z, Shuralyova I, Coe IR (2004). The adenosine transporter, mENT1, is a target for adenosine receptor signaling and protein kinase Cepsilon in hypoxic and pharmacological preconditioning in the mouse cardiomyocyte cell line, HL-1. *The Journal of pharmacology and experimental therapeutics* **310**(3)**:** 1190-1198.

Chen YH, Wu ML, Fu WM (1998). Regulation of acetylcholine release by intracellular acidification of developing motoneurons in Xenopus cell cultures. *J Physiol* **507 (Pt 1):** 41-53.

Chilian WM, Layne SM, Klausner EC, Eastham CL, Marcus ML (1989). Redistribution of coronary microvascular resistance produced by dipyridamole. *Am J Physiol* **256**(2 Pt 2)**:** H383-390.

Claycomb WC, Lanson NA, Jr., Stallworth BS, Egeland DB, Delcarpio JB, Bahinski A, Izzo NJ, Jr. (1998). HL-1 cells: a cardiac muscle cell line that contracts and retains phenotypic characteristics of the adult cardiomyocyte. *Proc Natl Acad Sci U S A* **95**(6)**:** 2979-2984.

Coe I, Zhang Y, McKenzie T, Naydenova Z (2002). PKC regulation of the human equilibrative nucleoside transporter, hENT1. *FEBS Lett* **517**(1-3)**:** 201-205.

Conti CR (1991). Adenosine: clinical pharmacology and applications. *Clin Cardiol* **14**(2)**:** 91-93.

Crawford CR, Patel DH, Naeve C, Belt JA (1998). Cloning of the human equilibrative, nitrobenzylmercaptopurine riboside (NBMPR)-insensitive nucleoside transporter ei by functional expression in a transport-deficient cell line. *The Journal of biological chemistry* **273**(9)**:** 5288-5293.

Cuffari C, Theoret Y, Latour S, Seidman G (1996). 6-Mercaptopurine metabolism in Crohn's disease: correlation with efficacy and toxicity. *Gut* **39**(3)**:** 401-406.

Dalton DW (1986). The cardiovascular effects of centrally administered 5-hydroxytryptamine in the conscious normotensive and hypertensive rat. *J Auton Pharmacol* **6**(1)**:** 67-75.

Dengler VL, Galbraith M, Espinosa JM (2014). Transcriptional regulation by hypoxia inducible factors. *Crit Rev Biochem Mol Biol* **49**(1)**:** 1-15.

Diaz J, Ni W, Thompson J, King A, Fink GD, Watts SW (2008). 5-Hydroxytryptamine lowers blood pressure in normotensive and hypertensive rats. *The Journal of pharmacology and experimental therapeutics* **325**(3)**:** 1031-1038.

Dos Santos-Rodrigues A, Grane-Boladeras N, Bicket A, Coe IR (2014). Nucleoside transporters in the purinome. *Neurochemistry international* **73:** 229-237.

Duan H, Hu T, Foti RS, Pan Y, Swaan PW, Wang J (2015). Potent and Selective Inhibition of Plasma Membrane Monoamine Transporter by HIV Protease Inhibitors. *Drug metabolism and disposition: the biological fate of chemicals* **43**(11)**:** 1773-1780.

Duan H, Wang J (2010). Selective transport of monoamine neurotransmitters by human plasma membrane monoamine transporter and organic cation transporter 3. *The Journal of pharmacology and experimental therapeutics* **335**(3)**:** 743-753.

Duan H, Wang J (2013). Impaired monoamine and organic cation uptake in choroid plexus in mice with targeted disruption of the plasma membrane monoamine transporter (Slc29a4) gene. *The Journal of biological chemistry* **288**(5)**:** 3535-3544.

Dubey RK, Gillespie DG, Mi Z, Suzuki F, Jackson EK (1996). Smooth muscle cell-derived adenosine inhibits cell growth. *Hypertension* **27**(3 Pt 2)**:** 766-773.

Eckle T, Kohler D, Lehmann R, El Kasmi K, Eltzschig HK (2008). Hypoxia-inducible factor-1 is central to cardioprotection: a new paradigm for ischemic preconditioning. *Circulation* **118**(2)**:** 166-175.

Eckle T, Krahn T, Grenz A, Kohler D, Mittelbronn M, Ledent C, Jacobson MA, Osswald H, Thompson LF, Unertl K, Eltzschig HK (2007). Cardioprotection by ecto-5'-nucleotidase (CD73) and A2B adenosine receptors. *Circulation* **115**(12)**:** 1581-1590.

Eltzschig HK, Abdulla P, Hoffman E, Hamilton KE, Daniels D, Schonfeld C, Loffler M, Reyes G, Duszenko M, Karhausen J, Robinson A, Westerman KA, Coe IR, Colgan SP (2005). HIF-1-dependent repression of equilibrative nucleoside transporter (ENT) in hypoxia. *The Journal of experimental medicine* **202**(11)**:** 1493-1505.

Eltzschig HK, Faigle M, Knapp S, Karhausen J, Ibla J, Rosenberger P, Odegard KC, Laussen PC, Thompson LF, Colgan SP (2006). Endothelial catabolism of extracellular adenosine during hypoxia: the role of surface adenosine deaminase and CD26. *Blood* **108**(5)**:** 1602-1610.

Eltzschig HK, Ibla JC, Furuta GT, Leonard MO, Jacobson KA, Enjyoji K, Robson SC, Colgan SP (2003). Coordinated adenine nucleotide phosphohydrolysis and nucleoside signaling in posthypoxic endothelium: role of ectonucleotidases and adenosine A2B receptors. *The Journal of experimental medicine* **198**(5)**:** 783-796.

Eltzschig HK, Kohler D, Eckle T, Kong T, Robson SC, Colgan SP (2009). Central role of Sp1-regulated CD39 in hypoxia/ischemia protection. *Blood* **113**(1)**:** 224-232.

Eltzschig HK, Thompson LF, Karhausen J, Cotta RJ, Ibla JC, Robson SC, Colgan SP (2004). Endogenous adenosine produced during hypoxia attenuates neutrophil accumulation: coordination by extracellular nucleotide metabolism. *Blood* **104**(13)**:** 3986-3992.

Endres CJ, Unadkat JD (2005). Residues Met89 and Ser160 in the human equilibrative nucleoside transporter 1 affect its affinity for adenosine, guanosine, S6-(4-nitrobenzyl)-mercaptopurine riboside, and dipyridamole. *Mol Pharmacol* **67**(3)**:** 837-844.

Engel K, Wang J (2005). Interaction of organic cations with a newly identified plasma membrane monoamine transporter. *Mol Pharmacol* **68**(5)**:** 1397-1407.

Engel K, Zhou M, Wang J (2004). Identification and characterization of a novel monoamine transporter in the human brain. *The Journal of biological chemistry* **279**(48)**:** 50042-50049.

Finegan BA, Lopaschuk GD, Gandhi M, Clanachan AS (1996). Inhibition of glycolysis and enhanced mechanical function of working rat hearts as a result of adenosine A1 receptor stimulation during reperfusion following ischaemia. *British journal of pharmacology* **118**(2)**:** 355-363.

Fishbein MC, Meerbaum S, Rit J, Lando U, Kanmatsuse K, Mercier JC, Corday E, Ganz W (1981). Early phase acute myocardial infarct size quantification: validation of the triphenyl tetrazolium chloride tissue enzyme staining technique. *Am Heart J* **101**(5)**:** 593-600.

Frank A, Bonney M, Bonney S, Weitzel L, Koeppen M, Eckle T (2012). Myocardial ischemia reperfusion injury: from basic science to clinical bedside. *Semin Cardiothorac Vasc Anesth* **16**(3)**:** 123-132.

Fraser JA, Middlebrook CE, Usher-Smith JA, Schwiening CJ, Huang CL (2005). The effect of intracellular acidification on the relationship between cell volume and membrane potential in amphibian skeletal muscle. *J Physiol* **563**(Pt 3)**:** 745-764.

Fredholm BB, Irenius E, Kull B, Schulte G (2001). Comparison of the potency of adenosine as an agonist at human adenosine receptors expressed in Chinese hamster ovary cells. *Biochemical pharmacology* **61**(4)**:** 443-448.

Furukawa J, Inoue K, Maeda J, Yasujima T, Ohta K, Kanai Y, Takada T, Matsuo H, Yuasa H (2015). Functional identification of SLC43A3 as an equilibrative nucleobase transporter involved in purine salvage in mammals. *Sci Rep* **5:** 15057.

Gaztanaga L, Marchlinski FE, Betensky BP (2012). Mechanisms of cardiac arrhythmias. *Rev Esp Cardiol (Engl Ed)* **65**(2)**:** 174-185.

Gordan R, Gwathmey JK, Xie LH (2015). Autonomic and endocrine control of cardiovascular function. *World journal of cardiology* **7**(4)**:** 204-214.

Gray JH, Owen RP, Giacomini KM (2004). The concentrative nucleoside transporter family, SLC28. *Pflugers Arch* **447**(5)**:** 728-734.

Griffiths EJ, Halestrap AP (1995). Mitochondrial non-specific pores remain closed during cardiac ischaemia, but open upon reperfusion. *Biochem J* **307 (Pt 1):** 93-98.

Grundemann D, Liebich G, Kiefer N, Koster S, Schomig E (1999). Selective substrates for non-neuronal monoamine transporters. *Mol Pharmacol* **56**(1)**:** 1-10.

Guo Y, Bolli R, Bao W, Wu WJ, Black RG, Jr., Murphree SS, Salvatore CA, Jacobson MA, Auchampach JA (2001). Targeted deletion of the A3 adenosine receptor confers resistance to myocardial ischemic injury and does not prevent early preconditioning. *J Mol Cell Cardiol* **33**(4)**:** 825-830.

Hart ML, Jacobi B, Schittenhelm J, Henn M, Eltzschig HK (2009). Cutting Edge: A2B Adenosine receptor signaling provides potent protection during intestinal ischemia/reperfusion injury. *J Immunol* **182**(7)**:** 3965-3968.

Hart ML, Kohler D, Eckle T, Kloor D, Stahl GL, Eltzschig HK (2008). Direct treatment of mouse or human blood with soluble 5'-nucleotidase inhibits platelet aggregation. *Arteriosclerosis, thrombosis, and vascular biology* **28**(8)**:** 1477-1483.

Hathaway DR, Konicki MV, Coolican SA (1985). Phosphorylation of myosin light chain kinase from vascular smooth muscle by cAMP- and cGMP-dependent protein kinases. *J Mol Cell Cardiol* **17**(9)**:** 841-850.

Hayer-Zillgen M, Bruss M, Bonisch H (2002). Expression and pharmacological profile of the human organic cation transporters hOCT1, hOCT2 and hOCT3. *British journal of pharmacology* **136**(6)**:** 829-836.

Hinschen AK, Rose'Meyer RB, Headrick JP (2003). Adenosine receptor subtypes mediating coronary vasodilation in rat hearts. *J Cardiovasc Pharmacol* **41**(1)**:** 73-80.

Hirschhorn R, Beratis N, Rosen FS (1976). Characterization of residual enzyme activity in fibroblasts from patients with adenosine deaminase deficiency and combined immunodeficiency: evidence for a mutant enzyme. *Proc Natl Acad Sci U S A* **73**(1)**:** 213-217.

Hua X, Kovarova M, Chason KD, Nguyen M, Koller BH, Tilley SL (2007). Enhanced mast cell activation in mice deficient in the A2b adenosine receptor. *The Journal of experimental medicine* **204**(1)**:** 117-128.

Hughes SJ, Cravetchi X, Vilas G, Hammond JR (2015). Adenosine A1 receptor activation modulates human equilibrative nucleoside transporter 1 (hENT1) activity via PKC-mediated phosphorylation of serine-281. *Cell Signal* **27**(5)**:** 1008-1018.

Itagaki S, Ganapathy V, Ho HT, Zhou M, Babu E, Wang J (2012). Electrophysiological characterization of the polyspecific organic cation transporter plasma membrane monoamine transporter. *Drug metabolism and disposition: the biological fate of chemicals* **40**(6)**:** 1138-1143.

Jin X, Shepherd RK, Duling BR, Linden J (1997). Inosine binds to A3 adenosine receptors and stimulates mast cell degranulation. *J Clin Invest* **100**(11)**:** 2849-2857.

Kanatsuka H, Lamping KG, Eastham CL, Dellsperger KC, Marcus ML (1989). Comparison of the effects of increased myocardial oxygen consumption and adenosine on the coronary microvascular resistance. *Circulation research* **65**(5)**:** 1296-1305.

Kang N, Jun AH, Bhutia YD, Kannan N, Unadkat JD, Govindarajan R (2010). Human equilibrative nucleoside transporter-3 (hENT3) spectrum disorder mutations impair nucleoside transport, protein localization, and stability. *The Journal of biological chemistry* **285**(36)**:** 28343-28352.

Kawabata H, Nakagawa K, Ishikawa K (2002). A novel cardioprotective agent, JTV-519, is abolished by nitric oxide synthase inhibitor on myocardial metabolism in ischemia-reperfused rabbit hearts. *Hypertension research : official journal of the Japanese Society of Hypertension* **25**(2)**:** 303-309.

Kher A, Meldrum KK, Wang M, Tsai BM, Pitcher JM, Meldrum DR (2005). Cellular and molecular mechanisms of sex differences in renal ischemia-reperfusion injury. *Cardiovasc Res* **67**(4)**:** 594-603.

Kin H, Zatta AJ, Lofye MT, Amerson BS, Halkos ME, Kerendi F, Zhao ZQ, Guyton RA, Headrick JP, Vinten-Johansen J (2005). Postconditioning reduces infarct size via adenosine receptor activation by endogenous adenosine. *Cardiovasc Res* **67**(1)**:** 124-133.

Koepsell H (2004). Polyspecific organic cation transporters: their functions and interactions with drugs. *Trends Pharmacol Sci* **25**(7)**:** 375-381.

Kohler D, Eckle T, Faigle M, Grenz A, Mittelbronn M, Laucher S, Hart ML, Robson SC, Muller CE, Eltzschig HK (2007). CD39/ectonucleoside triphosphate diphosphohydrolase 1 provides myocardial protection during cardiac ischemia/reperfusion injury. *Circulation* **116**(16)**:** 1784-1794.

Korkmaz-Icoz S, Radovits T, Szabo G (2018). Targeting phosphodiesterase 5 as a therapeutic option against myocardial ischaemia/reperfusion injury and for treating heart failure. *British journal of pharmacology* **175**(2)**:** 223-231.

Lam TI, Brennan-Minnella AM, Won SJ, Shen Y, Hefner C, Shi Y, Sun D, Swanson RA (2013). Intracellular pH reduction prevents excitotoxic and ischemic neuronal death by inhibiting NADPH oxidase. *Proc Natl Acad Sci U S A* **110**(46)**:** E4362-4368.

Lankford AR, Yang JN, Rose'Meyer R, French BA, Matherne GP, Fredholm BB, Yang Z (2006). Effect of modulating cardiac A1 adenosine receptor expression on protection with ischemic preconditioning. *American journal of physiology. Heart and circulatory physiology* **290**(4)**:** H1469-1473.

Ledent C, Vaugeois JM, Schiffmann SN, Pedrazzini T, El Yacoubi M, Vanderhaeghen JJ, Costentin J, Heath JK, Vassart G, Parmentier M (1997). Aggressiveness, hypoalgesia and high blood pressure in mice lacking the adenosine A2a receptor. *Nature* **388**(6643)**:** 674-678.

Lin BB, Hurley MC, Fox IH (1988). Regulation of adenosine kinase by adenosine analogs. *Mol Pharmacol* **34**(4)**:** 501-505.

Lindley ER, Pisoni RL (1993). Demonstration of adenosine deaminase activity in human fibroblast lysosomes. *Biochem J* **290 (Pt 2):** 457-462.

Loffler M, Morote-Garcia JC, Eltzschig SA, Coe IR, Eltzschig HK (2007). Physiological roles of vascular nucleoside transporters. *Arteriosclerosis, thrombosis, and vascular biology* **27**(5)**:** 1004-1013.

Mahmood A, Papayannis AC, Brilakis ES (2011). Pro-arrhythmic effects of intracoronary adenosine administration. *Hellenic J Cardiol* **52**(4)**:** 352-353.

Marro PJ, Baumgart S, Delivoria-Papadopoulos M, Zirin S, Corcoran L, McGaurn SP, Davis LE, Clancy RR (1997). Purine metabolism and inhibition of xanthine oxidase in severely hypoxic neonates going onto extracorporeal membrane oxygenation. *Pediatr Res* **41**(4 Pt 1)**:** 513-520.

Massmann V, Edemir B, Schlatter E, Al-Monajjed R, Harrach S, Klassen P, Holle SK, Sindic A, Dobrivojevic M, Pavenstadt H, Ciarimboli G (2014). The organic cation transporter 3 (OCT3) as molecular target of psychotropic drugs: transport characteristics and acute regulation of cloned murine OCT3. *Pflugers Arch* **466**(3)**:** 517-527.

Medina-Pulido L, Molina-Arcas M, Justicia C, Soriano E, Burgaya F, Planas AM, Pastor-Anglada M (2013). Hypoxia and P1 receptor activation regulate the high-affinity concentrative adenosine transporter CNT2 in differentiated neuronal PC12 cells. *Biochem J* **454**(3)**:** 437-445.

Meldrum KK, Meldrum DR, Hile KL, Burnett AL, Harken AH (2001). A novel model of ischemia in renal tubular cells which closely parallels in vivo injury. *J Surg Res* **99**(2)**:** 288-293.

Micheli V, Ricci C (1983). [Purine metabolism of the human erythrocyte]. *Quaderni Sclavo di diagnostica clinica e di laboratorio* **19**(1)**:** 1-37.

Morote-Garcia JC, Rosenberger P, Kuhlicke J, Eltzschig HK (2008). HIF-1-dependent repression of adenosine kinase attenuates hypoxia-induced vascular leak. *Blood* **111**(12)**:** 5571-5580.

Morote-Garcia JC, Rosenberger P, Nivillac NM, Coe IR, Eltzschig HK (2009). Hypoxia-inducible factor-dependent repression of equilibrative nucleoside transporter 2 attenuates mucosal inflammation during intestinal hypoxia. *Gastroenterology* **136**(2)**:** 607-618.

Morrison RR, Tan XL, Ledent C, Mustafa SJ, Hofmann PA (2007). Targeted deletion of A2A adenosine receptors attenuates the protective effects of myocardial postconditioning. *American journal of physiology. Heart and circulatory physiology* **293**(4)**:** H2523-2529.

Newby AC (1984). Adenosine and the concept of 'retaliatory metabolites'. *Trends Biochem Sci* **9**(2)**:** 42-44.

Ohta A, Sitkovsky M (2001). Role of G-protein-coupled adenosine receptors in downregulation of inflammation and protection from tissue damage. *Nature* **414**(6866)**:** 916-920.

Okada M, Bunag RD (1994). Selective enhancement in SHR of hypotension and bradycardia caused by NTS-injected serotonin. *Am J Physiol* **266**(2 Pt 2)**:** R599-605.

Paulmichl M, Gstraunthaler G, Lang F (1985). Electrical properties of Madin-Darby canine kidney cells. Effects of extracellular potassium and bicarbonate. *Pflugers Arch* **405**(2)**:** 102-107.

Pedata F, Corsi C, Melani A, Bordoni F, Latini S (2001). Adenosine extracellular brain concentrations and role of A2A receptors in ischemia. *Ann N Y Acad Sci* **939:** 74-84.

Pedley AM, Benkovic SJ (2017). A New View into the Regulation of Purine Metabolism: The Purinosome. *Trends Biochem Sci* **42**(2)**:** 141-154.

Pergola PE, Alper RH (1991). Vasopressin and autonomic mechanisms mediate cardiovascular actions of central serotonin. *Am J Physiol* **260**(6 Pt 2)**:** R1188-1193.

Philipp S, Yang XM, Cui L, Davis AM, Downey JM, Cohen MV (2006). Postconditioning protects rabbit hearts through a protein kinase C-adenosine A2b receptor cascade. *Cardiovasc Res* **70**(2)**:** 308-314.

Pijls NH, Tonino PA (2011). The crux of maximum hyperemia: the last remaining barrier for routine use of fractional flow reserve. *JACC Cardiovasc Interv* **4**(10)**:** 1093-1095.

Prystowsky EN, Niazi I, Curtis AB, Wilber DJ, Bahnson T, Ellenbogen K, Dhala A, Bloomfield DM, Gold M, Kadish A, Fogel RI, Gonzalez MD, Belardinelli L, Shreeniwas R, Wolff AA (2003). Termination of paroxysmal supraventricular tachycardia by tecadenoson (CVT-510), a novel A1-adenosine receptor agonist. *J Am Coll Cardiol* **42**(6)**:** 1098-1102.

Rahman MF, Askwith C, Govindarajan R (2017). Molecular determinants of acidic pH-dependent transport of human equilibrative nucleoside transporter 3. *The Journal of biological chemistry* **292**(36)**:** 14775-14785.

Riachi M, Bas F, Darendeliler F, Hussain K (2019). A novel 3'UTR mutation in the SLC29A3 gene associated with pigmentary hypertrichosis and non-autoimmune insulin-dependent diabetes mellitus syndrome. *Pediatr Diabetes*.

Riksen NP, Oyen WJ, Ramakers BP, Van den Broek PH, Engbersen R, Boerman OC, Smits P, Rongen GA (2005). Oral therapy with dipyridamole limits ischemia-reperfusion injury in humans. *Clinical pharmacology and therapeutics* **78**(1)**:** 52-59.

Rose JB, Naydenova Z, Bang A, Eguchi M, Sweeney G, Choi DS, Hammond JR, Coe IR (2010). Equilibrative nucleoside transporter 1 plays an essential role in cardioprotection. *American journal of physiology. Heart and circulatory physiology* **298**(3)**:** H771-777.

Roth GA, Huffman MD, Moran AE, Feigin V, Mensah GA, Naghavi M, Murray CJ (2015). Global and regional patterns in cardiovascular mortality from 1990 to 2013. *Circulation* **132**(17)**:** 1667-1678.

Ruel N, Nguyen KH, Vilas G, Hammond JR (2019). Characterization of 6-mercaptopurine transport by the SLC43A3-encoded nucleobase transporter. *Mol Pharmacol*.

SenGupta DJ, Lum PY, Lai Y, Shubochkina E, Bakken AH, Schneider G, Unadkat JD (2002). A single glycine mutation in the equilibrative nucleoside transporter gene, hENT1, alters nucleoside transport activity and sensitivity to nitrobenzylthioinosine. *Biochemistry* **41**(5)**:** 1512-1519.

Shah AM (2000). Inducible nitric oxide synthase and cardiovascular disease. *Cardiovasc Res* **45**(1)**:** 148-155.

Sievers F, Wilm A, Dineen D, Gibson TJ, Karplus K, Li W, Lopez R, McWilliam H, Remmert M, Soding J, Thompson JD, Higgins DG (2011). Fast, scalable generation of high-quality protein multiple sequence alignments using Clustal Omega. *Mol Syst Biol* **7:** 539.

Smits P, Williams SB, Lipson DE, Banitt P, Rongen GA, Creager MA (1995). Endothelial release of nitric oxide contributes to the vasodilator effect of adenosine in humans. *Circulation* **92**(8)**:** 2135-2141.

Stella L, de Novellis V, Marabese I, Berrino L, Maione S, Filippelli A, Rossi F (1998). The role of A3 adenosine receptors in central regulation of arterial blood pressure. *British journal of pharmacology* **125**(3)**:** 437-440.

Sukamoto T, Yamamoto T, Watanabe S, Ueki S (1984). Cardiovascular responses to centrally administered serotonin in conscious normotensive and spontaneously hypertensive rats. *Eur J Pharmacol* **100**(2)**:** 173-179.

Sundaram M, Yao SY, Ingram JC, Berry ZA, Abidi F, Cass CE, Baldwin SA, Young JD (2001). Topology of a human equilibrative, nitrobenzylthioinosine (NBMPR)-sensitive nucleoside transporter (hENT1) implicated in the cellular uptake of adenosine and anti-cancer drugs. *The Journal of biological chemistry* **276**(48)**:** 45270-45275.

Synnestvedt K, Furuta GT, Comerford KM, Louis N, Karhausen J, Eltzschig HK, Hansen KR, Thompson LF, Colgan SP (2002). Ecto-5'-nucleotidase (CD73) regulation by hypoxia-inducible factor-1 mediates permeability changes in intestinal epithelia. *J Clin Invest* **110**(7)**:** 993-1002.

Tang PCT, Yang C, Li RW, Lee SM, Hoi MP, Chan SW, Kwan YW, Tse CM, Leung GP (2016). Inhibition of human equilibrative nucleoside transporters by 4-((4-(2-fluorophenyl)piperazin-1-yl)methyl)-6-imino-N-(naphthalen-2-yl)-1,3,5-tr iazin-2-amine. *Eur J Pharmacol* **791:** 544-551.

Tao R, Kim SH, Honbo N, Karliner JS, Alano CC (2010). Minocycline protects cardiac myocytes against simulated ischemia-reperfusion injury by inhibiting poly(ADP-ribose) polymerase-1. *J Cardiovasc Pharmacol* **56**(6)**:** 659-668.

Thiel M, Chouker A, Ohta A, Jackson E, Caldwell C, Smith P, Lukashev D, Bittmann I, Sitkovsky MV (2005). Oxygenation inhibits the physiological tissue-protecting mechanism and thereby exacerbates acute inflammatory lung injury. *PLoS Biol* **3**(6)**:** e174.

Tsukamoto K, Kurihara T, Nakayama N, Isogai O, Ito S, Komatsu K, Kanmatsuse K (2000). Pressor responses to serotonin injected into the nucleus tractus solitarius of Sprague-Dawley rats and spontaneously hypertensive rats. *Clin Exp Hypertens* **22**(1)**:** 63-73.

Tutami LC, Mickle DAG, Weisel RD, Williams WG, Li RK (1994). An in vitro model to study myocardial ischemic injury. *Journal of tissue culture methods* **16**(1)**:** 1-9.

Verma S, Fedak PW, Weisel RD, Butany J, Rao V, Maitland A, Li RK, Dhillon B, Yau TM (2002). Fundamentals of reperfusion injury for the clinical cardiologist. *Circulation* **105**(20)**:** 2332-2336.

Visser F, Vickers MF, Ng AM, Baldwin SA, Young JD, Cass CE (2002). Mutation of residue 33 of human equilibrative nucleoside transporters 1 and 2 alters sensitivity to inhibition of transport by dilazep and dipyridamole. *The Journal of biological chemistry* **277**(1)**:** 395-401.

Walther DJ, Peter JU, Bashammakh S, Hortnagl H, Voits M, Fink H, Bader M (2003). Synthesis of serotonin by a second tryptophan hydroxylase isoform. *Science* **299**(5603)**:** 76.

Wang C, Lin W, Playa H, Sun S, Cameron K, Buolamwini JK (2013). Dipyridamole analogs as pharmacological inhibitors of equilibrative nucleoside transporters. Identification of novel potent and selective inhibitors of the adenosine transporter function of human equilibrative nucleoside transporter 4 (hENT4). *Biochemical pharmacology* **86**(11)**:** 1531-1540.

Wang J (2016). The plasma membrane monoamine transporter (PMAT): Structure, function, and role in organic cation disposition. *Clinical pharmacology and therapeutics* **100**(5)**:** 489-499.

Ward JL, Sherali A, Mo ZP, Tse CM (2000). Kinetic and pharmacological properties of cloned human equilibrative nucleoside transporters, ENT1 and ENT2, stably expressed in nucleoside transporter-deficient PK15 cells. Ent2 exhibits a low affinity for guanosine and cytidine but a high affinity for inosine. *The Journal of biological chemistry* **275**(12)**:** 8375-8381.

Watts SW (2005). 5-HT in systemic hypertension: foe, friend or fantasy? *Clinical science* **108**(5)**:** 399-412.

Watts SW (2016). Oh, the places you'll go! My many colored serotonin (apologies to Dr. Seuss). *American journal of physiology. Heart and circulatory physiology* **311**(5)**:** H1225-H1233.

Wiener N, Rosenblueth A (1946). The mathematical formulation of the problem of conduction of impulses in a network of connected excitable elements, specifically in cardiac muscle. *Arch Inst Cardiol Mex* **16**(3)**:** 205-265.

Wu X, Huang W, Ganapathy ME, Wang H, Kekuda R, Conway SJ, Leibach FH, Ganapathy V (2000). Structure, function, and regional distribution of the organic cation transporter OCT3 in the kidney. *American journal of physiology. Renal physiology* **279**(3)**:** F449-458.

Xi L, Das A, Zhao ZQ, Merino VF, Bader M, Kukreja RC (2008). Loss of myocardial ischemic postconditioning in adenosine A1 and bradykinin B2 receptors gene knockout mice. *Circulation* **118**(14 Suppl)**:** S32-37.

Xia L, Engel K, Zhou M, Wang J (2007). Membrane localization and pH-dependent transport of a newly cloned organic cation transporter (PMAT) in kidney cells. *American journal of physiology. Renal physiology* **292**(2)**:** F682-690.

Yamada Y, Goto H, Ogasawara N (1981). Adenosine kinase from human liver. *Biochim Biophys Acta* **660**(1)**:** 36-43.

Yang D, Koupenova M, McCrann DJ, Kopeikina KJ, Kagan HM, Schreiber BM, Ravid K (2008). The A2b adenosine receptor protects against vascular injury. *Proc Natl Acad Sci U S A* **105**(2)**:** 792-796.

Yang D, Zhang Y, Nguyen HG, Koupenova M, Chauhan AK, Makitalo M, Jones MR, St Hilaire C, Seldin DC, Toselli P, Lamperti E, Schreiber BM, Gavras H, Wagner DD, Ravid K (2006). The A2B adenosine receptor protects against inflammation and excessive vascular adhesion. *J Clin Invest* **116**(7)**:** 1913-1923.

Yang Z, Day YJ, Toufektsian MC, Ramos SI, Marshall M, Wang XQ, French BA, Linden J (2005). Infarct-sparing effect of A2A-adenosine receptor activation is due primarily to its action on lymphocytes. *Circulation* **111**(17)**:** 2190-2197.

Yao SY, Ng AM, Vickers MF, Sundaram M, Cass CE, Baldwin SA, Young JD (2002). Functional and molecular characterization of nucleobase transport by recombinant human and rat equilibrative nucleoside transporters 1 and 2. Chimeric constructs reveal a role for the ENT2 helix 5-6 region in nucleobase translocation. *The Journal of biological chemistry* **277**(28)**:** 24938-24948.

Yao SY, Sundaram M, Chomey EG, Cass CE, Baldwin SA, Young JD (2001). Identification of Cys140 in helix 4 as an exofacial cysteine residue within the substrate-translocation channel of rat equilibrative nitrobenzylthioinosine (NBMPR)-insensitive nucleoside transporter rENT2. *Biochem J* **353**(Pt 2)**:** 387-393.

Youdim MB, Edmondson D, Tipton KF (2006). The therapeutic potential of monoamine oxidase inhibitors. *Nat Rev Neurosci* **7**(4)**:** 295-309.

Young JD, Yao SY, Baldwin JM, Cass CE, Baldwin SA (2013). The human concentrative and equilibrative nucleoside transporter families, SLC28 and SLC29. *Molecular aspects of medicine* **34**(2-3)**:** 529-547.

Zhao ZQ, Corvera JS, Halkos ME, Kerendi F, Wang NP, Guyton RA, Vinten-Johansen J (2003). Inhibition of myocardial injury by ischemic postconditioning during reperfusion: comparison with ischemic preconditioning. *American journal of physiology. Heart and circulatory physiology* **285**(2)**:** H579-588.

Zhou M, Duan H, Engel K, Xia L, Wang J (2010). Adenosine transport by plasma membrane monoamine transporter: reinvestigation and comparison with organic cations. *Drug metabolism and disposition: the biological fate of chemicals* **38**(10)**:** 1798-1805.

Zhou M, Xia L, Wang J (2007). Metformin transport by a newly cloned proton-stimulated organic cation transporter (plasma membrane monoamine transporter) expressed in human intestine. *Drug metabolism and disposition: the biological fate of chemicals* **35**(10)**:** 1956-1962.

Ziegler JW, Ivy DD, Fox JJ, Kinsella JP, Clarke WR, Abman SH (1995). Dipyridamole, a cGMP phosphodiesterase inhibitor, causes pulmonary vasodilation in the ovine fetus. *Am J Physiol* **269**(2 Pt 2)**:** H473-479.

Appendices

Acknowledgements and preface

Data produced in this appendix was performed in the labs of Drs. Bourque (Supplementary Figure 1), Plane (Supplementary Figure 2 – 5) and Lopaschuk (Supplementary Figure 6) and not performed by me. The qPCR analysis of WT and ENT4-KO animals (Fig 4.29 – 4.34) was produced to complement functional data produced in the collaborator laboratories. These functional studies were performed concurrently with data produced in this thesis.

Methods

Animals used

WT and ENT4 KO mice (C57BL/6 background) were bred via homozygous mating pairs using standard husbandry procedures. Mice at 14-16 weeks of age were used for mesenteric vascular experiments and *in-vivo* vascular haemodynamics, and 24-28 weeks of age for heart perfusions. For tissue collection, mice were euthanized by isoflurane inhalation followed by decapitation according to the standards of the Canadian Council on Animal Care and protocols approved by the Animal Care Committee of the Faculty of Medicine and Dentistry, University of Alberta.

Haemodynamic measurements

Adult mice were kept spontaneously breathing under isoflurane anaesthesia (3-5% in 100% O_2) and maintained on a warm surgical table. Once surgical anaesthesia was achieved, mice were implanted with a pressure sensor (FISO Technologies Inc., Quebec, QC) in the left carotid artery for haemodynamic measurements, and a femoral venous catheter (Micro-renathane® - 0.010" o.d., 0.005" i.d.) for drug delivery. Once catheter implantation was completed, inspired isoflurane was set at 1.5% for the remainder of the experiment. To ensure stable haemodynamic parameters, blood pressure was allowed to equilibrate for a minimum of 25 minutes after cannulation, after which time baseline values were collected for 15 minutes. After baseline recordings, haemodynamic responses to a single bolus IV dose of methacholine (MCh 1 µg/kg), 5-HT (50 µg/kg), or sodium nitroprusside (SNP) (2 µg/kg) were measured, followed by a washout period of 15 minutes. To assess the contribution of NO to these responses, mice were administered the NOS inhibitor L-N^G-nitro-arginine methyl ester (L-NAME), given as an initial dose (60 mg/kg IV), followed by a maintenance dose (30 mg/kg) after 10 minutes. After an additional 5 minute wait period (after the second dose of L-NAME), a second bolus dose of the respective drug (MCh, 5-HT, SNP) was given at the doses noted above. All agents were dissolved in sterile saline.

Wire myography

The mesenteric bed was removed post mortem and placed in cold Krebs' buffer containing (mM): NaCl 119.0, $NaHCO_3$ 25.0, KCl 4.7, $MgSO_4$ 1.2, KH_2PO_4 1.18, glucose 11 and $CaCl_2$ 2.5. The superior mesenteric artery was isolated and cleaned of adhering fat and connective tissue, and cut into segments (~2 mm in length). Arterial segments were mounted between two gold-plated tungsten wires (20 µm diameter) in a Mulvany–Halpern myograph (model 400A, J.P. Trading, Denmark). Changes in isometric tension were recorded via a PowerLab acquisition system using Chart 5.0 software (AD Instruments, Colorado, USA). Tissues were maintained in Krebs' buffer gassed with 95% O_2/5% CO_2 at 37 °C and set to a pre-determined optimal resting tension of 5 mN (this value was determined from active length–tension curves). After an equilibration period of 30 minutes, endothelial function was assessed as percentage relaxation to acetylcholine (3 µM) following pre-stimulation with phenylephrine (3 µM; 75% of maximal tone). Arteries in which relaxation to acetylcholine was >90% of induced tone were deemed to have an intact endothelium. Arteries in which the percentage reversal of agonist-induced tone elicited by acetylcholine fell below this value were discarded. Cumulative concentration-response curves to acetylcholine and SNP were constructed in arteries in which tone was raised to 75% of maximum with phenylephrine (3 µM), relaxations were expressed as a percentage of induced tone. Cumulative concentration-response curves to phenylephrine and 5-HT were constructed in unstimulated arterial segments and expressed as a percentage of maximum response.

Pressure myography

Leak-free segments of second order mesenteric arteries (2-3 mm in length) were cleaned of adhering connective tissue and mounted between two glass cannulae in an arteriograph chamber (Living Systems Instrumentation, Vermont, USA) filled with Krebs' solution and secured with thin monofilament sutures. Arteries were viewed through an inverted microscope (Eclipse TE300, Nikon, Japan), and measurement of the artery internal diameter were made via an automated video dimension analyser (Living Systems Instrumentation, St. Albans, Vermont, USA). Pressure and diameter measurements were recorded via a PowerLab acquisition system using Chart 5.0 software (AD Instruments, Colorado, USA). Vessels were bathed in Krebs' buffer gassed with 95% O_2/5% CO_2 at 37°C, and intravascular pressure was maintained via a pressure servo-control system (Living Systems Instrumentation, St. Albans, Vermont, USA). Arteries that did not develop myogenic reactivity during an initial equilibration period of 30–40 minutes at 80 mmHg and 37°C were discarded. Following a 30 minute equilibration period with intravascular pressure

set at 80 mmHg, a pressure ramp was then applied by increasing the pressure to 120 mmHg in increments of 20 mmHg. Each pressure step was held for 2-3 minutes or until the diameter stabilised. Arteries were then bathed in Ca^{2+}-free Krebs' solution to reveal the maximum passive diameter.

Isolated working heart perfusion

Hearts from WT and ENT4 KO mice were perfused to evaluate cardiac function and metabolic changes. Mice were anesthetised with an intraperitoneal injection of sodium pentobarbital (60 mg/kg) after which their hearts were excised and perfused for 60 minutes. Hearts were perfused as isolated working preparations with oxygenated Krebs–Henseleit solution containing (in mM) 1.2 KH_2PO_4, 1.2 $MgSO_4 \cdot 7H_2O$, 2.5 $CaCl_2 \cdot 2H_2O$, 4.7 KCl, 25 $NaHCO_3$ and 118 NaCl. 5 mM [U-^{14}C]glucose and 0.8 mM [9,10-^{3}H]palmitate (pre-bound to 3% albumin) were added as energy substrates, in the presence or absence of 100 μU/mL insulin. Spontaneously beating hearts were perfused at an 11.5 mmHg left atrial preload and an 80 mmHg aortic afterload. Rate of glucose and palmitate oxidation were determined by the quantitative collection of $^{14}CO_2$ produced from [U-^{14}C]glucose, and $^{3}H_2O$ produced from [9,10-^{3}H]palmitate, respectively.

Results

In-vivo haemodynamic measurements

5-HT, MCh, and SNP each induced a significant reduction in diastolic blood pressure, this effect is consistently observed across genotypes (WT and ENT4-KO) and in both sexes (Supplementary Fig 1A, B and E). L-NAME did not affect 5-HT-mediated vasodilatation effects across the different experimental groups (Supplementary Fig 1C). However, L-NAME affected MCh-mediated vasodilatation differently in male and female animals. In the presence of L-NAME, MCh-mediated vasodilatation was significantly impaired in female ENT4-KO mice, compared to WT (Supplementary Fig 1D). In addition, L-NAME alone was able to increase diastolic blood pressure, with a significantly higher increase in diastolic blood pressure in males, compared to females. L-NAME-mediated vasoconstriction was significantly impaired in female ENT4-KO mice, compared to female WT (Supplementary Fig 1F).

Myogenic tone

Mesenteric vessels from male and female WT mice developed myogenic tone in response to increases in intravascular pressure from 60 and 80 mmHg, respectively (Supplementary Fig 2A and B). This myogenic tone response was completely absent in male ENT4-KO animals, but not female ENT4-KO animals (Supplementary Fig 2C and D). The passive diameters of the mesenteric vessels were not different between WT and ENT4-KO animals in both males and females (~210 µm internal diameter under Ca^{2+}-free conditions at 120 mmHg pressure).

Phenylephrine-induced vasoconstriction and SNP-mediated vasodilatation

Phenylephrine was able to induce vasodilatation in a similar manner across genotypes (WT and ENT4-KO) and in both sexes (Log EC_{50}~-5.8; Supplementary Fig 3A). WT and ENT4-KO male mice responded in a similar manner to endothelium-independent vasorelaxant SNP, while female ENT4-KO mice (relative to female WT) had a significantly greater sensitivity to SNP (Log EC_{50} of -8.14 ± 0.14 and -8.52 ± 0.09 for the WT and ENT4-KO arteries, respectively; Supplementary Fig 3C). On the other hand, male ENT4-KO mice (relative to male WT) had a significantly greater sensitivity to the endothelium-dependent vasorelaxant acetylcholine (Log EC_{50} of -6.91 ± 0.11 and -7.33 ± 0.05 for the WT and ENT4-KO arteries, respectively; Supplementary Fig 3D). Arteries from female WT and ENT4-KO did not show any difference in sensitivity to acetylcholine (Supplementary Fig 3E).

Endothelium-dependent relaxations

Acetylcholine concentration-response curves were generated in the absence and presence of the NOS inhibitor L-NAME (100 μM), the intermediate conductance K_{Ca} (IK_{Ca}) channel inhibitor TRAM-34 (1 μM) + the small conductance K_{Ca} (SK_{Ca}) channel inhibitor apamin (50 nM), or L-NAME + TRAM-34 + apamin. Inhibition of K_{Ca} channels produced a similar effect on acetylcholine-mediated vasodilatation in vessels from WT female and male mice (Supplementary Fig 4A and C), but L-NAME had a greater inhibitory effect on acetylcholine-mediated vasodilatation in female WT relative to male WT mice (13 ± 4% and 47 ± 7% relaxation by 1 μM acetylcholine in the presence of L-NAME in female WT and male WT arteries, respectively). TRAM-34/apamin had a greater inhibitory effect in arteries from female ENT4-KO animals, relative to female WT (49 ± 8% and 73 ± 7% relaxation to 1 μM acetylcholine in the presence of TRAM-34/apamin in the female ENT4-KO and WT tissues, respectively). Arteries from male ENT4-KO exhibited similar responses to all the agents used, relative to male WT (L-NAME, TRAM-34, apamin). Acetylcholine-mediated vasodilatation was completely inhibited in the presence of L-NAME + TRAM-34 + apamin, and this effect was consistently observed across genotypes (WT and ENT4-KO) and in both sexes.

Biphasic response to 5-HT

5-HT induced a biphasic response in mesenteric arteries, with a vasoconstriction of up to 1 μM followed by a vasodilatation at higher concentrations (Supplementary Fig 5). Arteries from male ENT4-KO animals exhibited a similar biphasic 5-HT response, relative to male WT (Supplementary Fig 5B). However, arteries from female ENT4-KO animals exhibited a significantly reduced sensitivity to the biphasic 5-HT response, compared to female WT (Supplementary Fig 5A).

Baseline measurements of cardiac function

Albeit not significant, hearts from male ENT4-KO animals showed a trend for a higher cardiac work, relative to male WT (Supplementary Fig 6A). A reduced cardiac efficiency with perfusion time observed in male WT hearts, was less evident in ENT4-KO male hearts (Supplementary Fig 6B). Under basal conditions (without insulin), the contribution of glucose and fatty acid oxidation to cardiac energy production (ATP and Acetyl-CoA) was similar in both WT and ENT4-KO male hearts (Supplementary Fig 6C – F). As expected, in the presence of insulin, the contribution of glucose oxidation to ATP and Acetyl-CoA production was significantly increased at the expense of fatty acid oxidation (Supplementary Fig 6E and F). This insulin sensitivity was similarly observed in the hearts of both male WT and ENT4-KO animals.

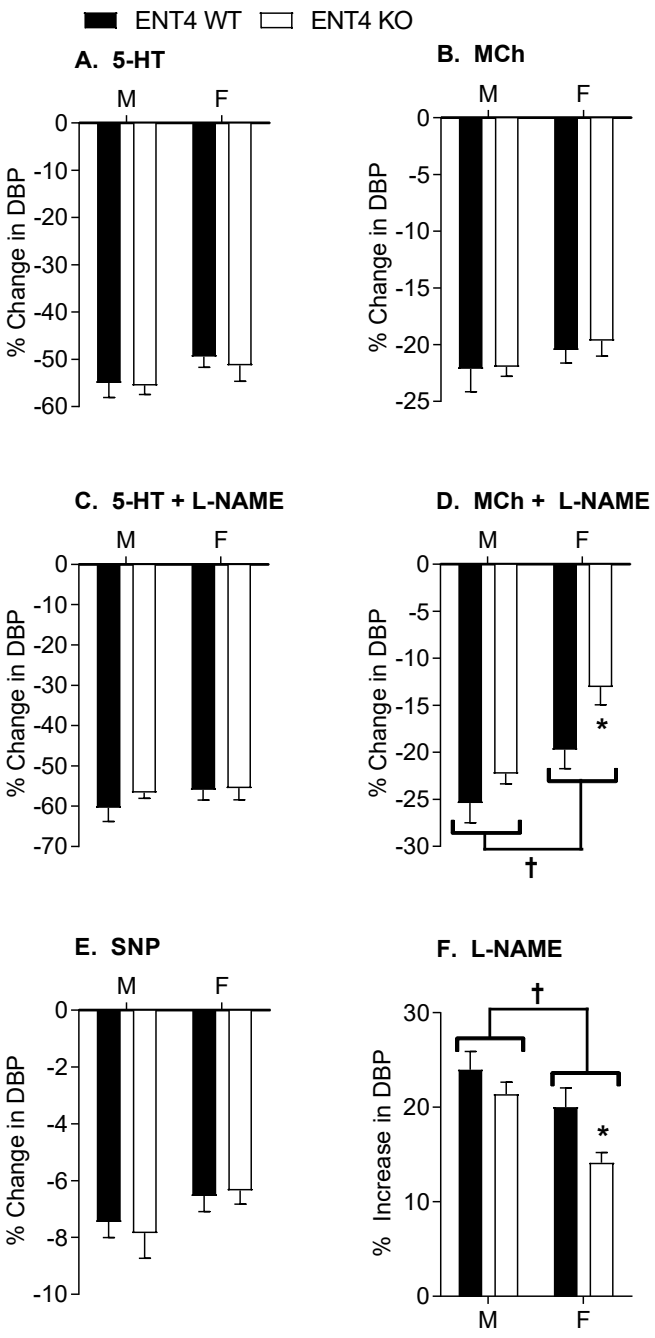

Supplementary Figure 1: *In-vivo* vascular haemodynamics in ENT4 WT and KO animals

Decrease in diastolic blood pressure induced by bolus infusions of 5-HT and methacholine, the absence (A, B) and presence (C, D) of the eNOS inhibitor L-NAME in male (M) and female (F) WT and ENT4-KO mice. (E) shows the effects of the endothelium-independent dilator SNP on diastolic blood pressure, and (F) shows increase in diastolic blood pressure induced by L-NAME alone. Each bar represents the mean ± SEM from 11 male WT, 11 female WT, 10 male ENT4-KO, and 8 female ENT4-KO mice. $^{*}p<0.05$ vs WT response and $^{\dagger}p<0.05$ between male and female responses as determined by 2-way ANOVA plus Bonferroni *post hoc* tests.

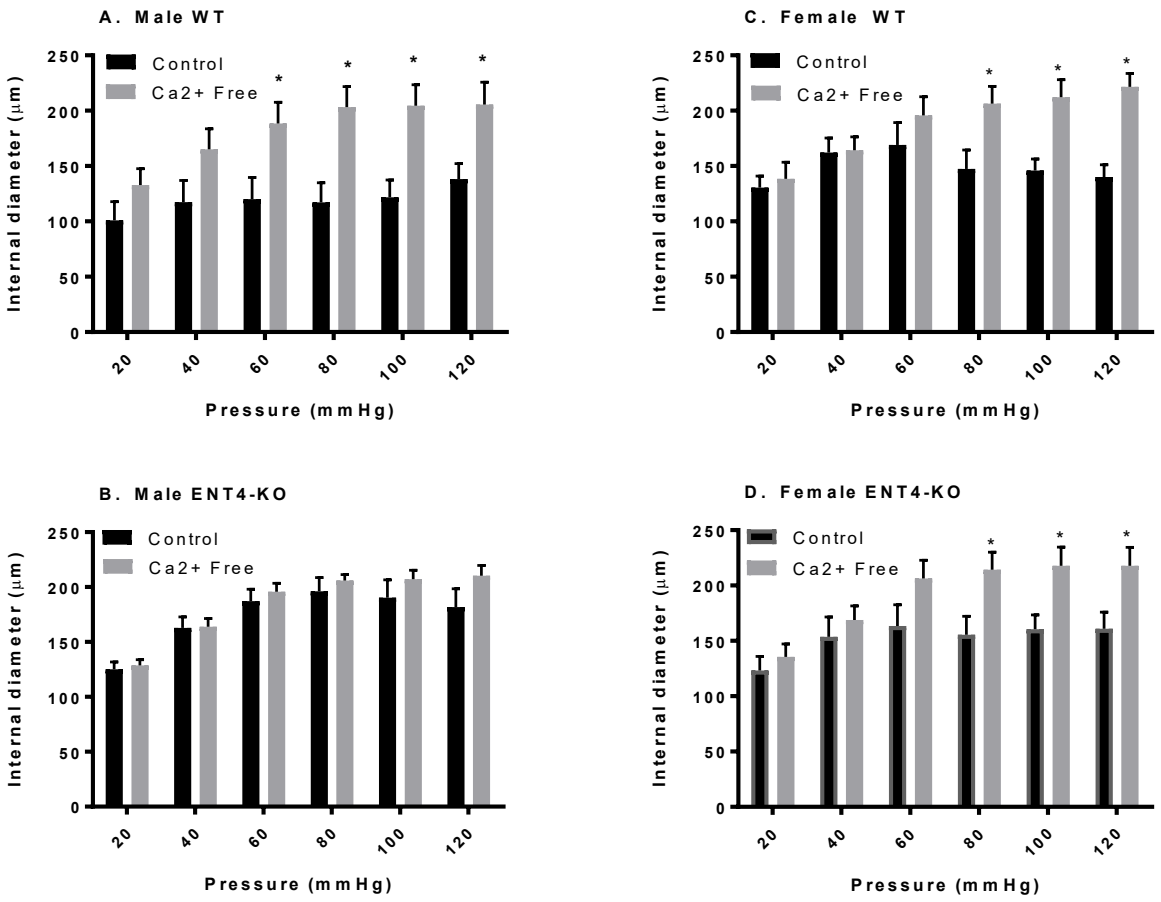

Supplementary Figure 2: Loss of myogenic tone in mesenteric arteries of male ENT4-KO mice

Second order mesenteric arteries isolated from male WT (A) and ENT4-KO (B) mice and female WT (C) and ENT4-KO (D) mice were subjected to incrementally increasing intravascular pressures between 20 and 120 mmHg (termed a pressure ramp), before internal diameters were measured. Pressure ramps were conducted in both normal Krebs' media (Control), and Ca^{2+}-free media (Ca^{2+} Free). Each bar represents the mean ± SEM from 5 experiments. $^{*}p<0.05$ vs control conditions as determined by Student's t-test.

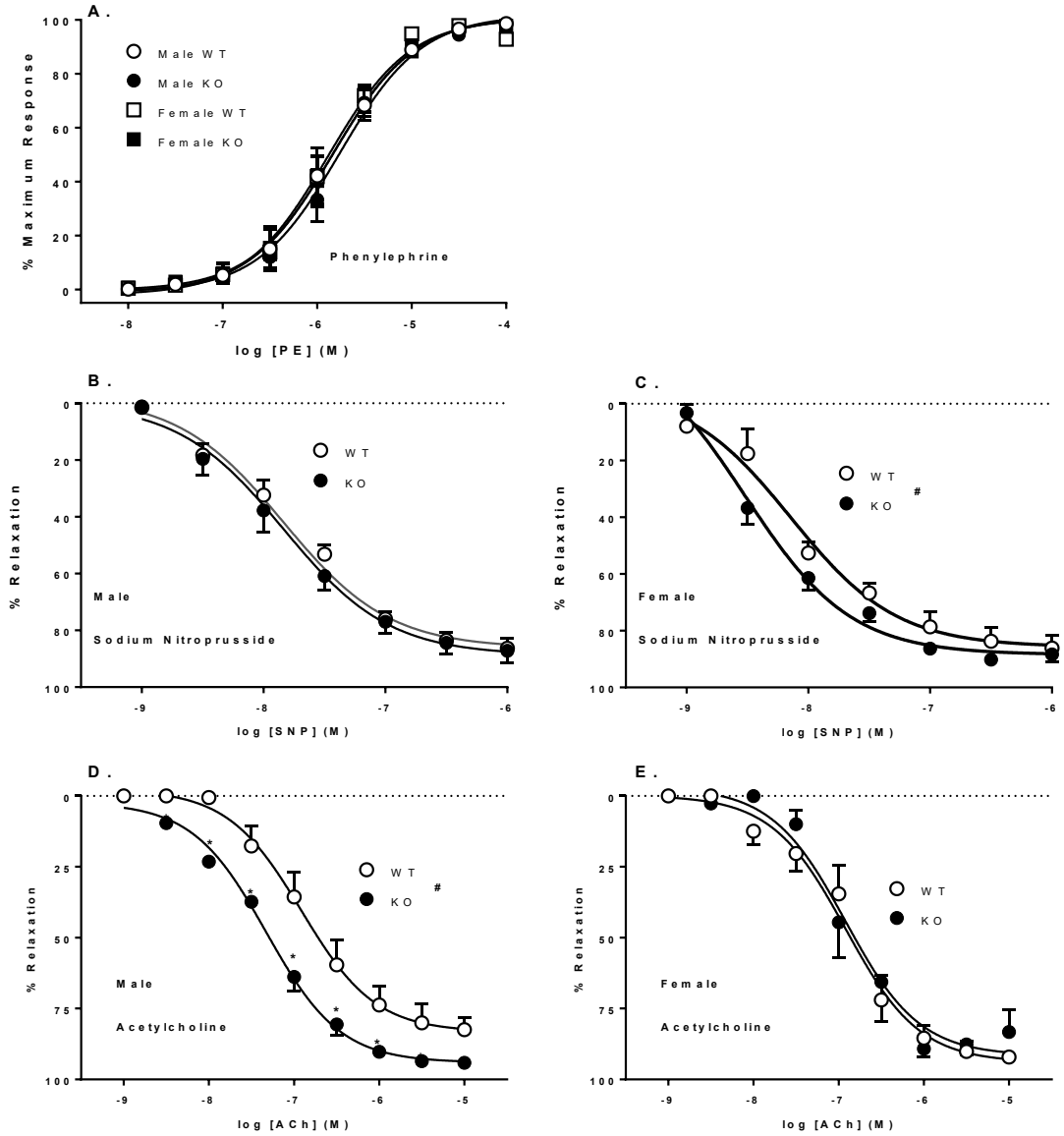

Supplementary Figure 3: Responsiveness of mesenteric resistance arteries to phenylephrine, acetylcholine and SNP

Mesenteric artery rings were isolated from male and female WT and ENT4-KO mice and mounted in a myograph under a resting tension of 5 mN. (A) shows the concentration-dependent increases in tone evoked by cumulative concentrations of phenylephrine. (B) and (C) indicate the relaxation of pre-stimulated mesenteric rings to cumulative concentrations of SNP in male and female mice, respectively, (D) and (E) show the relaxations induced by cumulative concentrations of acetylcholine in male and female mice, respectively. Data are represented as % of maximum response, and shown as mean ± SEM from 5 independent experiments. $^{*}p<0.05$ vs WT responses as determined by Student's t-test. $^{\#}$ Significant difference in log EC_{50} values calculated from curve fits of the WT and ENT4-KO data (Akaike's information criteria method, GraphPad Prism v 7.03).

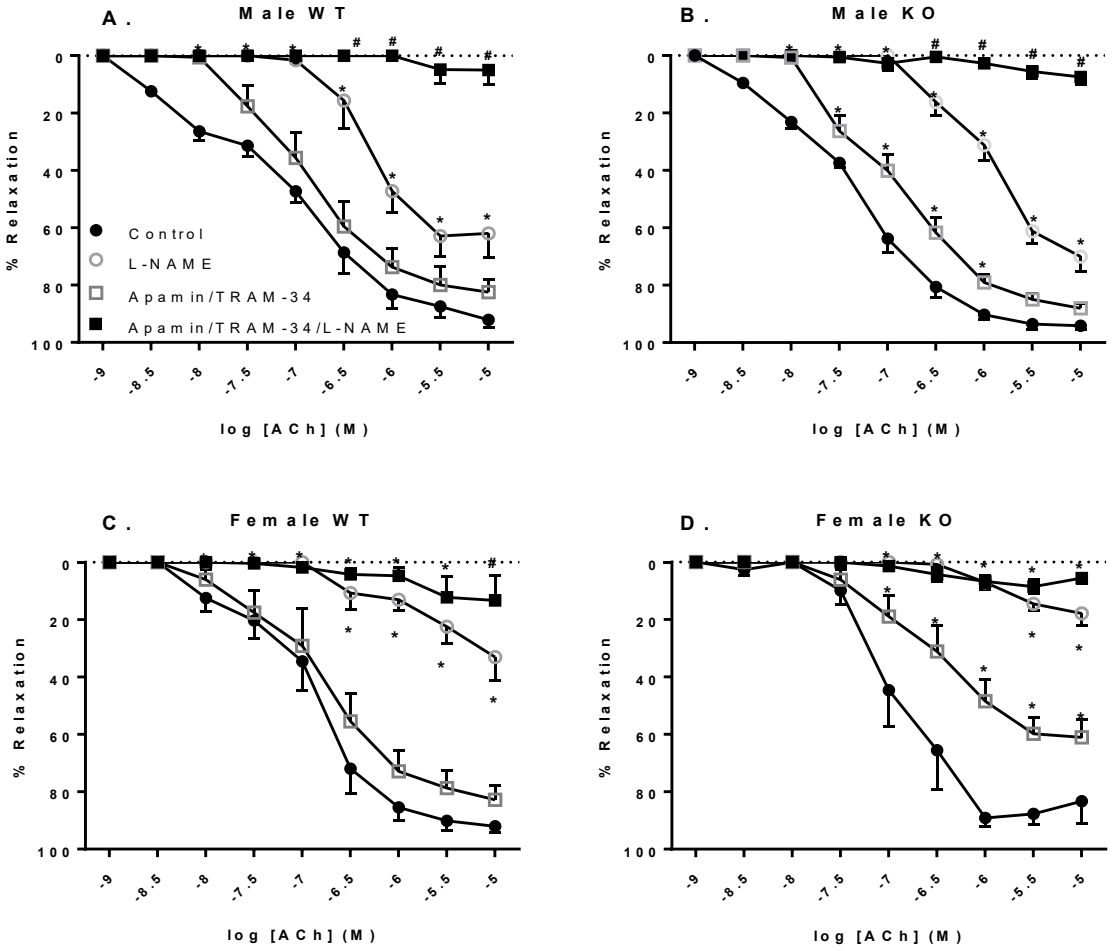

Supplementary Figure 4: Contribution of NO and K_{Ca} channels to the relaxant effect of acetylcholine in isolated mesenteric artery rings

Acetylcholine concentration response curves were generated, as described for supplementary Figure 3, in the absence and presence of L-NAME (to inhibit NO production), TRAM-34 + apamin (to inhibit K_{Ca} channels), or L-NAME + TRAM-34 + apamin (to inhibit both NO and K_{Ca}). Each point represents the mean ± SEM obtained using 5 male WT (A), 9 male ENT4-KO (B), 6 female WT (C), and 9 female ENT4-KO (D) arteries. Differences were assessed for significance by 2-way ANOVA plus Bonferroni *post hoc* tests with $p<0.05$ considered significant. * Significantly different from Control. # Significant difference between apamin/TRAM-34 and L-NAME/apamin/TRAM-34.

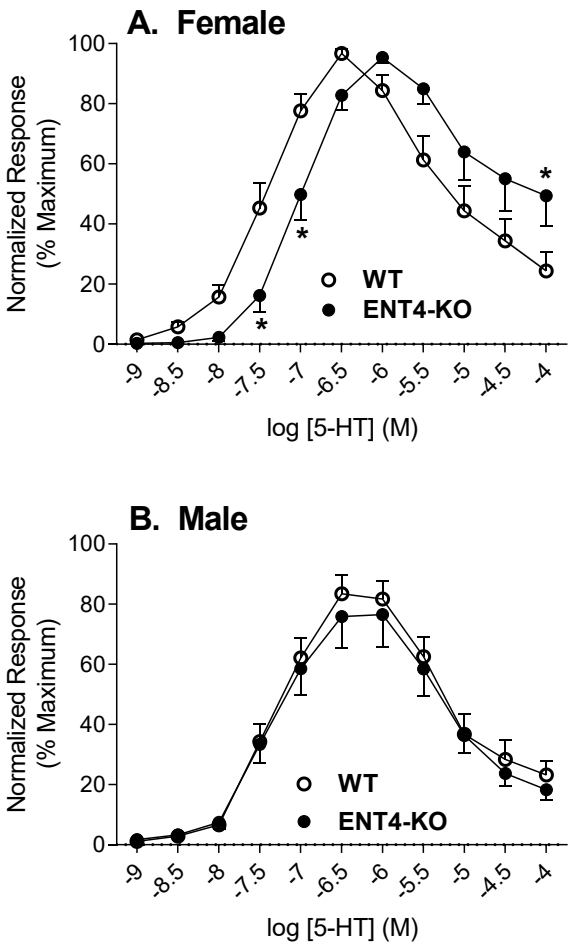

Supplementary Figure 5: Biphasic response of mesenteric resistance arteries to 5-HT

Mesenteric artery rings from female (A) and male (B) WT and ENT4-KO mice were exposed to increasing concentrations of 5-HT and the degree of vascular contraction shown as the % of maximum response of the tissue. Each point is the mean ± SEM from either 12 (A) or 10 (B) experiments. $^{*}p<0.05$ vs WT responses as determined by Student's t-test.

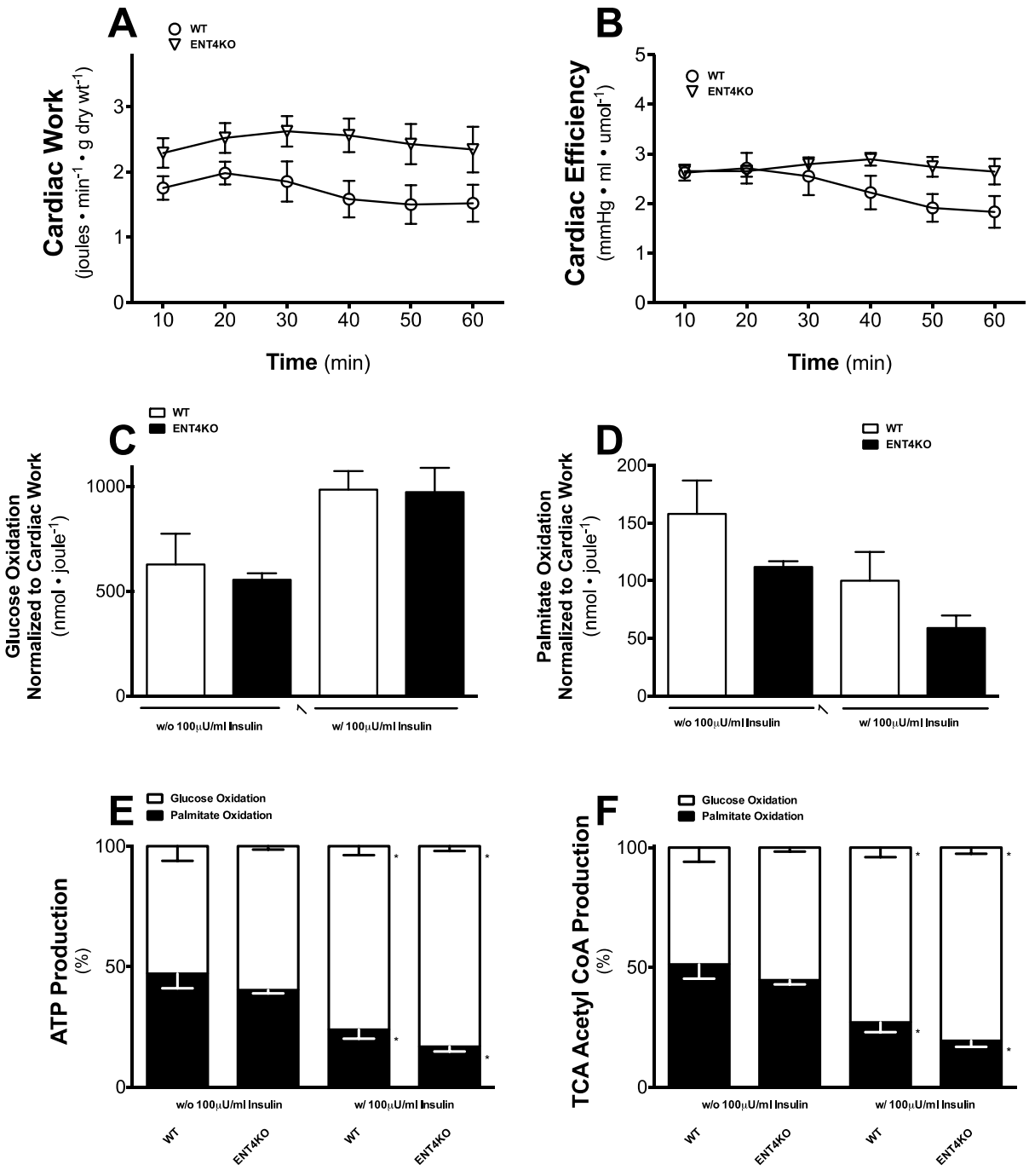

Supplementary Figure 6: Heart Perfusion data from 6-month male ENT4 WT and KO animals

Ex vivo assessment of cardiac function in the isolated perfused heart by a measure of cardiac work (A) and cardiac efficiency (B). Glucose (C) and palmitate (fatty acid) (D) oxidation normalised to cardiac work. ATP (E) and TCA acetyl CoA (F) production from glucose and palmitate oxidation. Data are expressed as mean ± SEM. n=6 for WT and n=8 for KO animals. No significant difference was observed as determined by multiple t-tests with correction for multiple comparisons using the Bonferroni–Dunn method (A, B) or Student's t-test (C, D). $^{*}p<0.05$ vs w/o insulin as determined by two-way ANOVA plus Bonferroni *post hoc* tests (E, F).